THE ANALYSIS OF TRIGLYCERIDE-RICH LIPOPROTEINS IN HUMAN SERUM

FOR CLINICAL STUDIES

A Dissertation

by

RICHA CHANDRA

Submitted to the Office of Graduate Studies of
Texas A&M University
in partial fulfillment of the requirements for the degree of

DOCTOR OF PHILOSOPHY

August 2006

Major Subject: Chemistry

THE ANALYSIS OF TRIGLYCERIDE-RICH LIPOPROTEINS IN HUMAN SERUM

FOR CLINICAL STUDIES

A Dissertation

by

RICHA CHANDRA

Submitted to the Office of Graduate Studies of
Texas A&M University
in partial fulfillment of the requirements for the degree of

DOCTOR OF PHILOSOPHY

Approved by:

Chair of Committee,   Ronald D. Macfarlane
Committee Members, David H. Russell
                              Manuel P. Soriaga
                              Rosemary L. Walzem
Head of Department, Emile E. Schweikert

August 2006

Major Subject: Chemistry

ABSTRACT

The Analysis of Triglyceride-Rich Lipoproteins in Human Serum for Clinical Studies.

(August 2006)

Richa Chandra, B.A., Austin College

Chair of Advisory Committee: Dr. Ronald D. Macfarlane

Since cardiovascular disease is one of the leading causes of mortality all over the world, it is becoming increasingly important and relevant to develop new analytical techniques for the analysis of the mechanisms of this complex disease as well as for clinical applications. The overall objective of this research was to develop an array of methods for the analysis of triglyceride rich lipoproteins (TRL) in human serum and to apply these methods to clinical samples.

TRL particles are mainly derived from dietary fats, which are positively correlated with cardiovascular disease. The mechanism behind which triglycerides cause cardiovascular disease is not well understood. The analysis of TRL by novel methods including density gradient ultracentrifugation and density profiling, gel electrophoresis, *in vitro* enzymatic assays, and capillary zone electrophoresis are presented here.

The development of a novel density profiling method for the remnant lipoproteins class of TRL and its application to clinical samples was successful. In addition, TRL were successfully evaluated for their composition by gel electrophoresis, *in vitro* enzymatic assays and capillary zone electrophoresis.

The results of these analyses demonstrate great potential for the use of these new methods as analytical tools for researchers in understanding the mechanism behind the onset of cardiovascular disease by TRL and their triglycerides as well as diagnostic tools for clinicians.

DEDICATION

To my parents Krishna and Renu Chandra

and my sister Natasha Chandra.

ACKNOWLEDGEMENTS

I would like to acknowledge my advisor Dr. Ronald D. Macfarlane for his unwavering support and invaluable advice in my academic career and life goals. I would like to thank him for always providing new perspectives and teaching me by example the importance of cardiovascular research and its relevance to all of our lives.

I would also like to thank my colleagues Leticia Espinosa and Ronald Henriquez for their collaborative efforts, advice and support over the years. Leticia Espinosa gave me valuable advice on the capillary electrophoresis and gel electrophoresis studies along with personal support over the years. I would like to acknowledge the support and collaborative efforts of Ronald Henriquez in the triglyceride distribution project development as well as the development of the capillary electrophoresis studies and thank him for his support as well.

I thank Dr. Rosemary Walzem for her invaluable support over the years of my academic career and for her collaborative efforts and advice on this project, especially the triglyceride distribution development, *in vitro* lipolysis studies, and capillary electrophoresis of TRL development. Dr. Walzem taught me how to study and think through complex biological mechanisms. I would like to thank Dr. Catherine J. McNeal at Scott & White Hospital, Temple, Texas for providing me an opportunity to work on a special case study of MMIHS and for her medical expertise and continual support in my research goals and career plans. I would also like to acknowledge Dr. John Pohl for his medical expertise in the special case study as well as his support in my career goals.

I would also like to acknowledge my committee members Dr. David Russell and Dr. Manuel Soriaga for their support during my academic career.

TABLE OF CONTENTS

LIST OF TABLES

LIST OF FIGURES

LIST OF ABBREVIATIONS

ACN	Acetonitrile
ALP	Atherogenic lipoprotein phenotype
Apo A-1	Apolipoprotein A-1
Apo A-2	Apolipoprotein A-2
Apo A-4	Apolipoprotein A-4
Apo B-100	Apolipoprotein B-100
Apo B-48	Apolipoprotein B-48
Apo C-1	Apolipoprotein C-1
Apo C-2	Apolipoprotein C-2
Apo C-3	Apolipoprotein C-3
Apo E-2	Apolipoprotein E-2
Apo E-3	Apolipoprotein E-3
Apo E-4	Apolipoprotein E-4
BGE	Background electrolyte
bTRL	Buoyant triglyceride-rich lipoprotein(s)
CH_3OH	Methanol
CM	Chylomicron(s)
CMR	Chylomicron remnant(s)
CsBiEDTA	Cesium bismuth ethylenediaminetetraacetic acid
CZE	Capillary zone electrophoresis

DAG	Diacylglycerol(s)
DGU	Density gradient ultracentrifugation
dHDL	Dense high density lipoprotein
DMSO	Dimethl sulfoxide
dTRL	Dense triglyceride-rich lipoprotein(s)
EDTA	Ethylenediaminetetraacetic acid
ELISA	Enzyme-linked immunosorbent assay
HDL	High density lipoprotein(s)
HL	Hepatic lipase
HSA	Human serum albumin
IDL	Intermediate density lipoprotein(s)
LCAT	Lecithin-cholesterol acyltransferase
LDL	Low density lipoprotein(s)
LDLr	LDL receptor
LDS	Lauryl alcohol sulfate, lithium salt
LP	Lipoprotein(s)
Lp(a)	Lipoprotein a
LpL	Lipoprotein lipase
LRP	LDL receptor-related protein
MAG	Monoacylglycerol(s)
MMIHS	Megacystis-Microcolon-Intestinal Hyperperistalsis Syndrome
mm	Millimeter

NaBiEDTA	Sodium bismuth ethylenediaminetetraacetic acid
Na$_2$CdEDTA	Disodium cadmium ethylenediaminetetraacetic acid
NBD	7-nitro-2,1,3-benz-oxadiazol-4-yl
RLP	Remnant lipoprotein(s)
rVLDL	VLDL remnant(s)
SDS	Sodium dodecyl sulfate
SDS-PAGE	Sodium dodecyl sulfate-polyacrylamide gel electrophoresis
TAG	Triglyceride(s) or triacylglycerol(s)
Thio-NADH	Thio-adenosine 5'-(trihydrogen diphosphate)
THL	Type III hyperlipoproteinemia
TPN	Total parenteral nutrition
Tris-HCl	Tris-hydrochloric acid
TRL	Triglyceride-rich lipoprotein(s)
VLDL	Very low density lipoprotein(s)
A	Absorbance
h	Height (cm)
L$_c$	Length of capillary (cm)
L$_d$	Length of capillary to detector window (cm)
μ_{eff}	Effective mobility (10^{-5} cm^2/Vs)
ρ	Density (g/mL)
π	Pi
r	Radius (cm)

t	Time (minutes or seconds)
U	Potential or voltage (V)
V	Volume

CHAPTER I

INTRODUCTION

Background on Cardiovascular Disease

Cardiovascular disease (CVD) today remains one of the leading causes of mortality in the United States, Europe and much of Asia. In recent years and today, health providers encourage people to change their lifestyles and to take advantage of the many new pharmacological approaches to lower their plasma cholesterol.[1] Since 1993, death from CVD has decreased 22.1%. In the United States as of this year, CVD is now the second leading cause of mortality and cancer now reigns as the first. In the next two decades, our nation will observe a huge increase in the disease burden as the baby boomer generation ages. This is largely preventable. According to the Department of Health and Human Services (DHHS), we can reverse the epidemic of heart disease through preventative strategies through action now. The DHHS is now focusing more heavily on an action plan for the prevention of cardiovascular disease to address the goals of *Healthy People 2010* established in January 2000. The focus of my research is to develop an analytical strategy for the detection of an emerging risk factor for CVD to aid the field of cardiovascular research in the direction of prevention of CVD and promotion of cardiovascular health.

_____

This dissertation follows the style of the *Journal of the American Chemical Society.*

Atherosclerosis is the accumulation of lipids within the artery wall, which causes an injury or lesion. This injury can cause an extensive inflammatory response with an accumulation of platelets and a pro-coagulant response. This pro-coagulant response can continue unabated thickening the arterial wall, which can eventually impede the blood flow. The majority of people and health care providers believe that atherosclerosis is limited to this manifestation of the disease and focus on the treatment of this manifestation. Rather, the process of atherogenesis is more complex with many causes leading to the initiation of the inflammatory response. For example, the causes of the arterial lesions can be due to levels and modifications of certain lipoproteins in the blood, free radicals from cigarette smoking, hypertension, diabetes, genetics, and/or a combination of any of these factors.[1] Since many of these causes can be controlled and observed, it is important to identify the causes or risk factors and develop techniques for better detection and evaluation.

In recent years, studies on the physiology of lipoproteins translated into the clinical setting as preventative tools fairly effectively in the form of measuring LDL (low density lipoprotein) cholesterol and HDL (high density lipoprotein) cholesterol. These are indirect measurements of the LDL and HDL concentrations.[2-5] Total plasma triglycerides are also clinically evaluated as another preventative tool, but their relationship to CVD was highly debated until recently.[4, 6, 7] Lipoproteins play a central role in atherosclerosis and this relationship is well established. LDL are atherogenic and HDL are cardio-protective.[3-5]

The clinical dyslipidemias that result in cardiovascular disease are well defined

and very specific. In general, a combination of certain phenotypes can be described as the metabolic syndrome. The American Heart Association describes the metabolic syndrome as involving abdominal obesity, atherogenic dyslipidemia, in which there are high triglycerides, high LDL cholesterol and low HDL cholesterol, elevated blood pressure, insulin resistance or glucose intolerance, among other risk factors.[8]

Atherogenic dyslipidemia or more specifically the "Atherogenic Lipoprotein Phenotype" is most relevant to the research presented here. Triglycerides or triacylglycerols (TAG) are a storage form of fat consisting of glycerol and three fatty acids. Triglyceride-rich lipoproteins (TRL) are the carriers of TAG. The relationship of plasma triglycerides (TAG) and triglyceride-rich lipoproteins (TRL) with heart disease is not well understood. The TAG are not a part of arterial plaque themselves, but rather probably have a more indirect mechanism that initiates the inflammatory events that lead to atherosclerosis.[4]

The Atherogenic Lipoprotein Phenotype (ALP) is characterized by small dense LDL particles. This is also associated with high levels of plasma TAG and low levels of HDL cholesterol. The characteristics of ALP are a good marker for risk assessment of CVD and myocardial infarction. It is also indicative of a defect in TAG metabolism.[6] Today, this definition is expanded for a more specific diagnosis to include the densities of LDL and HDL in association with elevated plasma TAGs more so than just with LDL- and HDL-cholesterol. Smaller dense LDL particles are more atherogenic as well as smaller dense HDL when associated with high plasma TAG levels.[4] This relationship requires further exploration in assisting our understanding of the mechanisms driving

cardiovascular disease.

Definition of Lipoproteins

Lipoproteins are aggregates of lipid and surface proteins (apolipoproteins) with some structural organization. Lipoproteins can be classified according to their origin, function, composition or even method of isolation (i.e. density separation versus immunoseparation). The lipid component can include cholesteryl esters and triacylglycerols (TAG). These components are hydrophobic and cannot travel alone through blood, which is a hydrophilic environment. The lipid component of lipoproteins also includes an amphipathic phospholipid bilayer that surrounds the hydrophobic core. The bilayer also contains non-esterified cholesterol or free cholesterol and the apolipoproteins.[9] The following figure illustrates the basic composition of an apo B-100 containing lipoprotein particle (Figure 1).
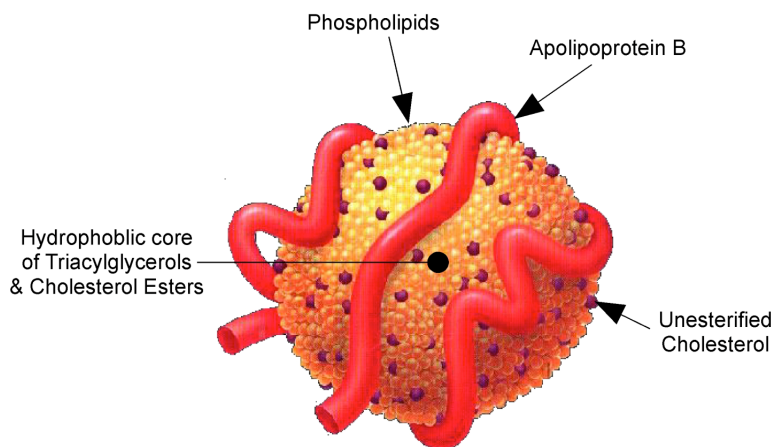
Figure 1. Basic composition of a lipoprotein (non-physiological structure)

Lipoprotein particles are classified mainly by their hydrated densities. It is important to keep in mind that this is an arbitrary classification system since the particles in reality exist more in a metabolic continuum and are constantly interchanging identities and roles.[10] This issue on arbitrary classification is addressed in the research presented here in the Results and Discussion. The lipoprotein classes defined by hydrated density vary in their sizes, lipid content, and apolipoprotein content as well. The following table details the variation of lipoprotein characteristics (**Table 1**).[5]

Table 1. Differential lipoprotein characteristics.

Lipoprotein Class	Density (g/mL)	Size (nm)	Major lipids	Major apolipoproteins
Chylomicron	<0.93	100-500	Dietary TAGs	B-48, C-II, E
VLDL	0.93-1.006	30-80	Endogenous TAGs	B-100, C-II, E
IDL	1.006-1.019	25-50	CEs and TAGs	B-100, E
LDL	1.019-1.063	18-28	CEs	B-100
HDL	1.063-1.210	5-15	CEs	A, C-II, E
Lp(a)	1.040-1.090	25-30	CEs	B-100 and glycoprotein

A convenient relationship between density and biological function exists in this classification system for lipoproteins. Generally, as density decreases, the ratio of TAGs to phospholipids and cholesterol decreases. This is why chylomicrons (CM) and VLDL are classified as triglyceride-rich lipoproteins (TRL). The main function of this class of lipoproteins is the transport of triglycerides. The following table provides the lipid and protein content of the TRL class in comparison to LDL and HDL, which are primarily cholesterol carriers (Table 2).[9]

Table 2. Compositional characteristics of the TRL class (CM or chylomicrons and VLDL) in comparison with LDL and HDL.

	CM	VLDL	LDL	HDL
Protein (% particle mass)	2	7	20	50
Triacylglycerols (% particle mass)	83	50	10	8
Cholesterol (% particle mass; free + esterified)	8	22	48	20
Phospholipids (% particle mass)	7	20	22	22

Significance of the Triglyceride-Rich Lipoprotein Problem

Triglyceride-rich lipoproteins (TRL) are the population of lipoproteins in human serum that are involved in the metabolism of dietary fats and contain most serum triglycerides as shown in Table 2.[11] TRL consist mainly of CM (chylomicrons) and VLDL (very low density lipoproteins). TRL remnants or RLP are particles derived from CM and VLDL and consist of CMR (chylomicron remnants) and rVLDL (VLDL remnants). This expands the TRL class to these four types of particles.[12]

The RLP portion of TRL (CMR and rVLDL) are considered the proatherogenic component of TRL.[12] RLP were listed as an emerging atherogenic risk factor by the Adult Treatment Panel of the American Heart Association in 2001.[8] In the literature, IDL (intermediate density lipoproteins) and RLP are traditionally described synonymously and interchangeably. IDL by definition have a density between VLDL and LDL. One of the most troubling aspects of analyzing "remnant-like lipoproteins" is in their elusive definition. For example, IDL are considered "density-isolated remnants" since they are separated based on their distinct density from VLDL and LDL.[13] The

following figure illustrates IDL in a density profile obtained in our laboratory by density

gradient ultracentrifugation in NaBiEDTA (Figure 2).
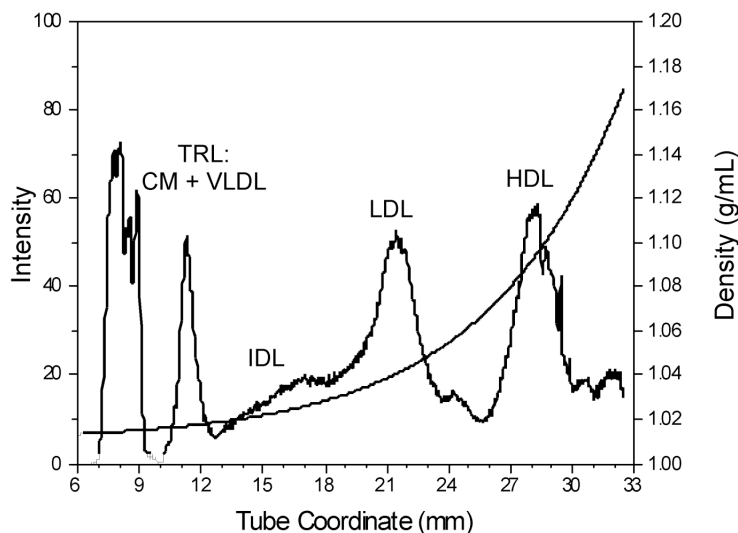
Figure 2. Density gradient ultracentrifugal separation of serum in NaBiEDTA showing IDL's distinct density.

RLP with certain apolipoprotein composition can be separated based on

immunoaffinity to certain antibodies and are therefore termed "immunoaffinity-

separated remnants." Overall, none of the methodologically-defined RLP complete our

understanding of a TRL remnant.[13] The definition of RLP separated based on

Nakajima's assay for differential immunoaffinity to anti-apo B-100 (JI-H) and anti-apo

A-1 is accepted in the research presented here. This assay is approved by the Food and

Drug Administration and its use predominates recent literature.[14-19] As described later in

the Results and Discussion, we prove that RLP, as defined by this assay[20] have distinct

densities from IDL.[21] Traditionally, this assay is used to measure RLP-cholesterol

specifically. In healthy patients, this RLP-cholesterol level ranges from 6.2 to 9.3 mg/dL.[7] RLP-cholesterol correlates to CVD when it is at a level of 12 mg/dL.[20]

Another significant feature of the TRL class is the fact that they are vehicles of TAG transport derived from both dietary and endogenous production. An elevated level of TAG is a risk factor for CVD in both males and females.[7, 22] Since the relationship between plasma TAG and atherosclerosis is not well understood,[4] it is pertinent to explore the metabolism of the TRL class as they are TAG carriers and are involved in TAG movement, distribution and clearance.

Functional and Structural Description of TRL

Chylomicrons (CM) are synthesized in the endoplasmic reticulum of intestinal absorptive cells. Their function is to transport dietary and biliary lipids from the intestine, through the lymphatic system, to the blood.[11] In contrast, VLDL particles are secreted from hepatocytes (liver cells) responsible for the transport of endogenous lipids from the liver to the blood.[12] RLP particles are formed by the metabolism of nascent CM and VLDL predominantly by the action of lipoprotein lipase (LpL) and to a lesser extent hepatic lipase (HL).[11] These enzymes remove triglycerides from the nascent particles.[23] The following figure is a simplified illustration of RLP content and formation from CM and VLDL by the action of LpL. (Figure 3)
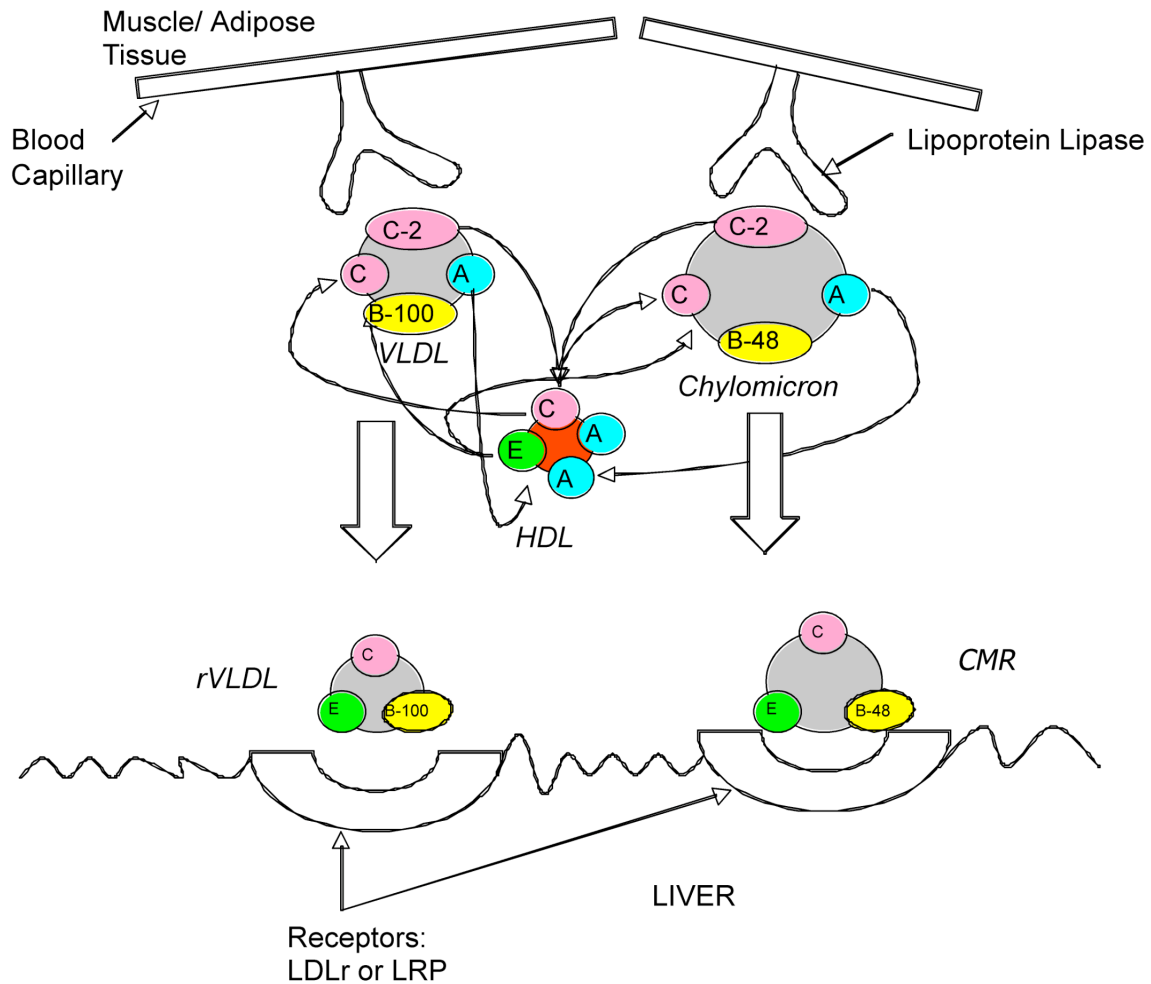
Figure 3. The metabolism and clearance of TRL particles from lipolysis to liver clearance.

As depicted in Figure 3, both CM and their remnants, CMR, contain a single apolipoprotein B-48 (apo B-48), the truncated version of full-length apo B-100. Apo B-48 is truncated at residue 2152 of the full length apo B-100.[11, 12, 24] Chylomicrons and their remnants contain triglycerides, cholesteryl esters, and some unesterified cholesterol surrounded by a monolayer of phospholipids and free cholesterol. In addition to apo B-48, these particles can have apo A-1 and apo A-4 along with apolipoproteins that are

acquired after secretion. Thus, apo E, apo C-1, apo C-2 and apo C-3 are transferred from HDL in circulation.[11, 12] VLDL remnants (rVLDL) contain a single molecule of apo B-100, apo A-1, A-2 and A-4, the three C apolipoproteins, and apo E. The apo B-100 of VLDL is full length with 4536 amino acids.[12] After VLDL is secreted, additional apo E and the C apolipoproteins are acquired from HDL.[11, 12]

The Metabolism of Triglyceride-Rich Lipoproteins

The TRL class has a varied formation and clearance pathway. The metabolism of TRL has a specific temporal sequence and can be divided into *forward cholesterol transport* and *reverse cholesterol transport.*[5] The entire process from chylomicron formation to LDL is known as *forward cholesterol transport.*[5]

Chylomicrons (CM) form in the small intestine one hour after a meal and are responsible for carrying dietary lipids. CM differ from VLDL, LDL and HDL, which are part of the endogenous pathway, in that they are part of the exogenous pathway metabolizing dietary fats.[25] As they travel through the body, they deliver their TAG content to muscle and adipose tissue through interaction with lipoprotein lipase (LpL). As a result of lipolysis, they become smaller and exchange apolipoproteins with HDL transforming into CMR (chylomicron remnants). Following uptake by liver receptors, the CMR release their content. Newly available CMR lipids can then be reassembled into a VLDL particle.[5] (Figure 3)

VLDL formation does not occur concurrently with CM formation as these particles are generated from CMR contents in the liver hours after a meal. VLDL carries

endogenous lipids and excess lipids absorbed by the liver from CM clearance and destruction. Like CM, these triglyceride-rich VLDL traverse the bloodstream to muscle and adipose tissue where they also deliver their TAG content through an interaction with LpL. As lipolysis proceeds, the VLDL become smaller and exchange apolipoproteins with HDL. The VLDL particle then becomes a rVLDL (VLDL remnant).[5] A general schematic of this process is depicted in Figure 3.

If the rVLDL particle loses more of its apolipoproteins and decreases more so in its size, it can then be classified as an IDL particle. The IDL particle is catabolized by hepatic lipase resulting in an LDL particle, which contains only apo B-100 on its surface. Two-thirds of LDL are derived from VLDL by this pathway.[5] Here is where the density based classification system is most obscure. The process of VLDL converting to LDL is VLDL → rVLDL → IDL → LDL; yet, rVLDL and IDL are often described synonymously. This is understandable considering that the process is a metabolic continuum, and until recently it was difficult to analyze and differentiate these metabolic intermediates.[21, 26]

Reverse cholesterol transport involves the interaction of TRL particles with HDL. HDL accepts unesterified cholesterol from TRL through lecithin-cholesterol acyltransferase (LCAT) by an apo A-1 interaction. While CM are hydrolyzed for their TAG content by LpL, all of the apo A-1, apo A-4, and eventually apo C-2 are also transferred to HDL.[11-13, 27]

Remnant lipoproteins bind to LpL, present on the surface of blood capillaries in muscle and adipose tissue, through apo C-2. The loss of Apo C-2 during *reverse*

cholesterol transport terminates the interaction with LpL and therefore lipolysis.[11-13, 27]

Basically, the TAG content is hydrolyzed, releasing diacylglycerol (DAG), 2-

monoacylglycerol (2-MAG), glycerol, and fatty acids into the capillary lumen. The

nascent TRL particles (CM and VLDL) are as a result transformed into remnants (CMR

and rVLDL). [11, 23, 25] The following figure is a simple depiction of the specific hydrolysis

reaction LpL catalyzes. (Figure 4)
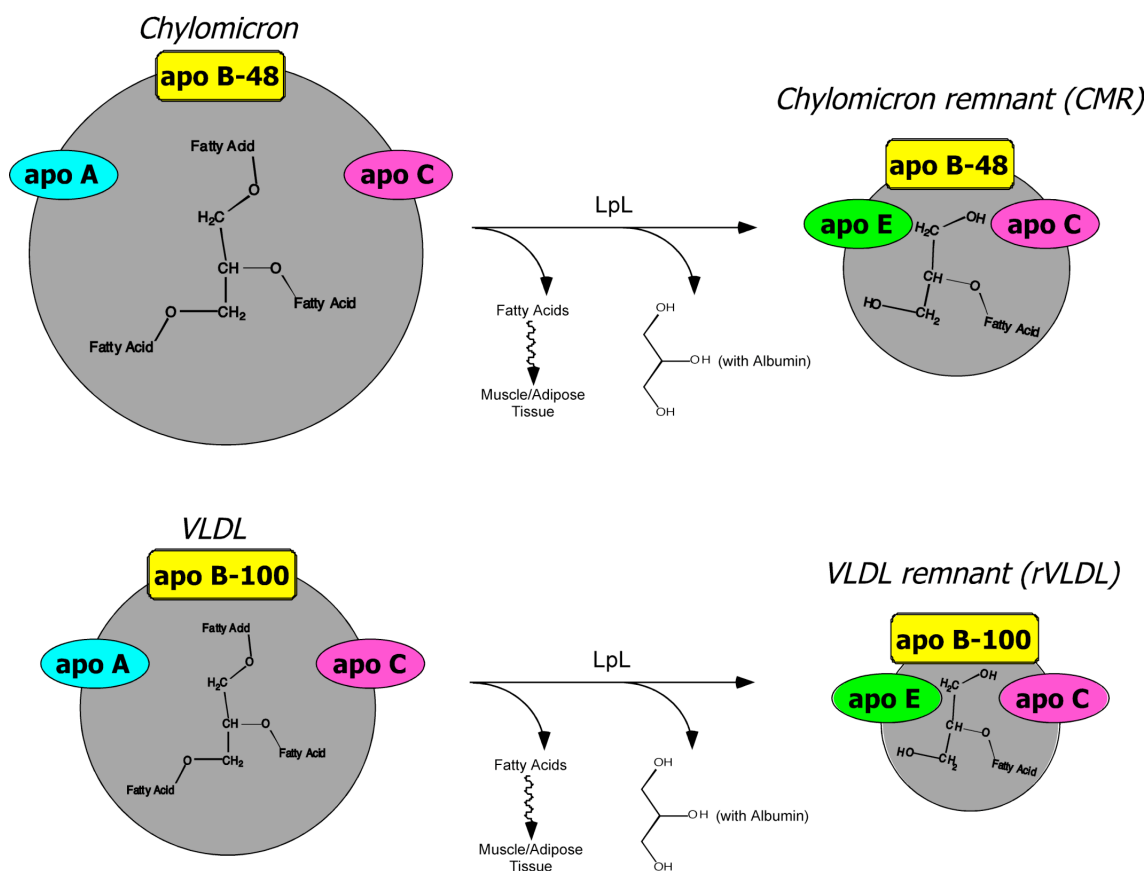
Figure 4. Triglyceride-rich lipoprotein TAG hydrolysis by lipoprotein lipase.

TRL, in general, are removed by the liver effectively in normolipidemic (healthy) subjects. After the loss of apo C-2, lipolysis is terminated and the RLP particle is transported to the liver. In the liver, hepatic lipase (HL) and lipoprotein receptors such as the LDL receptor (LDLr) and LDL receptor-related protein (LRP) capture the remnants for catabolism.[11-13, 27] Apo E remains on the remnant and is required for recognition by the LDLr and LRP.[11]

Apo B-100 on rVLDL interacts with the LDLr somewhere in the carboxyl terminal portion between amino acids 2800 and 4000, and it is possible that several domains of the protein are required for the proper conformation for interaction with the receptor.[24, 28] Some studies show that rVLDL interacts with the LDLr through apo E and not apo B-100. These studies also show that triglyceride enrichment of rVLDL decreases its affinity to LDLr. The affinity of apo B-100 to the LDLr in the liver is also dependent on the apo C-3 content of the lipoprotein particle.[28]

Isoforms of certain apolipoproteins can enhance or inhibit the clearance of RLP through the receptors in the liver. There are three common isoforms of apo E: apo E-2, apo E-3, and apo E-4. Apo E-2 has reduced affinity to the LDLr.[12, 29] This reduced affinity can be explained either by a specific amino acid substitution in this variant or a conformational change.[29, 30] Literature suggests the possibility of the interaction of several molecules of apo E with multiple LDL receptors. Multivalent binding could produce high affinity between remnants and their receptors.[24] Lipid association can also change the conformation of the binding domain of apo E, enhancing its interaction with the LDLr.[31]

Some studies suggest that certain C apolipoproteins inhibit apo E binding to receptors.[12, 24] This inhibition could be caused by displacement of apo E by high apo C concentration. Apo C-3 is known to particularly inhibit LpL. Both apo C-3 and apo C-2 correlate to increased cholesterol levels with delayed remnant clearance.[12] In addition, if VLDL particles have significant apo C content, then they are not recognized by the LDLr either through apo E or apo B-100.[24] Apo C-3 decreases the affinity of apo B-100 lipoprotein particles without triglyceride enrichment for the LDLr, whereas apo E increases the affinity. In TRL, apo C-2 and apo C-3 preclude interaction with the LDLr, and apo E enrichment can increase internalization of VLDL particles. The greater the apo C-3 content of TRL, the lower the affinity for LDLr.[28] In addition, apo C-1 content may also be positively correlated with the formation of atherosclerotic lesions.[32]

Chylomicron remnant (CMR) metabolism is slow and clearance can be saturated after a fat-containing meal. Hydrolysis of rVLDL is even slower than CMR. Larger rVLDL are taken up by the liver more rapidly than smaller rVLDL since they are more likely to interact with the LDL receptor.[11] Figure 3 illustrates the clearance of RLP as described here. TRL metabolism from formation to clearance is complex and intertwined with secondary factors such as dietary lipids and interaction with HDL. Understanding the complex processes involved in TRL metabolism is essential to understanding the relationship between diet and cardiovascular disease as well as TRL features and cardiovascular disease.

Atherogenicity of TRL

Recent evidence indicates that remnant lipoproteins (RLP) are the atherogenic component of TRL.[11, 12] TRL remnants produce fatty streaks and atherosclerotic lesions.[12] Remnant lipoproteins are atherogenic because they can penetrate arterial tissue and become trapped in the subendothelial space.[33] Remnant lipoproteins are a heterogeneous mixture of particles, and atherogenicity of the different particles may vary.[34] Atherosclerosis is manifested by cholesterol-loaded macrophages otherwise known as foam cells. Apo E plays an integral role in the uptake of VLDL by macrophages. If RLP do not clear through the liver and persist in circulation, they become susceptible to oxidation. Oxidized VLDL and rVLDL greatly stimulate cholesteryl ester loading in cultured macrophages.[35]

Type III hyperlipoproteinemia (THL) is the prototypic disorder of remnant metabolism.[33] THL patients tend to have higher concentrations of apo B-100, apo B-48, apo E, apo C-3, and plasma triglyceride concentration.[12] CMR and rVLDL play different roles in the expression of THL due to their distinct interactions with LpL.[36] THL is characterized by the apo E-2/2 genotype.[35, 37] Lower LDL levels are seen in apo E-2/2 individuals because there is less competition for the LDL receptor between the remnants and LDL.[12] The rVLDL are exposed to LpL more due to their longer residence time in plasma. This results in a more triglyceride-depleted and cholesterol enriched rVLDL particle. Cholesteryl ester enrichment makes these particles more atherogenic in terms of the role they play in plaque formation.[5]

Insulin resistance is known to increase the secretion of VLDL apo B-100 and cholesterol. It also decreases the activity of LDL receptors. [37] Insulin resistance leads to increased plasma RLP, and apo B-100 increases competition for hepatic receptors between CMR and rVLDL.[37] Atherosclerosis is the main cause of death in patients with type 2 diabetes/ diabetes mellitus.[18, 38] In diabetic patients, RLPs cause foam cell formation more easily.[39] Differential expression (THL and/or diabetes mellitus) in atherosclerosis caused by RLPs is due to the different metabolic properties of this heterogeneous population of lipoproteins.

In the postprandial state (following a meal), CM concentration is most elevated around three hours after meal. [12] In the postabsorbtive or fasting state, the few CM that are in circulation derive mainly from the absorption of lipids of the intestinal epithelium. When there is no LpL deficiency, CM are hydrolyzed rapidly resulting in CMR.[12] CMR have longer plasma residence time in patients with documented coronary artery disease, and delayed CMR removal is associated with patients with hypertriglyceridemia, low HDL concentration, and small dense LDL.[25]

Atherogenicity of Triglycerides (TAG)

The metabolism of exogenous particles (TAG carried in CM) is very rapid, and the slow rate of this clearance may be a risk factor for atherosclerosis.[25] Hypertriglyceridemia, elevated TAG levels, comes mainly in three forms of dyslipidemias, which are all associated with cardiovascular disease. Type I dyslipidemia is the most rare form. Increased TAG in the form of chylomicrons characterizes this disorder, and it is caused by impaired LpL activity.[5] Lipoprotein lipase impairment can be caused by either an LpL deficiency or deficiency of the LpL activator, apo C-2. This impairment results in extremely high levels of plasma TAG with "milky" or lipemic plasma. In normal subjects, LpL activity increases 3-6 hours after a high carbohydrate meal. However, even in normal subjects, the removal of TAG content from TRL particles by LpL is a kinetically saturable process. [40]

Type IV dyslipidemia is characterized by increased VLDL production due to an increase in TAG synthesis and normal cholesterol levels. This dyslipidemia is fairly common among patients suffering from cardiovascular disease. This disorder is genetic and is so referred to as *familial hypertriglyceridemia.* Type V dyslipidemia also involves increased TAG synthesis in addition to clearance impairment but is uncommon in comparison to Type IV dyslipidemia.[5] Type III dyslipidemia is more rare than all three types of dyslipidemias described above and is the prototypical disorder of RLP metabolism.[5]

Again, plasma TAG and TRL possess an indirect role in the development of atherosclerosis but directly correlate to many dyslipidemias involved in the onset of cardiovascular disease.[4] Comprehensive analytical methods involving the compositional analysis of TRL and their content are desirable for clinical applications to improve diagnostic capabilities.

Present Methods of Analysis

Density Gradient Ultracentrifugation

Density gradient ultracentrifugation is a standard method for the identification and separation of lipoproteins by density. The low density of lipoproteins allow for separation from denser proteins in serum by sequential flotation.[41, 42] The flotation rates of the different lipoprotein fractions decrease as the particle density increases. For example, chylomicrons are the least dense class of lipoproteins (>0.94 kg/L) and have a flotation rate greater than 400 S_f; whereas, HDL (high density lipoprotein) have a hydrated density between 1.063-1.21 kg/L and have a flotation rate between 0 and 9 S_f.[42]

The two main methods of ultracentrifugal separation of lipoproteins are rate zonal ultracentrifugation and isopycnic ultracentrifugation.[42] In both methods, salts such as NaCl, NaBr, and KBr are employed to float or sediment particles.[42, 43] Sucrose is also often used as a medium in ultracentrifugal separations.[44] The sedimentation and flotation rates are proportional to the applied centrifugal force, viscosity of the solution,

molecular weight of the particle, and the difference between the density of the particle and the density of the solution of choice.[42]

Rate zonal ultracentrifugation allows for a sequential flotation and separation of lipoprotein particles by adjustment of the solution density. The particles either float or sediment through a density gradient based on their densities. The sample is layered over or under the solution of different density.[42] In isopycnic ultracentrifugation, the particles move to zones where the gradient solution equals the particle's density. This method is often preferable to rate zonal ultracentrifugation in that it achieves more quantitative separation.[45] Often, density separations employ characteristics of both techniques and cannot be classified.[42] Either self-generating or pre-generated density gradients are used in centrifugal separations. Self-generating gradients are easy to produce and information regarding the resulting gradient is also easy to assess.[44]

Lipoproteins are traditionally separated by sequential flotation. This method can require days. Basically, a less dense solution is layered over serum, and buoyant lipoproteins float to the top after ultracentrifugation. The top fraction is then removed. The process is repeated with a slightly more dense solution each time, centrifuged, and recovered by aspiration.[41, 46] In recent years, single spin separations were reported involving sucrose, CsBiEDTA, and other metal ion complexes of EDTA. These procedures involve shorter centrifugation times and simplify sample preparations. [44, 47-49]

TRL are traditionally analyzed by ultracentrifugation.[34, 50] Ultracentrifugation allows for the separation of IDL in between the densities of VLDL and LDL ($1.006 < d < 1.019$ g/mL). IDL cholesterol is most often used as an index of RLP

concentration. There is no standardized procedure for this measurement. As aforementioned, IDL isolated in this manner does not include the less catabolized and more triglyceride-rich RLPs.[26] In the past, ultracentrifugation was deemed "tedious and time-consuming." The fractions isolated in this manner are heterogeneous and cross-contamination between fractions is common as well.[43] Most of the TRL class cannot achieve equilibrium in salt solutions since they have densities lower than water.[48]

Following a density gradient separation, particles can be visualized in many ways. Lipophilic stains such as Fat Red[51] and Sudan Black B[52] can stain the serum sample prior to the separation. Recently, a fluorescent probe, NBD C_6-ceramide (Figure 5), has been used in concert with density gradient ultracentrifugation to visualize lipoproteins. Lipoproteins can be visualized with low concentrations of this probe.[21, 48, 49] Also, a strong correlation between NBD C_6-ceramide with LDL and HDL cholesterol concentrations has previously been observed.[53]
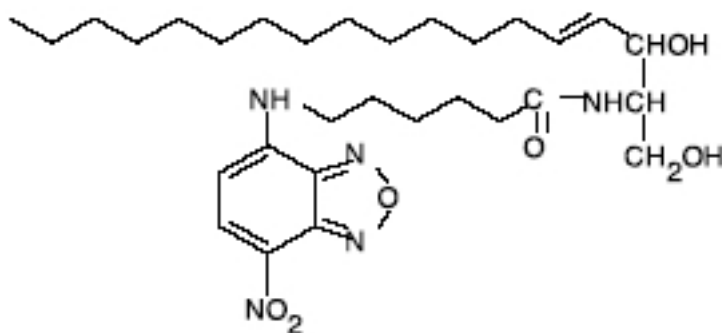
Figure 5. Structure of NBD C6-ceramide.

NBD C_6-ceramide is lipoprotein specific in serum, but can alter the electrophoretic mobility of LDL and HDL.[54] This indicates that it can affect the physical properties of serum lipoproteins. However, fluorescence staining has inherent advantages in terms of sensitivity and selectivity.[55] Fluorescence staining in conjunction with density-gradient ultracentrifugation has been effectively established as the method of choice for lipoprotein fingerprinting by density profiling.[21, 44, 49, 56]

Recovery of the lipoprotein fractions allows for further analyses. If the particles can be visualized following an ultracentrifugal separation, the fractions can be removed by aspiration by placing the pipette below the surface of the liquid. In addition, tube slicing techniques may be employed to recover the fractions. Tube slicers are commercially available as well as fraction collectors that cause displacement of fractions upward by a heavy liquid introduced at the bottom of the tube.[42] In addition, in our laboratory, we developed a novel freeze/cut method involving slow freezing of a tube in liquid nitrogen followed by slicing with a reciprocating saw.[21]

Immunoaffinity Separations

Immunoaffinity analyses involve a protein and antibody reaction that allows selective detection or separation. Nakajima's immunoseparation assay, which is commercially available through Polymedco Inc., is the most recent technological development in RLP measurement.

In this assay, a monoclonal antibody to apo B-100 that recognizes VLDL but not rVLDL and a monoclonal antibody to apo A-1, which recognizes HDL and nascent chylomicrons, is employed to separate the RLP from all other serum lipoproteins.[19, 34] The antibody does not recognize apo B-48 since it reacts with an epitope beyond the C-terminus. The antibody can react with practically all LDL particles and most VLDL particles through apo B-100 except those that are enriched in cholesterol and apo E.[12, 16, 34]

The hypothesis as to why the anti-apo B-100 does not bind to apo B-100 on rVLDL is that there is a homologous region of interaction between apo B and apo E where the antibody cannot bind.[19] The assay removes all HDL, chylomicrons, LDL and VLDL.[38] Incubation of the assay takes place in a mixer with built-in magnetic bars that drive steel beads up and down in each cup. After incubation, the supernatant (RLP, unbound fraction) is transferred for cholesterol analysis in a chemistry analyzer (Cobas MIRA S). Only CMR and rVLDL remain in the unbound fraction. This immunoseparation assay is used to determine RLP-cholesterol as a measurement of cholesterol in the unbound fraction.[38] The following figure illustrates a general schematic of the immunoseparation assay. (Figure 6)

RLP — △ RLP   ● LDL + nascent VLDL   ○ HDL   ⊕ Sepharose 4B + anti-apo B-100   ⊕ Sepharose 4B + anti-apo A-1
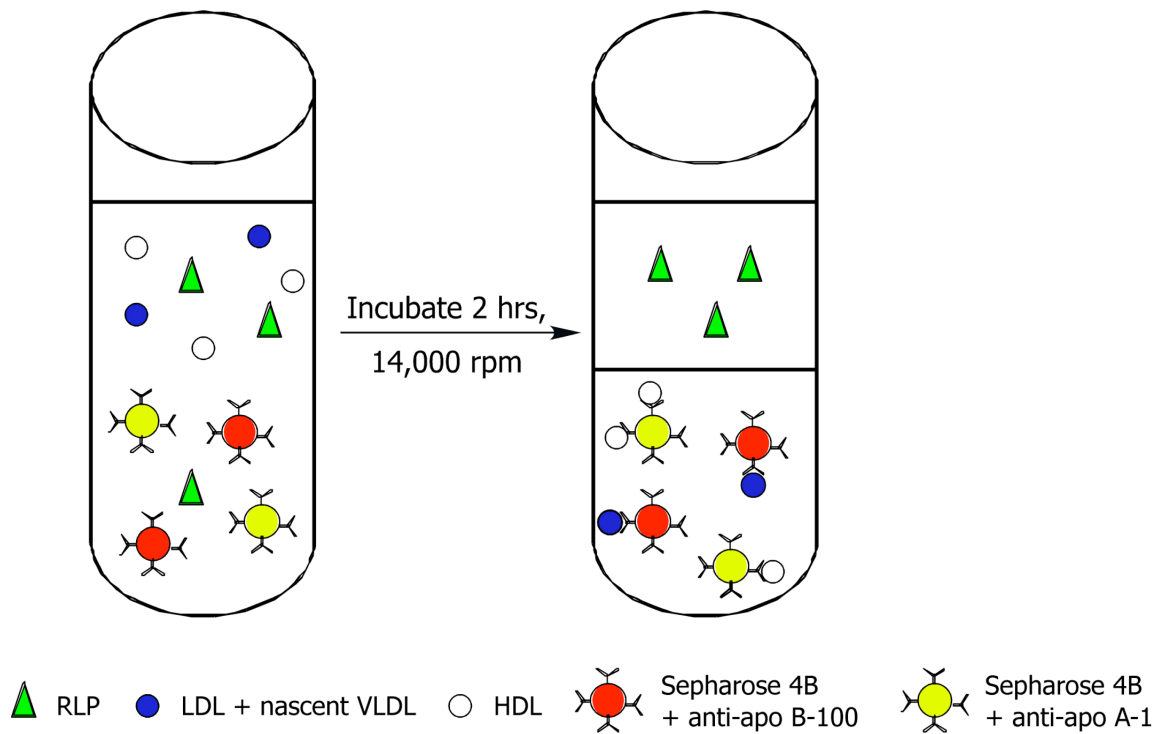
Figure 6. A general schematic of the RLP immunoseparation assay.

The Polymedco assay is approved by the Food and Drug Administration for the diagnosis of type III dyslipidemia when RLP-cholesterol: total serum TAG ratio is > 0.23. This assay is a valid measure of proatherogenic RLPs, but a more standardized and cost-effective analysis for clinical use to predict cardiovascular events independently is desired.[16, 34]

Other immunoaffinity assays are also employed in the analysis of apolipoprotein content in TRL. Site-differential enzyme-linked immunosorbent assays (ELISAs) measure apo B-100, apo E, and apo B-48.[26, 50] Sequential immunoaffinity chromatography or immunoprecipitation also measures lipoproteins with apo B, apo E, and apo C content.[26]

Cholesterol and Triglyceride Analyses

Many analytical techniques for the measurement of cholesterol and triglyceride content of lipoproteins exist. Currently, the CDC (Center for Disease Control) approved measurement of total cholesterol comes from the work of Sperry and Brand. This is a colorimetric assay based on the hydrolysis of cholesterol esters and the reaction of purified cholesterol with a color-producing reagent.[57]

Routine laboratory measurement of cholesterol is based on enzymatic methods and has largely replaced the chemical approach of Sperry and Brand. These methods are more specific and can be automated. Generally these methods involve the hydrolysis of cholesterol esters by cholesterol esterase, an enzyme, to release cholesterol and fatty acids. The cholesterol is then oxidized by cholesterol oxidase to produce hydrogen peroxide (H_2O_2) as a side product. Measurement of H_2O_2 is the most common method to quantitate cholesterol. The H_2O_2 molecule reacts with two chromogenic substrates by peroxidase to produce a quinonimine dye that can then be measured at 500 nm. [58]

Likewise, most clinical laboratories utilize enzymatic methods to analyze triglyceride (TAG) concentration. This measurement involves hydrolysis of triglycerides into glycerol and fatty acids by lipase. Glycerol is then phosphorylated by a kinase to produce glycerol-1-phosphate. This molecule is then oxidized to produce H_2O_2, and as in the case of the enzymatic cholesterol assay, H_2O_2 is reacted with two chromogenic substances to produce quinoneimine dye that can then be visually detected by

spectrometry.[59] The following figure details the reactions necessary for the measurement of triglycerides in this manner. (Figure 7)
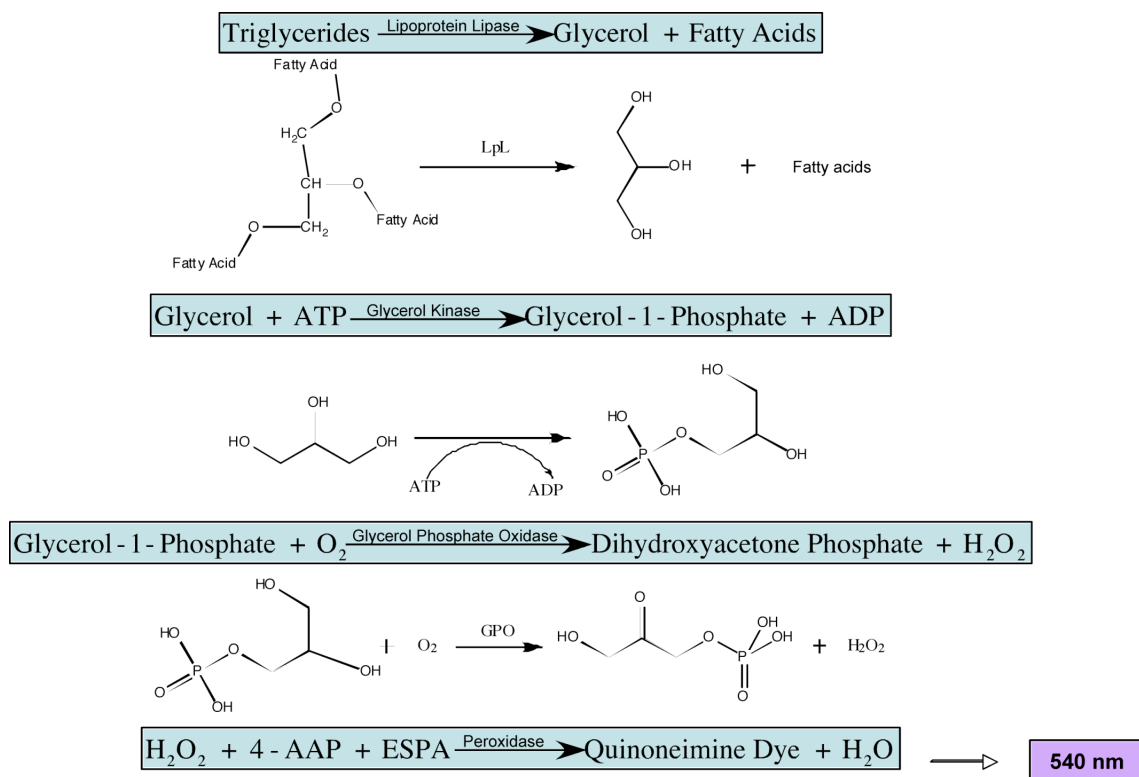
Figure 7. True triglyceride enzymatic assay (Sigma Aldrich).

An important interference in this assay to consider is that TAG concentration is measured from the glycerol. If there is glycerol present in the sample, it can cause an overestimation of the TAG concentration. Therefore, it is common to take two measurements, one with all the reactions above and one with all the reactions except the first lipolysis step. This allows for a measurement of the free glycerol, which can then be subtracted from the total value to provide a "true triglyceride" measurement.[59] However,

most clinical laboratories do not actually make this glycerol measurement since high concentrations of glycerol are not common in most subjects.[60] Micro-enzymatic determinations of cholesterol and triglycerides can be performed in conjunction with lipoprotein separation by density gradient ultracentrifugation with a good detection limit and sensitivity to measure cholesterol and TAG level in lipoprotein subclasses.[61]

In the past, remnant lipoprotein cholesterol was measured as a ratio between VLDL cholesterol and VLDL triglyceride concentration in patients with the apo E-2 phenotype. This ratio was compared to the VLDL cholesterol: VLDL triglyceride concentration in patients of the normal apo E phenotype, apo E-3/3, and the excess in cholesterol was defined as the RLP-cholesterol. It was found that the combination of RLP-cholesterol calculated in this way along with IDL-cholesterol related to the progression of cardiovascular disease.[12]

With RLP-cholesterol, as isolated by the Polymedco assay, a detection limit of 0.12 mg/dL is needed since the samples are diluted 61-fold. The traditional oxidase-peroxidase assays do not have a sufficient detection limit to accurately analyze dilute samples. An enzymatic cycling method was developed using cholesterol dehydrogenase (CD) that can detect $0.10 * 10^{-3}$ mmol/L. In this method, cholesterol ester hydrolase hydrolyzes esterified cholesterol to free cholesterol and fatty acids. The cholesterol is then reversibly oxidized in the presence thio-NAD and thio-NADH. The thio-NADH is measured by change in absorbance per minute at 404 and 500 nm to measure the cholesterol concentration. This CD enzymatic cycling method is more sensitive and creates a more linear calibration curve that passes through the origin. RLP-cholesterol >

0.194 mmol/L is a cardiovascular risk factor, and when it is diluted 61-fold with the immunoaffinity gel solution the concentration of the supernatant is <0.003 mmol/L.[62] RLP-triglycerides are measured by CDC-standardized enzymatic methods.[63] In addition, cholesteryl esters, TAG, free cholesterol, MAG (monoacylglycerols) and phospholipids can be detected simultaneously by high performance liquid chromatography. These measurements are highly accurate for the TRL subclasses, but lipids classes that are in lower concentrations such as MAGs and free fatty acids are difficult to detect.[64]

Electrophoresis

Electrophoresis is a separation technique for analytes that are charged in a buffer solution where an electric field is applied. Two formats of electrophoretic separations exist: slab electrophoresis and capillary electrophoresis. Generally, slab electrophoresis is described as a form of gel electrophoresis. Such methods are routinely used in the field of biochemistry and date back to 1930s. Capillary electrophoresis is an instrumental version of electrophoresis and has been extensively used in the last twenty years.[65] Many electrophoresis techniques are used to detect the different forms of TRL and their apolipoprotein composition.

Agarose gel electrophoresis separates RLPs based on their charge. Also, RLPs can be separated according to size by polyacrylamide gel electrophoresis (PAGE). Both of these techniques are useful for detection but not accurate quantification.[26] Isoelectric focusing gel electrophoresis determines the genotypes of apolipoproteins. For example,

in type III dyslipidemia, patients are homozygous for the apo E-2 isoform. These isoforms can be detected by isoelectric focusing gel electrophoresis.[35]

Various truncated forms of apo B-100 have been detected by gel electrophoresis including apo B-74 (410,000 Da) and apo B-26 (145,000 Da). Further fragmentation of apo B-74 yields apo B-44 (240,000 Da), and apo B-30 (170,000 Da). These are all derived from apo B-100 by proteolytic fragmentation by serum enzymes.[66] Apo B-48 is not derived from apo B-100 as described previously. It is difficult to quantify apoB-48 by gel staining since it is small in mass compared to apo B-100. Capillary electrophoresis and specific antibodies can better quantify apo B-48.[15, 33]

Capillary electrophoresis is a fast technique that uses small amounts of sample and reagents. It separates analytes of different sizes and charges. Now, automated instrumentation makes this technique available for routine use in clinical laboratories. Capillary zone electrophoresis (CZE) is the simplest form of capillary electrophoresis since it involves a low viscosity buffer in which the analytes migrate from one end to another based on their electrophoretic mobility (proportional to a charge to mass ratio).[67] Today, capillary electrophoresis technology is being marketed to non-specialists and even replacing 1D SDS-PAGE (sodium dodecyl sulfate polyacrylamide gel electrophoresis) that is routinely used in biochemistry laboratories.[68]

Capillary electrophoresis has much potential in the analysis of lipoproteins in that it can help our understanding of metabolic lipoprotein heterogeneity.[69] Most separation methods such as ultracentrifugal, immunological, and chromatographic techniques, produce a heterogeneous separation and often do not agree with each other.[53, 69]

Capillary isotachophoresis in conjunction with NBD C_6-ceramide staining can separate the lipoprotein classes directly from serum or plasma. It is the only technique that can quantify CM and IDL currently.[53] In capillary isotachophoresis, a discontinous electrolyte system is used to produce "zones" that migrate in order of decreasing mobility until a steady state of stacked zones exists. This separation technique distinguishes IDL, VLDL, and LDL.[67, 69] This technique may become the standard in monitoring disorders of lipoprotein metabolism.[67]

In addition to analysis of intact lipoproteins, capillary electrophoresis is used to analyze apolipoprotein (surface proteins) of the lipoprotein particles as well. The lipoprotein particles are delipidated by different techniques prior to the electrophoretic separation.[70, 71] By adding a detergent to the separation buffer, the apolipoproteins can be separated effectively through inhibition of protein-protein interactions.[70] In this manner, the apolipoproteins of HDL and LDL have been characterized by capillary zone electrophoresis.[71, 72]

Determination of LpL and Apo C-2 Deficiencies

RLP are formed from their nascent TRL counterparts by the action of LpL via interaction with RLP surface constituent apo C-2. Both LpL and apo C-2 play intregral roles in the metabolism of TRL to RLP. LpL deficiency evidences extreme hypertriglyceridemia caused by an accumulation of CM and VLDL in plasma.[73] Famililial LpL deficiency is diagnosed clinically by a specific assay of LpL activity in plasma following an intravenous injection of heparin. Heparin releases the LpL from the

endothelial cells into circulation. This is an invasive procedure and causes a depletion of LpL in the patient following the injection. Apo C-2 deficiency is traditionally diagnosed by titration of plasma with normal apo C-2 in the presence of bovine milk LPL. In addition, 2-D gel analysis can verify deficiency of apo C-2.[40]

The capillary isotachophoresis technique described previously is also used to determine LpL activity indirectly by a "precursor/product" concept. The ratio of RLP to the nascent TRL particles is used to determine whether LpL has effective enzymatic activity.[53]

Triglyceride-rich lipoproteins are a heterogeneous class of particles with unique and complex metabolic and compositional features. Some of these features may relate to the various correlations with cardiovascular disease presented here. It is paramount to develop new analytical strategies to understand the complex features of this lipoprotein class to further our understanding of their relation to heart disease. Development of new analytical techniques for this class will potentially assist the scientific and clinical community in the prevention of cardiovascular disease and promotion of cardiovascular health.

CHAPTER II

MATERIALS AND METHODS

Materials

The RLP immunoseparation gel containing antibodies to apo B-100 and apo A-1 on sepharose beads and RLP buffer (5 mM tris-HCl) was purchased from Polymedco, Inc. (Cortlandt Manor, NY). NBD C_6-ceramide was purchased from Molecular Probes (Eugene, OR). An aqueous solution of CsBiEDTA was synthesized as described previously.[48] The $Na_2CdEDTA$ was synthesized as described previously as well.[49] NaBiEDTA ($C_{10}H_{12}N_2O_8NaBi\cdot4H_2O$) was purchased from TCI America (Portland, Oregon). Sucrose ($C_{12}H_{22}O_{11}$) was purchased from EM Science (Darmstadt, Germany).

Tris-Acetate SDS-PAGE mini-gels 3-8% NuPAGE®, Novex® Tris-Acetate SDS Running Buffer (20X), and NuPAGE® LDS Sample Buffer (4X) were purchased from Invitrogen (Carlsbad, CA). The phosphorylase b, cross linked molecular weight markers (catalog number 9012-69-5), 2-mercaptoethanol, and an apo B-100 standard were purchased from Sigma-Aldrich (St. Louis, MO). Western blot analysis was performed in conjunction with the SDS-PAGE analysis with a WesternBreeze® Immunodetection Kit from Invitrogen (Carlsbad, CA). A polyclonal apolipoprotein B antibody (Catalog number AB742) from Chemicon International (Temecula, CA) was employed in this immunodetection.

Cholesterol analysis was performed with Infinity^{TM} cholesterol reagent, Lipid Control Levels 1 and 2, and cholesterol standard purchased from Thermo Electron Corporation (Waltham, MA). The triglyceride measurements were performed from the following reagents purchased from Sigma-Aldrich (St. Louis, MO): triglyceride reagent (catalog number T2449), free glycerol reagent (catalog number F6428), and glycerol standard (catalog number G7793). Lipoprotein lipase (catalog number L2254) was also purchased from Sigma-Aldrich (St. Louis, MO).

Solutions for the background electrolyte in capillary zone electrophoresis were made from sodium borate ($Na_2B_4O_7 \bullet 10H_2O$) from Fisher Scientific (Hampton, NH) and a mixture of 70% sodium dodecyl sulfate or lauryl sulfate ($C_{12}H_{25}O_4SNa$) with 25% myristyl sulfate content ($C_{14}H_{30}0_4SNa$) and 5% cetyl sulfate ($C_{16}H_{33}O_4SNa$) from Sigma-Aldrich (St. Louis, MO). Human serum albumin (catalog number A-1653, Sigma-Aldrich, St. Louis, MO) standard and cholesterol standard from the cholesterol assay above were utilized as standards for the capillary zone electrophoresis analyses.

Method 1. Remnant Lipoprotein Density Profiling

Subject Selection

Serum samples were selected from our serum library on the basis of the following features as determined by lipoprotein density profiling: elevated VLDL and IDL levels. Subjects without these features were deemed normolipidemic or "healthy" subjects. Our serum library consists of donated serum from patients at Scott & White Hospital, Temple, TX as well as anonymous donors from our laboratory and community. Serum samples were collected from donors in Vacutainer-brand serum collection tubes (Beckton Dickinson Systems, Franklin Lakes, NJ). Serum was stored at -86ºC until needed.

Immunoseparation Assay

This immunoseparation assay isolates RLP from other serum lipoprotein based on antibodies to apo A-1 and apo B-100. The RLP immunoseparation gel was prepared according to instructions provided by Polymedco, Inc. with some modifications. The RLP immunoseparation gel was mixed manually by inversion of the container until it was completely suspended. The total volume of the assay was altered to 900 µL, and the assay was performed in 1.5 mL Eppendorf tubes. A 900 µL aliquot of the suspended RLP immunoseparation gel was transferred to the Eppendorf tubes for each sample. The gel was then centrifuged for 5 minutes at 800 rpm at 4ºC. Following the centrifugation, 680 µL of the supernatant was discarded and replaced with 680 µL of the RLP buffer

(0.05 M tris-HCl). The gel was mixed with this buffer prior to re-centrifugation. The centrifugation was repeated three times, and for the third time, only 620 µL of the RLP buffer was added. For each assay, 60 µL of serum and 4 µL of a 1 mg/mL NBD C_6-ceramide in DMSO were added to the RLP gel and RLP buffer prior to incubation. The tubes were then placed on an M-60 orbital mixer (Labnet International, Inc.) and incubated at 1400 rpm for 2 hours. After mixing, the gel was allowed to settle for 15 minutes. Following the incubation, the RLP was recovered by removal of 660 µL of the supernatant by pipette. This supernatant contained the RLP and serum proteins that did not react to the antibodies present in the immunoseparation gel.

Ultrafiltration

Ultrafiltration was performed in order to remove the tris-HCl buffer and concentrate the RLP for further analysis by density gradient ultracentrifugation. Ultrafiltration of the recovered RLP was performed in a 100,000 nominal molecular weight cutoff centrifugal filter (Millipore) mounted in a 1.5 mL Eppendorf tube according to manufacturer's instructions. Briefly, the filter was inserted into an Eppendorf tube after which 330 µL of the RLP supernatant was added to the sample reservoir without touching the membrane. The cap on the tube was then sealed over the filter inside the tube. The sample was spun at 14,000 rpm for 6 minutes. Following the centrifugation, the remaining 330 µL of the RLP supernatant was added to the sample reservoir without touching the membrane. Again, the tube was sealed with the filter in it and centrifuged at 14,000 rpm for 6 minutes. The filter was inverted in a new Eppendorf

tube and centrifuged at 800 rpm for 3 minutes to collect the RLP. Approximately 60 μL of RLP and serum proteins were recovered.

Ultracentrifugation

Ultracentrifugation of the RLP and serum was performed to obtain density profiles as follows. The density gradient ultracentrifugation protocol using 0.240 M CsBiEDTA and/or 0.2 M NaBiEDTA as the density gradient forming solute described previously was followed for both total serum and RLP samples with minor modifications.[48] For serum density profiling, 60 μL of serum and 2 μL of the 2 mg/mL NBD C_6-ceramide in DMSO were diluted to 140 μL in H_2O followed by the addition of 1100 μL of the CsBiEDTA or NaBiEDTA. A 1000 μL aliquot of this solution was ultracentrifuged in a 1.0 mL, 34 mm long, polycarbonate thickwall ultracentrifugation tube (Product Number 343778, Beckman-Coulter, Palo Alto, CA) at 120,000 rpm for 6 hours at 5ºC in an Optima TLX ultracentrifuge, TLA 120.2 fixed-angle rotor (Beckman-Coulter, Palo Alto, CA). Similarly for the RLP density profiling, 60 μL of the RLP (concentrated by ultrafiltration) was diluted to 140 μL in H_2O followed by the addition of 1100 μL of the CsBiEDTA. A 1000 μL aliquot of this solution was also ultracentrifuged under the same conditions as the serum. Following the spin, 200 μL of H_2O was layered on top of the tube contents for each sample. The water layering allowed for the separation of buoyant and dense TRL.

Image Analysis

Following the spin and layering, an image of the tube was obtained and analyzed using a digital Optronics Microfire Camera (S99808, Goleta, CA) with a Fiber-Lite MH-100 Illuminator, (MH100A, Edmund Industrial Optics). The light source described here is a metal halide continuous light source. The camera is a digital color microscope camera (S99808, Optronics, Goleta, CA). The camera and light source were placed orthogonally to each other on an optical bench to illuminate the sample suspended in a post holder. Two filters matching the excitation and emission characteristics of NBD C_6 ceramide from Schott Glass (Elmsford, NY) were chosen. A blue-violet filter (BG-12) with a bandwidth centered at 407 nm and a yellow emission filter (OG-515) with a bandwidth centered at 570 nm were used as the excitation and emission filters respectively. Specific settings for the Microfire camera software were an exposure of 15.8 mS with a gain of 1.000 and a target intensity of 30% to illuminate the tube prior to image capture.

The image of the tube following ultracentrifugation was then converted to a density profile using the described method.[49] Briefly, the image was converted from pixel values into intensities versus tube coordinates (0-34 mm) of the polycarbonate ultracentrifugation tube by Origin 7.0 software to create a lipoprotein density profile. This entire protocol was applied in the same manner to all subjects to obtain the total serum and RLP density profiles.

Method 2. Separation of bTRL and dTRL

This method describes the use of different solvents to resolve the bTRL from the dTRL lipoprotein class by layering following an ultracentrifugal separation. Some of these separations were also monitored as a function of time to determine the migration of the bTRL qualitatively.

Layering of Water as a Function of Time

In this study, the migration of bTRL was studied in a water layer as a function of time. Following the ultracentrifugation protocol, a 200-μL layer of water was added to the tube contents to separate TRL. The separation of the dTRL (dense TRL) and bTRL (buoyant TRL at the meniscus) fractions was carried out by layering with water following an ultracentrifugal spin. The separation was examined as a function of time. Two solutions with 50 μL of fasting serum from a normolipidemic subject, Subject 1, 545 μL water, 600 μL of the CsBiEDTA, and 5 μL of NBD C_6-ceramide were prepared. These samples were ultracentrifuged under the same conditions described above. Following the spin, 200 μL of water was layered by pipette on top of the tube contents. Images of these tubes were taken at 10-minute intervals over the period of one hour to follow the migration of particles in the dTRL fraction to the meniscus.

Layering of Water or Acetonitrile as a Function of Time

Another time-based migration study was performed by layering with water ($\rho =$

1.00 g/mL) or acetonitrile ($\rho = 0.79$ g/mL) following a density gradient ultracentrifugal

separation in a lower density gradient solution, 0.1 M CsBiEDTA ($\rho = 1.04$ g/mL) of

lesser volume. Two solutions of a postprandial serum sample from Subject 2 were

prepared as follows. A low density CsBiEDTA solution was prepared from the stock

described above by combining 225 µL of the stock CsBiEDTA with 225 µL of water. To

this mixture, 100 µL of serum and 2 µL of 1 mg/mL NBD C_6-ceramide were added.

From each of these two solutions, a 500 µL aliquot was ultracentrifuged for 3 hours at

120,000 rpm and 5 ºC. Images of both tubes were recorded at the same settings

described before following the ultracentrifugal separation. One tube was then layered

with 500 µL of water, and the other was layered with 500 µL of acetonitrile. Images of

these samples were recorded over a period of 80 minutes.

Layering of Water versus 50% (v/v) Methanol and 100% Methanol

Separation at the layered meniscus was also compared in water, 50% (v/v)

methanol in water, and 100% methanol. These samples were prepared with 60 µL of

serum, 1100 µL of the CsBiEDTA or $Na_2CdEDTA$, 140 µL water, and 2 µL of (2

mg/mL) NBD C_6-ceramide. A 1000 µL aliquot of each of the samples was subjected to

ultracentrifugal separation at 120,000 rpm for 6 hours at 5 ºC. After the spin, the tubes of

CsBiEDTA and $Na_2CdEDTA$ were layered with water, 50% methanol, or 100%

methanol. Again, images of the tubes were analyzed at the same setting described above.

Method 3. Apolipoprotein Analysis

TRL fractions isolated from density gradient ultracentrifugation following a

freeze/cut recovery in liquid nitrogen were analyzed by gel electrophoresis for their

apolipoprotein content. In this analysis, apo B-100 and apo B-48 content was examined

in bTRL and dTRL fractions in order to determine the separation of the apoB-100

containing TRL (VLDL and rVLDL) from the apo B-48 containing TRL (CM and

CMR).

SDS-PAGE (sodium dodecyl sulfate-polyacrylamide gel electrophoresis) was

performed on a 3-8% Tris-Acetate gradient slab minigel (Invitrogen, Carlsbad, CA).

Lipoprotein fractions were collected from the polycarbonate tube by a freeze/slice

method where the tube was first frozen in liquid nitrogen and then cut for collection. The

following equation is used to determine cut points in the tube.

$$mm_f = 1.058 * mm_l - 1.645 \qquad\qquad \text{(Equation 1)}$$

The mm_l represents the tube coordinate in mm from the lipoprotein density profile. Since, the density gradient solution expands upon freezing, this equation corrects for the expansion yielding a frozen state cut point, mm_f. In addition, 8.76 mm was subtracted from the frozen state cut point to adjust for the tube's position on a micrometer/tube holder assembly used.

After collection, the lipoprotein fractions were concentrated by ultrafiltration as described above according to manufacturer's instructions in 100,000 nominal molecular weight cutoff centrifugal filters (Millipore). The fractions were then prepared for SDS-PAGE (sodium dodecyl sulfate polyacrylamide gel electrophoresis) under reduction conditions in LDS Sample Buffer (Invitrogen). A high molecular weight phosphorylase b standard and an apo B-100 standard were prepared in the same manner and used to determine identities of protein bands in the TRL fractions. Briefly, 10 µL of a sample was mixed with 9 µL of LDS sample buffer and 1 µL of 10% (v/v) 2-mercaptoethanol in water. The samples were reduced by incubation for 10 minutes at 70 ℃. The electrophoresis was performed in an XCell SureLock ^{TM} Electrophoresis Cell (Invitrogen) with an electrophoresis power supply (EPS 3500 XL, Pharmacia Biotech) at a constant voltage of 150 V and power at 5 W for 1 hour and 15 minutes.

Following the electrophoresis, the gel was silver stained by the standard non-fixing silver staining method of Blum, et al in order to visualize the separated proteins.[74] Briefly, the gel was rinsed in water that was replaced three times for 5 minutes each. The gel was then incubated in a fixative solution of 10% (v/v) glacial acetic acid, 30% (v/v) ethanol in water for one hour. The fixative solution was replaced and the gel was incubated in the solution for an additional hour. The gel was then rinsed for 20 minutes in a 20% (v/v) ethanol solution. The gel was rinsed again in water for 20 minutes. The gel was sensitized for approximately 1 minute in a 0.02% (w/v) sodium thiosulfate solution. The gel was rinsed in water three times for brief periods of 20 seconds. Finally, the gel was stained in a 0.2% (w/v) silver nitrate solution. Following the silver nitrate staining, the gel was rinsed in water to remove any free silver nitrate for a brief period of 5 seconds. Lastly, the stained bands were developed in a 3% (w/v) sodium carbonate, 0.025% (v/v) formaldehyde, and 10 mg/L sodium thiosulfate solution. The development was stopped by incubating the gel in 20% (w/v) tris, 10% (v/v) glacial acetic acid solution. The gel was then stored in water and scanned. The protein bands on the gel were then analyzed by Kodak 1D Image Analysis software.

Method 4. RLP Cholesterol Determination

The cholesterol content for the RLP isolated by immunoseparation was determined by enzymatic cholesterol assay with visible spectroscopic detection.

<u>RLP Immunoseparation Assay</u>

The RLP immunoseparation assay was followed as described above with minor modifications. The total volume of RLP immunoseparation gel with antibodies was 300 µL and 240 µL of this volume was supernatant. In the supernatant, 5, 10, and 15 µL of serum were assayed maintaining a constant final volume of 300 µL for the assay. Again, the tubes were incubated for 2 hours at 14,000 rpm, and the gel was allowed to settle for 15 minutes following the incubation. The supernatant was aspirated as described above and cholesterol analysis was performed on the recovered RLP in solution.

Cholesterol Determination

Cholesterol analysis was performed according to the manufacturer's instructions (Thermo Electron Corporation) as follows. The RLP buffer, 0.05 M tris-HCl, (Polymedco) was used as the blank. Serum, blank, cholesterol standard, and cholesterol reagent were brought to room temperature. A 3 µL aliquot of each was then pipetted into a 96 well microtiter plate with visible light transmittance properties. Then 300 µL of the cholesterol reagent was added to each well. The plate with the samples and added cholesterol assay reagent was incubated at 37 ºC for 5 minutes. The absorbance of the samples was recorded at a wavelength of 500 nm. The average absorbance value of the blank was subtracted from all the absorbance values to obtain corrected absorbance values. The cholesterol concentrations for the RLP samples were then calculated from the linear regression equation of prepared cholesterol standards.

Method 5. Triacylglycerol Distribution

In this method, the triglyceride content and the MAG (monoacylglycerol), DAG (diacylglycerol), and glycerol content were measured in different lipoprotein fractions separated by density gradient ultracentrifugation. These values were used to determine relative distribution throughout the lipoprotein classes as a function of density.

Density Gradient Ultracentrifugation & Fraction Collection

The ultracentrifugation protocol in *Method 1* was followed in NaBiEDTA followed by freezing tubes in liquid nitrogen for freeze and cut recovery of all fractions of the tube also described above. In addition, some of the fractions were collected by aspiration.

Triglyceride Measurement

Triglyceride measurements were performed according to manufacturer's instructions (Sigma Aldrich). These reactions are detailed in Figure 7. Briefly, the glycerol standard, blank (water), and 3 µL aliquots of the lipoprotein fractions and serum were assayed with a 300 µL volume of prepared triglyceride working in a 96 well microtiter plate. The plate was incubated for 5 minutes at 37 ºC after which absorbance values at 540 nm were measured for all standards, blank, fractions, and serum. The absorbance of the blank was subtracted to obtain corrected absorbance values for the

standard and samples. The triglyceride concentration was determined by the following equation.

$$\frac{A_{sample} - A_{blank}}{A_{standard} - A_{blank}} \times \text{Conc. of Standard (2.5 mg/mL)} \qquad \text{(Equation 2)}$$

The absorbance values at 540 nm for the sample (A_{sample}) and standard ($A_{standard}$) were corrected by subtracting the absorbance value of the blank or water (A_{blank}). The triglyceride concentrations were then calculated against the absorbance ($A_{standard}$) and theoretical concentration of the glycerol standard (2.5 mg/mL or 250 mg/dL).

Free Glycerol Measurement

The same protocol above was applied for the free glycerol measurement. The standards, blank and samples were assayed with just the free glycerol reagent instead of the triglyceride working reagent with the same volumes to determine free glycerol concentration. In this measurement since only the free glycerol reagent was used, there was no additional lipolysis from lipoprotein lipase, which is in the triglyceride working reagent. Therefore, triglycerides were not accounted in this measurement. Again, the absorbance values were corrected with the blank and concentrations were determined by calibration against the standard in the same manner described above.

True Triglyceride Determination

The "true triglyceride" values for the fractions were calculated as a difference between the initial triglyceride measurement and the free glycerol measurement. By subtracting the measurement of free glycerol/MAG/DAG, the true triglycerides were determined.

TAG Distribution and Percent Recovery

The following figure illustrates the cylindrical shape of a fraction cut from the polycarbonate tube after freezing in liquid nitrogen (Figure 8).
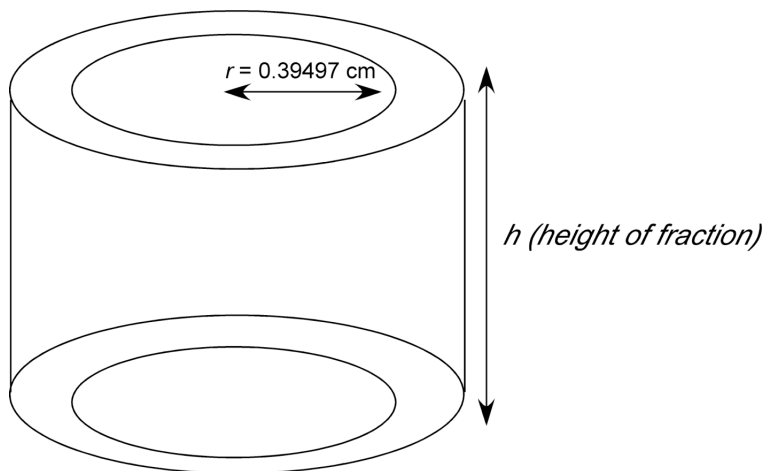
Figure 8. The cylindrical shape of a fraction cut from a polycarbonate ultracentrifugation tube.

The heights of the fractions were determined from the difference between tube cutting coordinates of the lipoprotein fractions. The height values were used to calculate the volume of each fraction based on the measured inner radius of the polycarbonate

tubes (0.39497 cm) by the following equation for the volume of a cylinder.

$$V = \pi * r^2 h = \pi(0.39497cm)^2(h)$$
(Equation 3)

The shape of the bottom fraction or the dense HDL/serum protein fractions did not conform to a cylinder, and so, its volume was calculated as the difference between the total volume of the tube (1200 μL) and the calculated volumes of the rest of the fractions.

Percent recovery of TAG from the density gradient ultracentrifugation was determined by converting the TAG concentrations to mass values (mg) for each fraction and adding the individual TAG masses for all the fractions of a tube. This additive mass value was then divided by the mass of TAG found in serum extrapolated to the volume of serum ultracentrifuged in the tube.

Lastly, an assumption of 100% recovery was made to determine the distribution of TAG as percentage values by using a multiplier (X) in the following equation.

$$\frac{(Av_a + Bv_b + Cv_c + Dv_d + Ev_e + Fv_f)X}{1200uL} = [TAG_{TOTAL}]\ in\ serum \qquad \text{(Equation 4)}$$

The TAG_{TOTAL} is the concentration of TAG in serum in the aliquot of serum that is ultracentrifuged. The variables A through F represent the raw TAG concentrations of the six fractions sliced from the ultracentrifuged tube. The v variables are the volumes associated with each respective fraction calculated from Equation 3. The total volume of the tube following the ultracentrifugation and layering is 1200 µL. Finally, the unitless multiplier X was determined from these measured quantities and was used to determine the extrapolated TAG concentration of each fraction by multiplying the raw concentrations (A through F). These values were then represented as a percentage of the total TAG concentration in the tube (TAG_{TOTAL}).

Method 6. In vitro *Lipolysis*

In this study, serum samples were incubated with lipoprotein lipase to induce triglyceride hydrolysis in an *in vitro* setting. These serum samples were then examined by density gradient ultracentrifugation to determine changes in the lipoprotein density profile as well as subsequent triglyceride distribution analysis to determine the extent of triglyceride hydrolysis and generation of glycerol/MAG/DAG in the lipoprotein fractions isolated by density gradient ultracentrifugation.

Determination of Incubation Time and LpL Concentration

Different concentrations of LpL (1000 U/0.49 mL stock) were examined with constant volumes of fasting serum for different periods of incubation in an *in vitro* setting. A 100 µL volume of serum was incubated with 14 µL of LpL of different concentrations for 2, 4, 6, and 8 hours at 37 ºC. The lipolysis was quenched by refrigeration at -20 ºC. Four different concentrations of LpL solutions in water were examined for the four incubation periods: 0 U/µL (control or water), 0.04 U/µL, 12.24 U/µL, and 28.57 U/µL.

Triglyceride Distribution following *in vitro* Lipolysis

In addition, *in vitro* lipolysis assays with the 0 U/µL LpL (control) and 0.11 U/µL LpL with shorter varied incubation periods of 30 minutes, 60 minutes, 90 minutes and 120 minutes were also applied to fasting serum samples. The same ultracentrifugation protocol was followed for the above LpL assays by using a 60-µL aliquot of each assay (serum and LpL or serum and water), which was ultracentrifuged in 0.2 M NaBiEDTA as described before. Image analysis was performed as described in Chapter II, *Method 1,* Image Analysis. Again, fractions were collected by the freeze/cut manner described in Chapter II, *Method 3* and relative distribution of triglycerides was determined as described in Chapter II, *Method 5* for the fasting serum.

Method 7. TRL Analysis by Capillary Zone Electrophoresis

To further characterize the TRL class, intact triglyceride-rich lipoprotein fractions collected from preparative density gradient ultracentrifugation in 20% (w/v) sucrose were examined by capillary zone electrophoresis in two uniform electrolyte solutions for their relative migration time, electrophoretic mobilities, and intensities.

Fraction Collection

Preparative density gradient ultracentrifugation in 20% (w/v) sucrose solution was employed to collect TRL and RLP samples for capillary electrophoresis analysis. Serum (200 µL) or RLP solutions (60 µL from RLP immunoseparation assay) were prepared in water to a final volume of 400 µL. These sample solutions were layered over 800 µL of 20% (w/v) sucrose in a polycarbonate ultracentrifuge tube. The tube contents were ultracentrifuged at 100,000 rpm for 4.5 hours at 20 ºC with a 2-minute acceleration before the spin and 3-minute deceleration after the spin. These tubes were not layered and were frozen in liquid nitrogen following the spin. TRL and RLP fractions at the meniscus were collected from the tube by cutting. TRL and RLP fractions collected from 3 tubes were combined to yield a high concentration of lipoproteins. In addition, some tubes were layered with only half the concentration of serum with 100 µL of serum and 100 µL of water mixed. Following the ultracentrifugation, a 200-µL layer of water was added to shift the meniscus and divide the TRL into buoyant and dense TRL fractions. These fractions, too, were frozen in liquid nitrogen and subsequently cut for collection and analysis.

The immunoseparation assay described in *Method 1* was used to prepare RLP that was analyzed by capillary electrophoresis prior to preparative ultracentrifugation in 20% (w/v) sucrose. The immunoprecipitated RLP contains the serum proteins. These proteins are removed by density gradient ultracentrifugation.

Concentration by Ultrafiltration

After obtaining the relevant sucrose gradient fractions from the frozen tubes, the

TRL and RLP fractions were concentrated by ultrafiltration in 100,000 nominal

molecular weight cutoff filters according to manufacturer's instructions (Millipore).

Briefly, ~75-200 µL of the total TRL or RLP harvested from tubes were combined with

an additional volume of 12.5 mM sodium borate buffer to yield aliquots of 400 µL. This

entire volume was subjected to centrifugation at 14,000 rpm for 3 minutes in order to

remove the sucrose gradient solution. The volume was replaced with the 12.5 mM

sodium borate buffer to yield a total volume of 400 µL. The aliquots were again

centrifuged at the same settings. Finally, a 75-100 µL aliquot of the TRL or RLP was

recovered by inverting the filters and centrifuging at 800 rpm for 3 minutes.

Background Electrolyte Systems

Two background electrolyte (BGE) solutions were prepared for the

electrophoretic separations. The first BGE was prepared with sodium borate in water at a

concentration of 12.5 mM with a measured pH of 9.22. This BGE buffer was used as a

sample buffer for all the electrophoretic separations described below to ensure no sample

delipidation occurred. The second buffer system was prepared in water at a

concentration of 12.5 mM sodium borate, 3.5 mM 70% SDS, and 20% ACN (v/v) with a

measured pH of 9.20. Electrophoretic separations were carried out in both of the above

buffers.

Capillary Cartridge Assembly

Prior to the electrophoretic separations, a capillary cartridge was assembled according to instructions provided by Beckman Instruments (Fullerton, CA). Briefly, an untreated fused silica capillary (Catalog Number TSPO75375, Polymicro, Pheonix, AZ) of a 76 μm inner diameter and 360 μm outer diameter was prepared to a total length of 47.2 cm and with a detector window at 41.4 cm.

Capillary Zone Electrophoresis (CZE) Separation

The CE separations were performed in a Beckman P/ACE Model 5510 capillary electrophoresis instrument equipped with a photodiode array detector (Beckman Coulter, Inc.). Deionized water was injected (8 seconds) as an electroosmotic flow marker (EOF) followed by a sample injection of 10-15 seconds at 17 kV for variable electrophoretic separation time periods. Both BGE solutions were used to carry out the separations, but all TRL and RLP samples were placed in the 12.5 mM sodium borate in water BGE solution. Fractions corresponding to the lipoprotein subclasses were detected at 214 nm. Following the separation and detection, fractions were analyzed for migration times, effective electrophoretic mobilities, and relative intensities.

In addition, the TRL and RLP samples were also analyzed with new capillary electrophoresis instrumentation (P/ACE^{TM} MDQ Capillary System, Beckman Coulter Inc.) equipped with a multiwavelength photodiode array detector and 32 Karat software (Beckman Coulter). The electrophoretic separation were carried out in the 12.5 mM sodium borate, 3.5 mM 70% SDS, and 20% ACN (v/v) BGE solution in an untreated fused silica capillary (Part 338454, Beckman Coulter) compatible with the new instrumentation with a 75 µm inner diameter and a 375 µm outer diameter. The total length of the capillary in this system was 62 cm, and the length of the capillary to the detector window was 50 cm. The samples were injected by pressure at 0.5 psi for 4 seconds and the EOF marker (water) was injected at 0.5 psi for 3 seconds prior to the electrophoretic separation. The separation was carried out at 17.5 kV for a period of 25 minutes. Electropherograms of the samples and standards were examined at 214, 234, and 280 nm for relative migration times and intensities with the accompanying 32 Karat software.

Method 8. Postprandial Study

Subject 2 donated blood over a 9 hour period starting with a baseline draw. After the baseline draw, Subject 2 received a high-fat meal containing 1010 calories and 640 calories from fat. The meal specifically contained 71 g of total fat of which there was 28 g of saturated fat and 3 g of trans fat, 125 mg cholesterol, 53 g of carbohydrates, 2 g of dietary fiber, 12 g of sugar, and 40 g of proteins. After the meal, blood was drawn at every hour for the following 8 hours. From these serum draws, total lipoprotein profiles and RLP density profiles were obtained in NaBiEDTA as described previously. The relative integrated intensities of the lipoprotein fractions from both the total lipoprotein profiles and the RLP profiles were analyzed with the Origin 7.0 software.

Method 9. Special Case Study: Hypertriglyceridemia and Megacystis-Microcolon-Intestinal Hyperperistalsis Syndrome

An RLP immunoseparation assay followed by RLP density profiling and apolipoprotein analysis by SDS-PAGE was performed on fasting and nonfasting serum from an 8-month old baby girl suffering from hypertriglyceridemia and megacystis-microcolon-intestinal hyperperistalsis syndrome. The subject was fed by total parenteral nutrition (TPN) with minimal lipids intravenously and in this state a "nonfasting" serum sample was obtained. The subject was taken off the TPN and a "fasting" serum sample was obtained 4 hours later.

The RLP Density Profiling method in CsBiEDTA described in *Method 1* and the SDS-PAGE apolipoprotein analysis described in *Method 3* were applied to the fasting and nonfasting samples from this subject to obtain a total lipoprotein profile, and RLP profile, and apolipoprotein content in the TRL fractions. Specific metabolic features of this subject were addressed by this analysis to assist in the diagnosis of this particular ailment. The differential density profiling method of the RLP profile determined lipoprotein lipase efficacy as well as the efficacy of TRL synthesis by the liver and/or small intestine and clearance efficacy of TRL by the liver.

CHAPTER III

RESULTS AND DISCUSSION

Remnant Lipoprotein Density Profiling (Differential Density Lipoprotein Profiling)

<u>Objective</u>

We developed a technique, which couples Nakajima's RLP immunoseparation assay with ultracentrifugal density gradient separation in CsBiEDTA to define and separate RLP by density. The novel coupling of the two methods shows the efficacy of the immunoseparation assay and defines the densities of the RLP relative to other TRL. We demonstrate that Nakajima's immunoseparation assay does effectively separate components of the TRL class from other serum lipoproteins: HDL, LDL, and most VLDL.[21]

<u>Total Lipoprotein Density Profiling</u>

Before performing an RLP immunoseparation, a density profile is obtained by density gradient ultracentrifugation. Figure 9 is a density profile of serum components from Subject 1 in a CsBiEDTA gradient. The serum is separated in CsBiEDTA in a polycarbonate tube of 34 mm length. The serum lipoprotein fractions separate according to their densities in the gradient at different tube coordinate positions. This profile shows the typical features of a serum density profile including serum proteins at a tube

coordinate of 28 mm, HDL subclasses from 21 mm to 26 mm, LDL centered at 18 mm,

IDL at 13 mm, and the meniscus containing buoyant and dense TRL at about 10 mm.
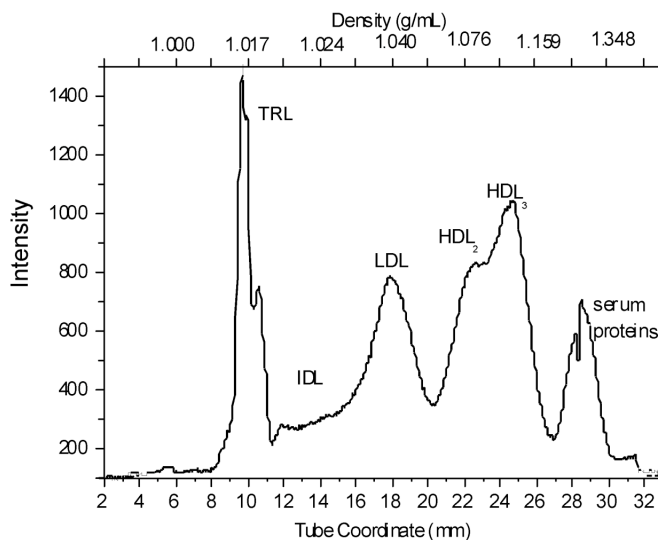
Figure 9. Lipoprotein density profile (unlayered) for Subject 1 in CsBiEDTA.

As shown in Figure 10, the buoyant and dense TRL are resolved by layering 200

µL of H_2O shifting the meniscus about 4 mm. The more buoyant and hence larger TRL

separate from the less buoyant, smaller TRL components upon layering of water. The

two fractions at the top of the tube consist of CM and VLDL with the meniscus

containing the more buoyant, triglyceride-rich portion leaving behind the denser and less

buoyant counterparts of the TRL class. The more buoyant TRL immediately follow the

shifting meniscus as the water is added, whereas the denser TRL remain behind due to

lower flotation velocity (Figure 10).
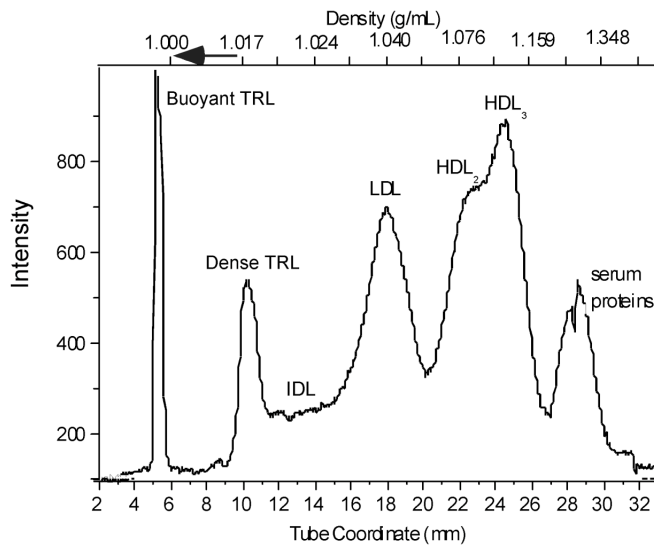
Figure 10. Lipoprotein density profile (layered with water) for Subject 1 in CsBiEDTA.

The meniscus region between the buoyant and dense TRL does not follow the density gradient of the CsBiEDTA in the rest of the tube. The density of this region is essentially the density of H_2O and is labeled as such. Figure 10 is an example of a density profile in CsBiEDTA of a normolipidemic subject (Subject 1) with features of minimal dense TRL and IDL. The features of a typical lipoprotein density profile in a CsBiEDTA gradient include the meniscus (buoyant TRL), dense TRL, IDL, LDL, and HDL regions primarily. Fluorescence arising from the IDL fraction is detected above the background fluorescence at density values between the dense TRL and LDL fraction. Other unique characteristics of this profile are the apparent HDL_2 and HDL_3 subclasses of the HDL region. At the bottom of the tube at 28 mm, serum proteins, mainly albumin separate from the lipoprotein classes. A discontinuity dividing this fraction originates

from light scattering from a seam on the surface of the polycarbonate tube and is not due to any serum component.

RLP Density Profiling in CsBiEDTA

Figure 11 is the RLP profile of Subject 1. This RLP profile shows an effective removal of the LDL and IDL subclasses by the RLP immunoseparation assay. Again, by adding H_2O immediately following the ultracentrifugation spin, a portion of the more buoyant TRL migrates in the shifting meniscus at the density of water. Hence, two density-distinct RLP fractions remain at the corresponding buoyant and dense TRL densities.
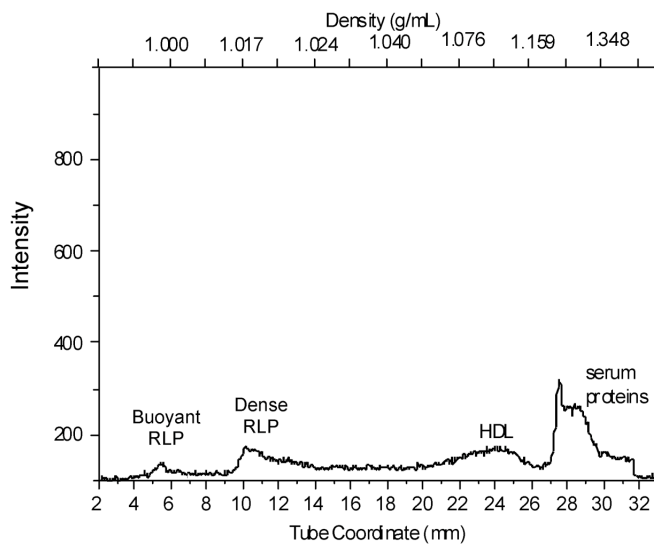
Figure 11. RLP density profile (layered with water) for Subject 1 in CsBiEDTA.

Interestingly, approximately 5% of the HDL is not removed by the immunoseparation. As described before, the RLP immunoseparation includes antibodies to apo B-100 and apo A-1. Remnant particles do not react to these antibodies. Although rVLDL contain an apo B-100, the immunoreactivity to this particular monoclonal antibody is compromised. It is this fact upon which the immunoseparation is based since normal VLDL retain immunoreactivity between their apo B-100 and the antibody as well as LDL. In addition, CMR unlike their nascent counterparts (CM) have no apo A-1. Serum proteins have no immunoreactivity to these antibodies and also appear in the RLP density profile.

Moreover, small and dense HDL in the form of HDL_3 due to their size have increased dissociation of apo A-1.[75, 76] The mechanism behind this is the uptake of triglycerides by HDL, which leads to an increase in lipolysis by hepatic lipase.[75, 77] HDL become smaller in size and more vulnerable to losing apo A-1.[75, 78] Small, dense triglyceride-rich HDL is observed in people suffering from hypertriglyceridemia. In these subjects, HDL_3 dominates over HDL_2.[75, 79] HDL generally have an apo A-1 constituent to which the antibody in the RLP immunoseparation can react.

Therefore, most HDL is also removed by the assay. However, if the HDL has lost its apo A-1 due to triglyceride-enrichment, it would appear in the RLP density profile. This is yet another facet to the RLP density profile and an extension of the RLP immunoseparation assay as dense triglyceride-rich HDL lacking apo A-1 can be detected along with buoyant and dense RLP.

In this subject the HDL seen in the RLP density profile (Figure 11) is indeed of the denser form (HDL$_3$) as both HDL classes are detected in the total lipoprotein profile (Figure 10). It is likely that the HDL seen here has lost its apo A-1. The percent of RLP in total TRL at each density is relatively minimal. The buoyant TRL at the meniscus consist of only 0.04% buoyant RLP, and the dense TRL consist of 17.81% dense RLP. The RLP that separates at the IDL density is insignificant as it is almost completely removed.

Figure 12a is an example of a profile that satisfies the criteria of elevated VLDL and the presence of IDL (Subject 3). These characteristics are typically good indicators of elevated RLP.
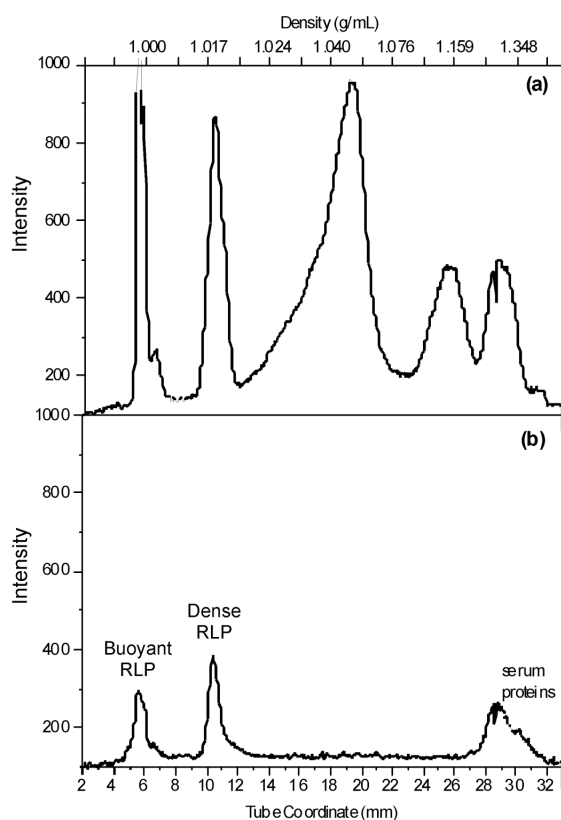
Figure 12. Lipoprotein density profile (a) and RLP density profile (b) for Subject 3 in CsBiEDTA following the layering of water.

Many features of this profile are similar to Subject 1's profile in Figure 10. Both profiles exhibit lipoprotein fractions at the meniscus (buoyant TRL), dense TRL, IDL, LDL, and HDL densities. However, Subject 3's profile features elevated dense TRL and IDL in contrast to Subject 1's profile.

Subject 3's RLP profile in Figure 12b dramatically demonstrates the efficacy of the immunoseparation assay in its removal of all non-RLP lipoprotein fractions. The apo B-100 antibody removes most VLDL, IDL, and LDL. The apo A-1 antibody removes the CM and HDL. Again, two density-distinct RLP fractions remain in the profile. The

buoyant TRL at the meniscus consist of 22.9% buoyant RLP content. The dense RLP at the dense TRL density is 28.6% of the nascent fraction. It is interesting to note that lipoprotein particles at the density value of IDL are not a significant feature of the RLP density profiles. The RLP fraction at the IDL density is only 3.5% of the nascent particles in Subject 2's serum.

Postprandial versus Fasting Samples

The RLP immunoseparation assay and the ultracentrifugation protocol in CsBiEDTA were performed on fasting and postprandial samples from Subject 2. The postprandial serum sample from this subject was obtained 5 hours after ingestion of a high-fat content, fast food burger. The fasting serum sample was obtained prior to the meal. The RLP profiles for both samples are overlaid with the density profiles for the fasting in Figure 13a and postprandial serum samples in Figure 13b.
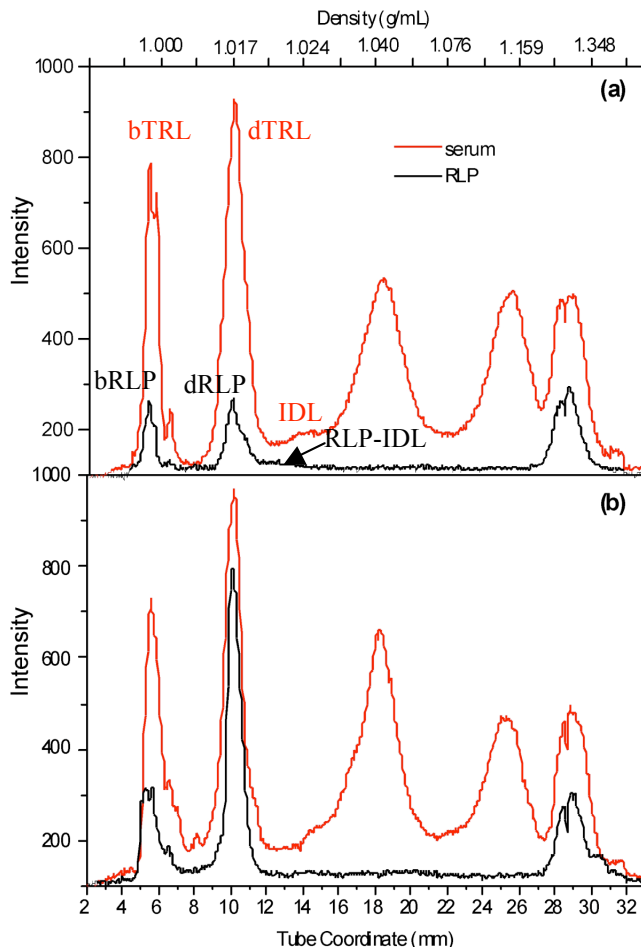
Figure 13. (a) Lipoprotein (red line) and RLP density profiles (black line) in CsBiEDTA following the layering of water for Subject 2 in the fasting state (b) Lipoprotein (red line) and RLP density profiles (black line) in CsBiEDTA following the layering of water for Subject 2 in the postprandial state.

Once more, the RLP fractions separate at density values corresponding to their nascent counterparts, and minimal RLP separates at the density corresponding to IDL. Subject 3's RLP profiles reconfirm the effectiveness of the removal of non-RLP lipoproteins by the immunoseparation. In addition, there is a marked increase in dense RLP from the fasting to postprandial samples. An interesting finding is the fact that the overall dense TRL content does not appreciably increase from the fasting to postprandial

state at the fifth hour after the meal according to our results. The percentages of RLP:

TRL at each density for the fasting and postprandial samples from Subject 3 are

tabulated in the following table (Table 3).

Table 3. Percentage of RLP at TRL and IDL densities for fasting and postprandial samples of Subject 2.

Samples	Integrated area, %
Fasting Samples	
buoyant RLP/buoyant TRL	13.5
dense RLP/dense TRL	12.6
RLP-IDL/(IDL + RLP-IDL)	0
Postprandial Samples	
buoyant RLP/buoyant TRL	29.4
dense RLP/dense TRL	53.5
RLP-IDL/(IDL + RLP-IDL)	5.8

These numbers indicate the extent of the increase in RLP in the postprandial

state. The data provide the ratio of the remnant particle of interest to its corresponding

nascent TRL particle plus the remnant itself. For example, the ratio of "Buoyant RLP:

Buoyant TRL" signifies the ratio of the buoyant remnant particles to the nascent buoyant

TRL particles plus the buoyant remnant particle itself. This is definitive evidence of the

presence of RLP in circulation following a fat-containing meal.

Summary on Remnant Lipoprotein Density Profiling

The residence and dynamics of clearance of the buoyant and dense RLP in the

hours following a meal can potentially be measured by this new methodology. This

would provide insight into the clearance rate of RLP by the liver in a particular subject. It could also provide useful information in regard to the atherogenicity of these particles and in the assessment of an individual's risk factor for developing coronary heart disease.

In addition, the RLP density profile provides more information regarding the metabolism of TRL. As previously discussed, the first stage of catabolism of TRL involves activation of LpL on the endothelium of capillaries in adipose and muscle tissue by apo C2 on the surface of the TRL particles which results in the hydrolysis of associated triglycerides to free fatty acids and formation of RLPs (Figure 13).[11, 80] Therefore, the presence of RLP in the RLP density profile provides indirect confirmation of the presence of LPL activity as well as apo C2.

In essence, a precursor/product concept is applied here in the metabolism of nascent TRL to RLP to confirm this enzyme's activity as well as the presence of apo C2.[53] This precursor/product concept was previously used to assess the efficacy of LpL consistent with the same line of reasoning.[53] The usage of RLP density profiling to establish functionality of a lipolytic cascade is a simpler technique compared to traditional methods to determine the possibility of familial LPL deficiency since it does not require systemic heparinization.

Traditionally, famililial LpL deficiency is diagnosed clinically by a specific assay of LpL activity in plasma following an intravenous injection of heparin. Heparin releases the LpL from the endothelial cells into circulation. This is an invasive procedure and

causes a depletion of LpL in the patient following the injection.[40] Our method eliminates the need for this entire procedure and only requires a serum blood draw.

Separation of bTRL and dTRL

Objective

The use of different solvents to resolve the bTRL from the dTRL lipoprotein class by layering following an ultracentrifugal separation is presented here. Without any additional separation, TRL separate together at the meniscus following a density gradient ultracentrifugation in any gradient solution. This is due to the fact that VLDL have densities less than 1.006 g/mL and CM have densities less than 0.95 g/mL. The density of the solvent limits the separation of TRL in gradient solutions. The solvent of choice is usually water with a density of 1.000 g/mL. In this study, an additional solvent layer is added to the serum solution separated by density gradient ultracentrifugation in order to attempt a further separation of the TRL subclasses. Some of these separations were also monitored as a function of time to determine the migration of the buoyant (bTRL) qualitatively.

Layering of Water as a Function of Time

The migration of bTRL to the meniscus upon layering of water was monitored as a function of time. The following figure illustrates the stability of the total lipoprotein profile in CsBiEDTA over a 60-minute period following the layering of water for

Subject 1's serum (Figure 14).
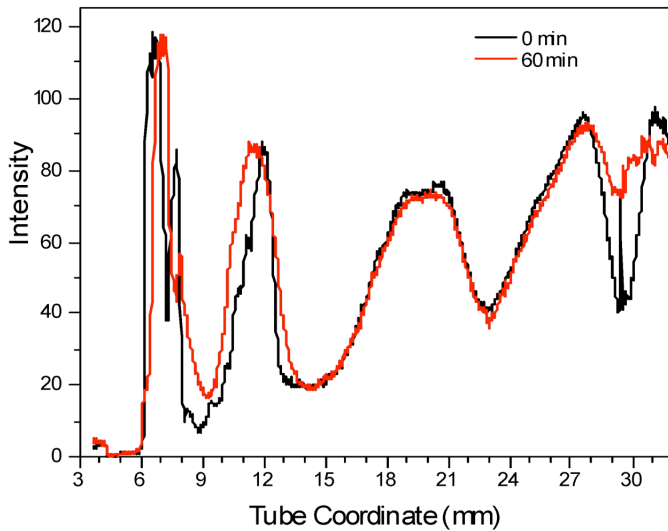
Figure 14. Changes in the total lipoprotein density profile in CsBiEDTA for Subject 1 over 60 minutes.

Overall, the total lipoprotein profile does not change. The CsBiEDTA gradient is stable in the LDL region and the location of this class does not change during the 60-minute time frame. Some resolution between HDL and the serum proteins is lost. The bTRL and dTRL also lose resolution, which may be attributable to bTRL migration to the meniscus or changes in the CsBiEDTA gradient at the top due to the addition of the water layer. A 60-minute time delay following the layering of water in a 200 μL volume does not present an advantage in terms of bTRL and dTRL separation.

Layering of Water or Acetonitrile as a Function of Time

Another time-based migration study was performed by layering with water (ρ = 1.00 g/mL) or acetonitrile (ρ = 0.79 g/mL) following a density gradient ultracentrifugal separation in a lower density gradient solution, 0.1 M CsBiEDTA (ρ = 1.04 g/mL) of lesser volume. To observe the migration of the bTRL to the meniscus serum from Subject 2 was separated by ultracentrifugation in this CsBiEDTA solution in a smaller volume of 500 µL. Following the ultracentrifugal separation, a 500-µL layer of water was added. This allowed for a greater volume range for the bTRL migration and separation to occur. The following figure shows the initial ultracentrifugal separation of Subject 2's serum in 0.1 M CsBiEDTA as well as the initial layering of water at time zero (Figure 15).
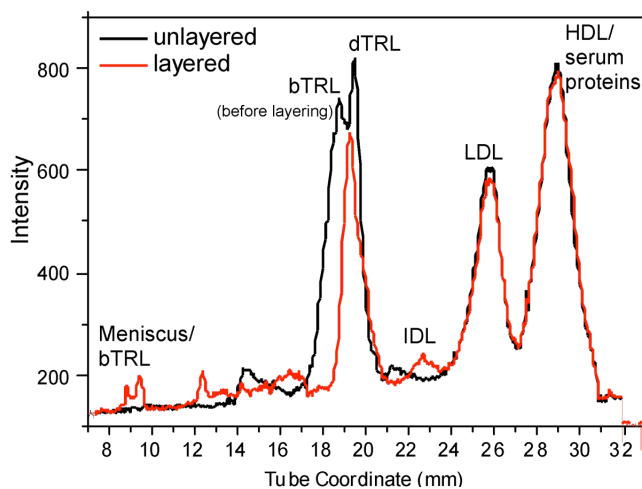
Figure 15. Migration of bTRL to the water meniscus in a 0.1 M CsBiEDTA density profile at time 0.

It is apparent that the initial layering of water does not facilitate a clean separation of the bTRL over a 500-µL volume (Figure 15). An appreciable level of fluorescence background is present in between the meniscus and dTRL following the layering. Also, it appears that the addition of the water layer pushes the IDL closer to the LDL probably due to mixing of the CsBiEDTA at the unlayered meniscus with the water layer. However, the separation does achieve resolution for the IDL class. The HDL is not resolved from the serum proteins in this gradient but is resolved from the LDL class. The migration of the bTRL was monitored over a total time period of 80 minutes following the initial water layer at time zero. The following figure illustrates the migration of the bTRL in the water layer over the first 20 minutes following the layering (Figure 16).
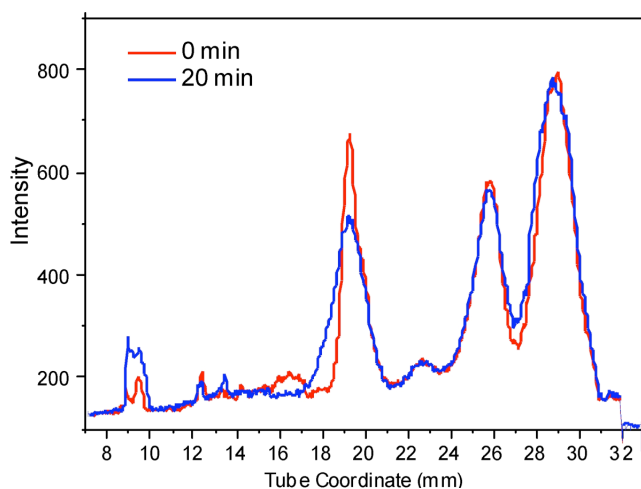
Figure 16. Migration of bTRL to the water meniscus in a 0.1 M CsBiEDTA density profile from 0 to 20 minutes.

In Figure 16, a further migration of bTRL is observed as fluorescence intensity increases at the meniscus and decreases at the dTRL shifting some of the intensity from this class to lower density. Still, fluorescence background exists between the meniscus and dTRL possibly indicating the migration of bTRL or an unclean separation. The IDL, LDL, and HDL/proteins are stable at their densities in this gradient with minimal loss of resolution between the LDL and HDL. The figure that follows represents the bTRL migration from 20 to 60 minutes (Figure 17).
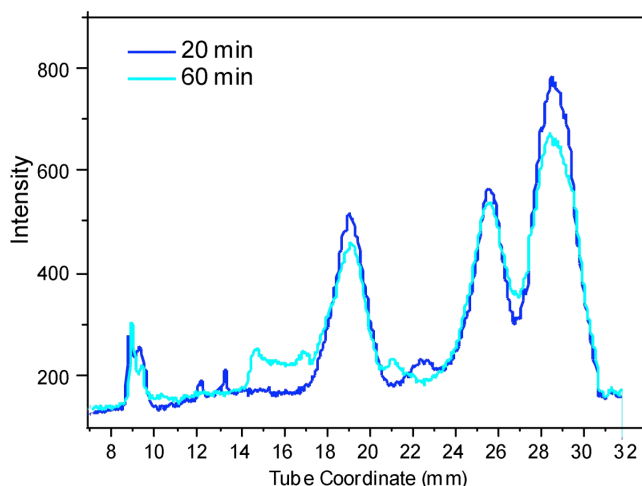
Figure 17. Migration of bTRL to the water meniscus in a 0.1 M CsBiEDTA density profile from 20 to 60 minutes.

At 60 minutes following the water layering, many changes in the density profile occur. First of all, fluorescence intensity is diminished at the HDL/serum proteins class. Also, some resolution is lost between the LDL and HDL/serum proteins, and IDL shifts to a lower tube coordinate (21 mm). Further migration of bTRL from the dTRL class

occurs as fluorescence intensity increases at a lower tube coordinate to the left of the

dTRL class in the form of two peaks at 15 and 17 mm. The fluorescence intensity at the

meniscus increases slightly with the elimination of background fluorescence at tube

coordinates 12 and 13 mm. The changes in fluorescence intensity at the dTRL and IDL

are most likely due to the mixing of the water layer and the pre-formed CsBiEDTA

gradient established by ultracentrifugation. The following figure represents the last

period of bTRL migration from 60-80 minutes (Figure 18).
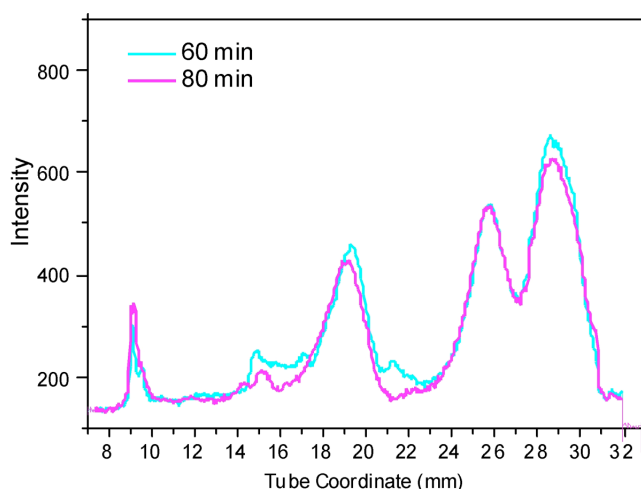
Figure 18. Migration of bTRL to the water meniscus in a 0.1 M CsBiEDTA density profile from 60 to 80 minutes.

At 80 minutes following the layering, the LDL again has stable fluorescence

intensity and position; however, HDL/serum proteins remain at a stable density but again

lose fluorescence intensity. IDL resolution is effectively lost at this stage. Nevertheless,

further bTRL migration occurs shifting from the previous 17 mm peak to 15 mm. The

previous 15 mm peak migrates to a lower tube coordinate as well at 14 mm. The

meniscus fluorescence intensity increases only slightly in this final time frame.

Overall, the slow migration of bTRL through an extended water layer over a low-density gradient solution shows some promise for separation of bTRL and dTRL classes into more resolved classes differentiated by their flotation velocities. Further examination of these classes is needed to determine differences beyond flotation velocity in these TRL classes.

Acetonitrile was also examined as another solvent system for bTRL and dTRL separation efficacy over a 500-µL volume of a 0.1 M CsBiEDTA ultracentrifugal separation. The separation of the TRL classes through a 500-µL acetonitrile layer over a period of 80 minutes is presented here. The following figure shows the initial ultracentrifugal separation of Subject 2's serum in 0.1 M CsBiEDTA as well as the initial layering of 500 µL of acetonitrile (ACN) at time zero (Figure 19).
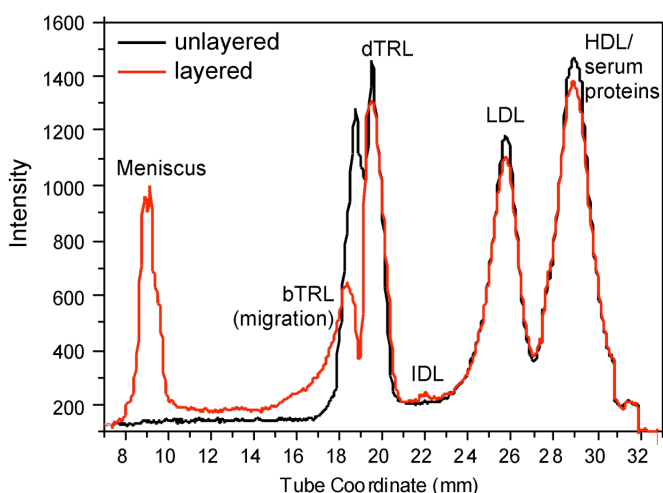
Figure 19. Migration of bTRL to the acetonitrile meniscus in a 0.1 M CsBiEDTA density profile at time 0, RRH serum, separation of bTRL and dTRL, ACN layer layering.

Clearly, the initial layering of ACN facilitates a cleaner separation of the bTRL over a 500-µL volume than water as previously illustrated (Figure 15). A distinguishable IDL peak appears between the dTRL and LDL closer to the LDL due to mixing of the CsBiEDTA at the unlayered meniscus with the ACN layer. Acetonitrile has favorable characteristics as a solvent for the study of bTRL migration since it has a density of 0.78 g/mL and has a high dielectric constant like water. This allows for NBD C_6-ceramide fluorescence to be detected only in the lipoproteins without background fluorescence arising from the solvent itself. The migration of the bTRL was monitored over a total time period of 80 minutes following the initial water layer at time zero. The following figure compares the migration of the bTRL in the water layer in both postprandial and fasting samples from Subject 2 (Figure 20).
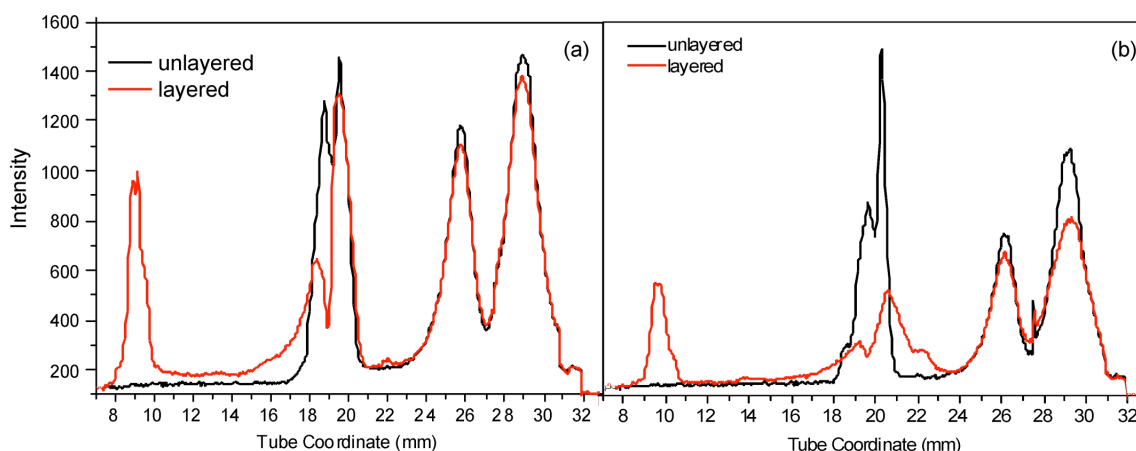
Figure 20. Migration of bTRL to the acetonitrile meniscus in a 0.1 M CsBiEDTA density profile at time 0 for (a) postprandial serum and (b) fasting serum from Subject 2.

The two panels presented in Figure 20 are juxtaposed for comparison of fasting and postprandial TRL separations from the same subject. Figure 20(a) is a reproduction of Figure 19. In Figure 20(b), we can see the difference in bTRL and dTRL separation from a fasting sample of the same subject. Even in the fasting state, some bTRL begin migrating to the meniscus upon layering of ACN. In addition, the fluorescence intensity at the meniscus, bTRL, LDL, and HDL is less intense than in the postprandial state. IDL still appears between the dTRL and LDL with some resolution loss at the dTRL in the fasting serum separation. Figure 21 shows the migration of the bTRL class from the dTRL class in the first 20 minutes following the ACN layering (Figure 21).
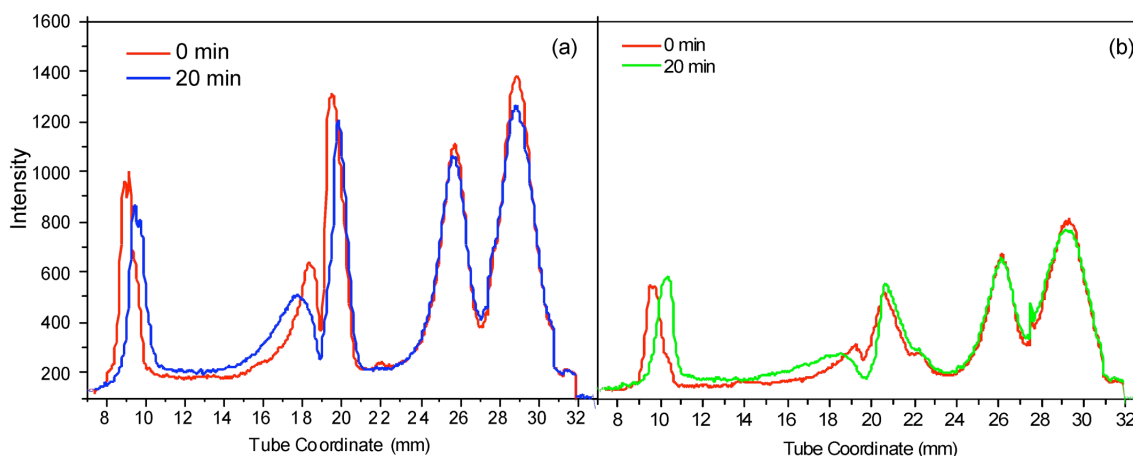
Figure 21. Migration of bTRL to the meniscus in acetonitrile over a 0.1 M CsBiEDTA density profile from 0 to 20 minutes for (a) postprandial serum and (b) fasting serum from Subject 2.

Again, further migration of the bTRL towards the meniscus occurs after 20 minutes of the initial layering for both the postprandial and fasting serum samples. The

remaining fractions appear stable in their densities. The following figure illustrates the final migration examined of the bTRL from 60 to 80 minutes (Figure 22).
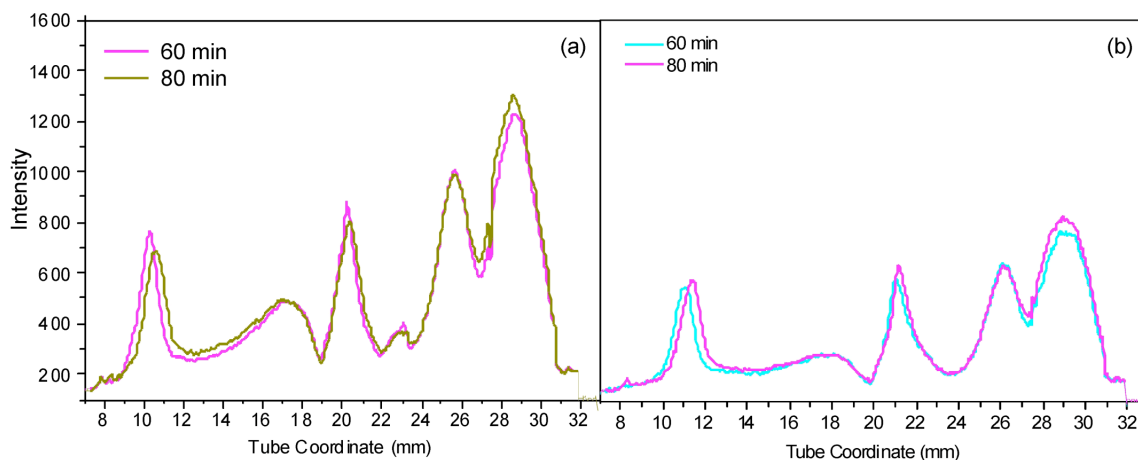
Figure 22. Migration of bTRL to the meniscus in acetonitrile over a 0.1 M CsBiEDTA density profile from 60 to 80 minutes for (a) postprandial serum and (b) fasting serum from Subject 2.

By 60 minutes, the bTRL achieve significant resolution from the dTRL class in both the fasting and postprandial samples. After 80 minutes, the peak ceases its migration in the ACN layer. The separation was followed for an additional 40 minutes, not presented here, in which the separation and resolution of the classes did not change.

As seen in the case of the water layering, the slow migration of bTRL through an extended ACN layer over a low-density gradient solution shows promise for separation of bTRL and dTRL classes into more resolved classes differentiated by their flotation velocities. Just as in the case of the water layering, further examination of these classes by secondary techniques is needed to determine differences beyond a cursory

examination of flotation velocity in these TRL classes. These techniques are also necessary to examine the structural integrity of a lipoprotein in solvents such as acetonitrile.

Layering of Water versus 50% (v/v) Methanol and 100% Methanol

Another comparison on bTRL separation was performed following ultracentrifugal separations in CsBiEDTA compared with $Na_2CdEDTA$ followed by layering of the following solvents: water, 50% (v/v) methanol, or 100% methanol. Normal volume separations (1000 µL) by density gradient ultracentrifugation were carried out for postprandial serum from Subject 2 in 0.2 M CsBiEDTA. A 200-µL layer was water was added to the tube contents following the ultracentrifugal separation. The following figure illustrates the separation of bTRL from dTRL in water immediately following the ultracentrifugal separation in CsBiEDTA for postprandial serum from Subject 2 (Figure 23).
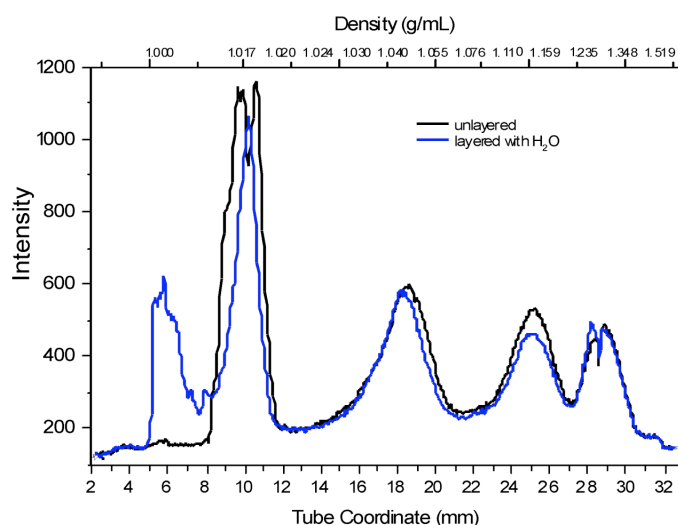
Figure 23. Separation of bTRL and dTRL in a 0.2 M CsBiEDTA density profile following the layering of water.

In this separation, dTRL falls at a density of 1.017 due to the formation of the CsBiEDTA gradient formed by ultracentrifugation. The bTRL class is at the density of water, 1.000 g/mL. The addition of a water layer, shifts the bTRL to a lower density and lower tube coordinate as well as causing a loss of resolution for the dTRL due to the similar densities of water and the CsBiEDTA gradient at the top of the tube. Following the same separation, a 200-µL layer of 50% methanol in water was also added (Figure 24).
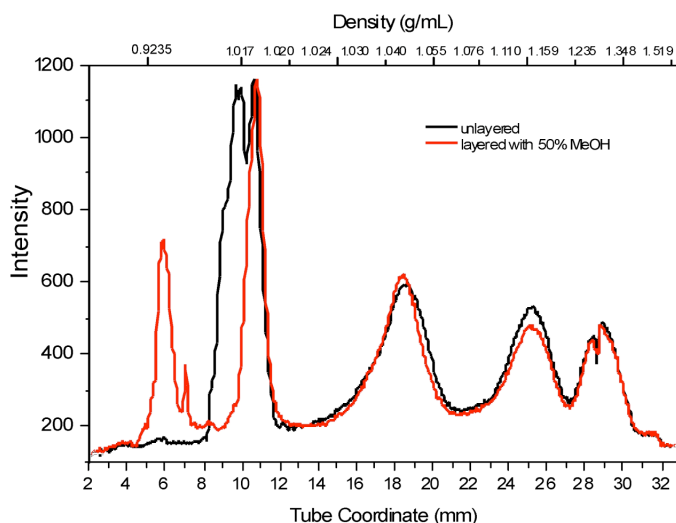
Figure 24. Separation of bTRL and dTRL in a 0.2 M CsBiEDTA density profile following the layering of 50% methanol.

Separation of bTRL from dTRL in a 50% methanol medium offers a cleaner separation in terms of disturbance of the dTRL. Since the density of 50% methanol in water (0.9235 g/mL) is more distinct from the CsBiEDTA (1.017 g/mL) in this portion of the tube, the layering can be performed with more ease and less perturbation. Furthermore, in the water separation (Figure 23), some of the dTRL in the form of VLDL may also migrate to the meniscus at the density of water. At a density of 0.9235 g/mL (Figure 24), less of the VLDL would migrate from the dTRL to the meniscus, and the chylomicrons would separate more effectively into the bTRL fraction. A 100% methanol solution was also layered over the tube contents (Figure 25).

Figure 25. Separation of bTRL and dTRL in a 0.2 M CsBiEDTA density profile following the layering of 100% methanol.

The layering of 100% methanol over the tube contents, though performed with ease, destroys the bTRL and dTRL fractions. This can be seen as the TRL peak in the unlayered separation, separates into two peaks with significant background fluorescence intensity in between. At some critical concentration of methanol between 50% and 100%, the TRL lipoproteins lose structural stability as evidenced here in this separation (Figure 25).

Likewise, similar separations of bTRL and dTRL in water, 50% methanol in water, and 100% methanol layers were examined following an ultracentrifugal separation of postprandial serum from Subject 2 in $Na_2CdEDTA$. The following figure demonstrates the separation of bTRL and dTRL in a water layer following ultracentrifugal separation in $Na_2CdEDTA$ (Figure 26).
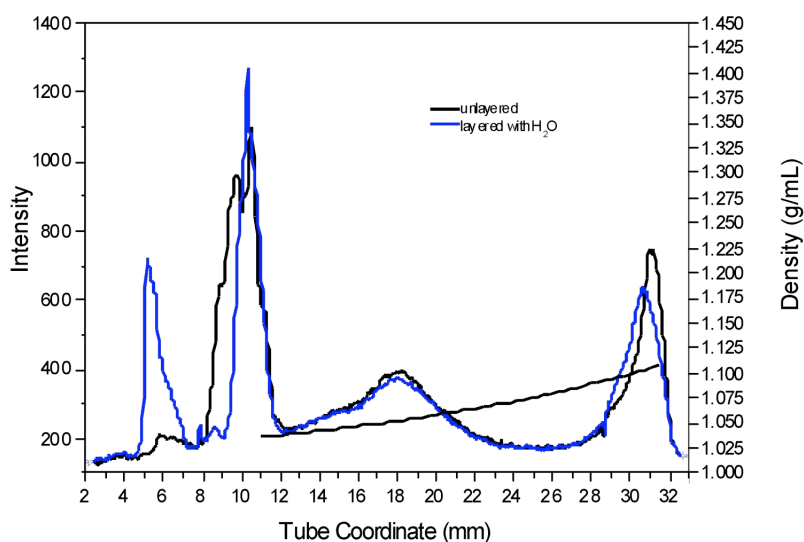
Figure 26. Separation of bTRL and dTRL in a 0.2 M Na₂CdEDTA density profile following the layering of water. RRH postprandial serum separation of bTRL and dTRL.

The separation of the lipoprotein classes in the 0.2 M Na₂CdEDTA gradient is quite different from the CsBiEDTA separations. The HDL and serum proteins achieve no separation; LDL and HDL are well separated. However, the LDL and TRL classes have less resolution than in a 0.2 M CsBiEDTA ultracentrifugal gradient separation. The density at the dTRL fraction in this gradient separation is greater than in CsBiEDTA. Since the water layer has a greater difference in density from the Na₂CdEDTA gradient at the top of the tube, the layering can be performed with greater ease. Hence, less of the dTRL class is disrupted and remains more intact at the Na₂CdEDTA and water interface than as previously seen in a water layer separation in CsBiEDTA (Figure 23). A 50% methanol in water layer separation of bTRL and dTRL was also examined over a Na₂CdEDTA ultracentrifugal separation (Figure 27).
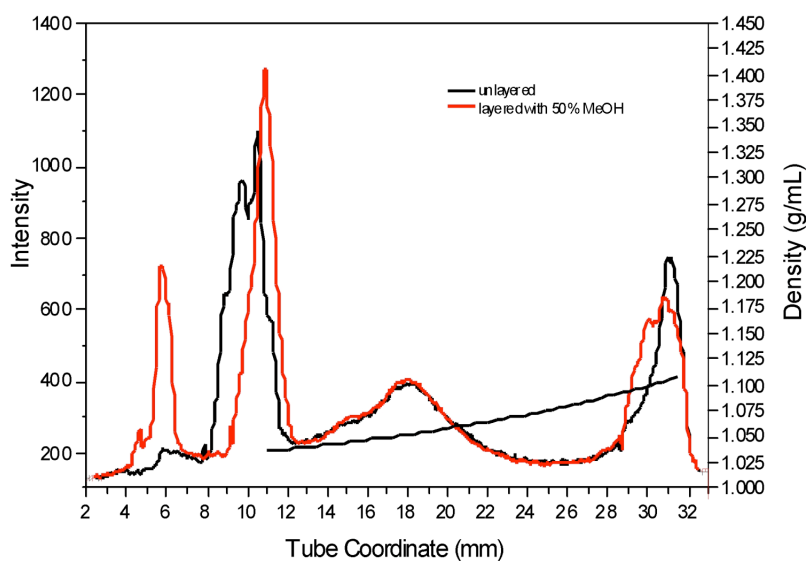
Figure 27. Separation of bTRL and dTRL in a 0.2 M Na$_2$CdEDTA density profile following the layering of 50% methanol.

The difference between a water layer and 50% methanol layer separation over a Na$_2$CdEDTA ultracentrifugal separation is not as dramatic as in CsBiEDTA. This is due to the fact that the density of the Na$_2$CdEDTA gradient at the unlayered TRL position (between 1.025 and 1.050 g/mL) is higher than in CsBiEDTA. The bTRL migration and separation is, therefore, similar in water and 50% methanol. A longer migration period would need to be monitored for the 50% methanol layer versus the water layer to examine the efficacy of the separation over an extended time period to prove whether either layer contributes to a more resolved separation of the bTRL and dTRL classes. A 100% methanol layer was also applied in the separation of bTRL and dTRL over a Na$_2$CdEDTA ultracentrifugal gradient separation (Figure 28).
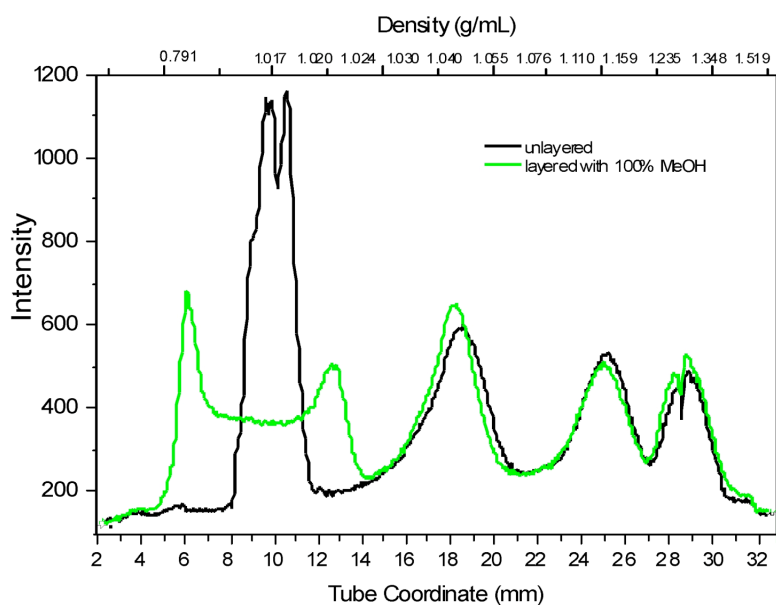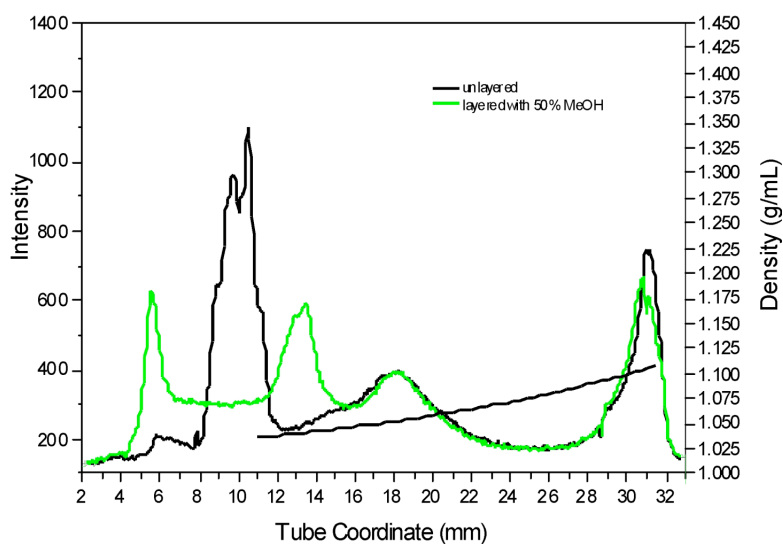
Figure 28. Separation of bTRL and dTRL in a 0.2 M Na2CdEDTA density profile following the layering of 100% methanol.

The result here (Figure 28) is similar to the 100% methanol layer separation of bTRL and dTRL over a 0.2 M CsBiEDTA separation presented previously (Figure 25). The TRL class separates into two peaks at 6 mm and 13.5 mm with elevated background fluorescence intensity between the two peaks due to loss of lipoprotein structural integrity. In addition, the dTRL and LDL class lose further resolution as the dTRL collides with a portion of the LDL class around 14-15 mm.

The layering studies presented here prove that a careful balance in methanol and water concentration is necessary for the effective separation of bTRL and dTRL and maintenance of lipoprotein structural integrity. Further compositional analysis on the bTRL fraction separated in 50% methanol presented later provides more information in regard to lipoprotein stability in this solvent. The densities of the layering solution and gradient solution need to be sufficiently distinct for ease in layering and in the

prevention of density disruption for the dTRL class and gradient at the interface. Both acetonitrile and 50% methanol show promise as separation solvents for bTRL. It is important to determine the structural stability of the bTRL in these solvents prior to their establishment as solvents of choice for layering and separation of TRL.

Summary on Separation of bTRL and dTRL

In the examination of different layering solvents, both acetonitrile and 50% methanol in water show the greatest promise in terms of separating the least dense TRL subclasses in the form of CM and CMR, which have a densities less than 0.95 g/mL. These solutions can be layered on the meniscus following a density gradient ultracentrifugal separation with relative ease due to their difference in density with the density gradient solutions. Water offers the least clean separation of the TRL subclasses since it has a density in between the VLDL and CM. Also, water is not as easy to layer since its density is not as distinct from the density gradient solutions. However, lipoprotein particles are most stable in their structure in water. The structural stability of the TRL particles in acetonitrile and 50% methanol in water needs to be evaluated.

Apolipoprotein Analysis

Objective

TRL fractions isolated from density gradient ultracentrifugation following a freeze/cut recovery in liquid nitrogen were analyzed by gel electrophoresis for their apolipoprotein content. This technique was used to identify the bTRL and dTRL fractions and to determine the separation of apo B-48 containing TRL (CM and CMR) from apo B-100 containing TRL (VLDL and rVLDL).

SDS-PAGE Analysis

After isolating bTRL (in water and 50 % methanol), dTRL, and LDL fractions by density gradient ultracentrifugation, SDS-PAGE (sodium dodecyl sulfate polyacrylamide gel electrophoresis) was performed to analyze these lipoprotein classes for identification by apolipoprotein content. The following figure details the apolipoprotein content of these various subclasses along with a molecular weight ladder standard (phosphorylase b) and apo B-100 standard (Figure 29).
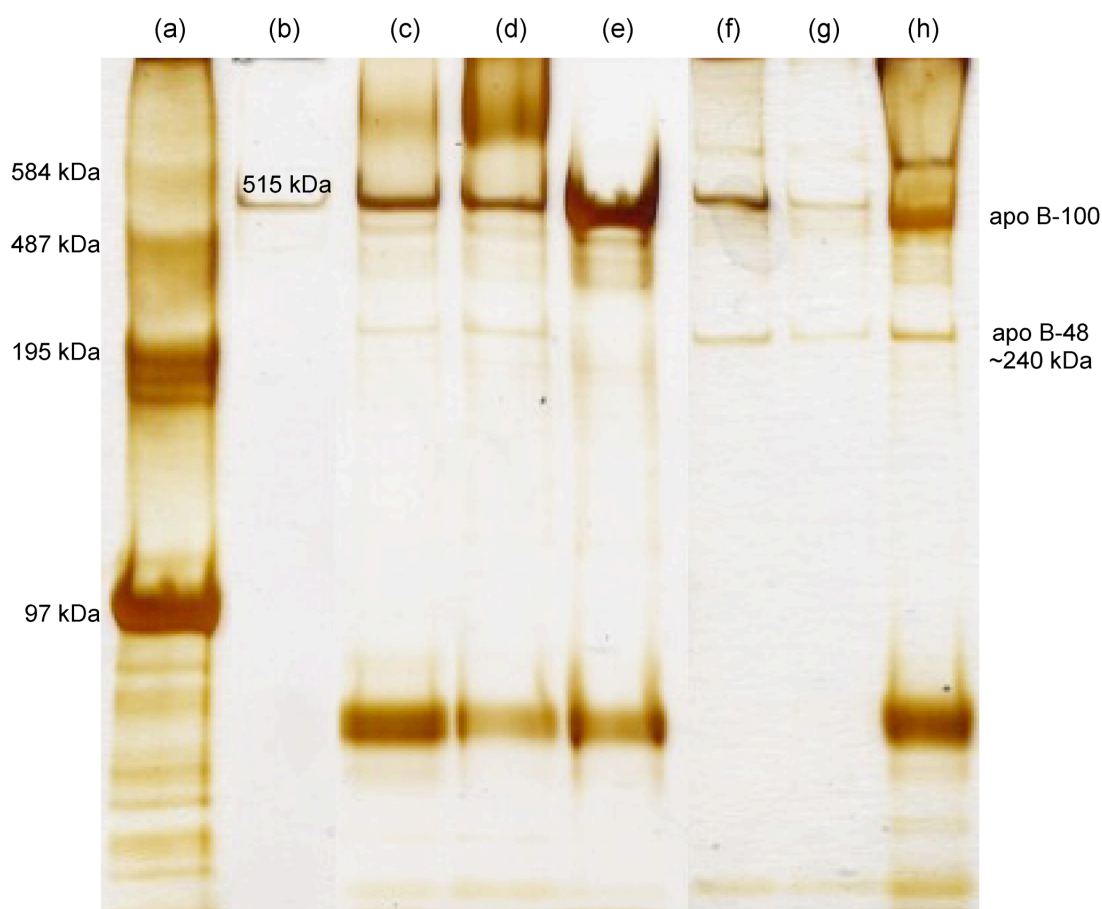
Figure 29. SDS-PAGE analysis of (a) phosphorylase b standard, (b) apo B-100 standard, (c) Subject 1 buoyant TRL, (d) Subject 1 dense TRL, (e) Subject 1 LDL, (f) Subject 2 buoyant TRL (water), (g) Subject 2 buoyant TRL (50% CH₃OH in H2O), and (h) Subject 2 dense TRL in a 3-8% tris-acetate gel.

The buoyant and dense TRL fractions were identified for their apolipoprotein

content by SDS-PAGE analysis as illustrated in Figure 29. Lanes (a) and (b) are the

phosphorylase b and apo B-100 standards respectively. These standards were used to

identify the apo B-100 and apo B-48 bands in the TRL and LDL fractions. The

molecular weights corresponding to the phosphorylase b standard are listed to the left of

the gel image in Figure 29. The apo B-100 standard has a molecular weight of 515 000

Da as shown in Figure 29, lane (b).

Lanes (c) and (f) show the apo B-48 and apo B-100 content of the buoyant TRL class in the meniscus separated by the layering of water in Subjects 1 and 2, respectively. Lane (e) is the LDL fraction from Subject 1 and was used as an experimental control. This fraction contains a large amount of apo B-100 and no apo B-48 as is expected of LDL particles. This helps determine the apo B-48 band in the bTRL and dTRL fractions along with molecular weight identification from the standards.

Lane (g) is a meniscus separation of TRL from Subject 2 by layering of 50% methanol in water ($\rho = 0.925$ g/mL). This separation shows great potential of further separating buoyant TRL from dense TRL in that the apo B-100 content was reduced in this fraction in comparison to the meniscus separation of buoyant TRL in water Figure 29, lane (f). The apo B-48 content does not change as significantly, which indicates that CM and CMR separate from the apo B-100 containing TRL (VLDL and rVLDL) fairly effectively in a 50% methanol in water layer.

Summary on Apolipoprotein Analysis

This analysis proves that the bTRL and dTRL fractions have a mixture of apo B-100 and apo B-48 containing lipoproteins. The separation by water layering does not separate CM and CMR from VLDL and rVLDL. However, the 50% methanol layering decreases the amount of apo B-100 at the meniscus and shows promise in providing a better separation. It is not clear from this analysis if the 50% methanol layer destroys some of the lipoprotein content. It is likely that density-based separation will not be most

suitable method for separating the TRL subclasses from each other.

RLP Cholesterol Determination

Objective

      A modified technique to determine RLP cholesterol was developed utilizing the RLP immunoseparation assay and an enzymatic cholesterol analysis. The challenge in this study was achieving a limit of detection suitable for the dilution of RLP isolated by the immunoseparation. Traditionally, RLP cholesterol isolated by the commercially available Polymedco kit is diluted 61-fold. Due to this dilution, RLP samples typically have cholesterol concentration below the limit of detection of traditional enzymatic cholesterol assays (oxidase-peroxidase assays). However a commercial kit which utilizes an enzymatic cycling method based on the rate of change in absorbance of two chromogenic products at 404 and 500 nm is very sensitive. This method involves the use of instrumentation that can measure multiple absorbance values as a function of time.[62]

Enzymatic Cholesterol Analysis

      The cholesterol content for RLP isolated by immunoseparation was determined by enzymatic cholesterol assay with visible spectroscopic detection. RLP was initially collected by the immunoseparation assay using three variable volumes of serum prior to the separation. Cholesterol analysis was performed following isolation of RLP in the 5 mM tris-HCl buffer. The following figure illustrates a calibration curve for prepared

cholesterol standards (Figure 30).
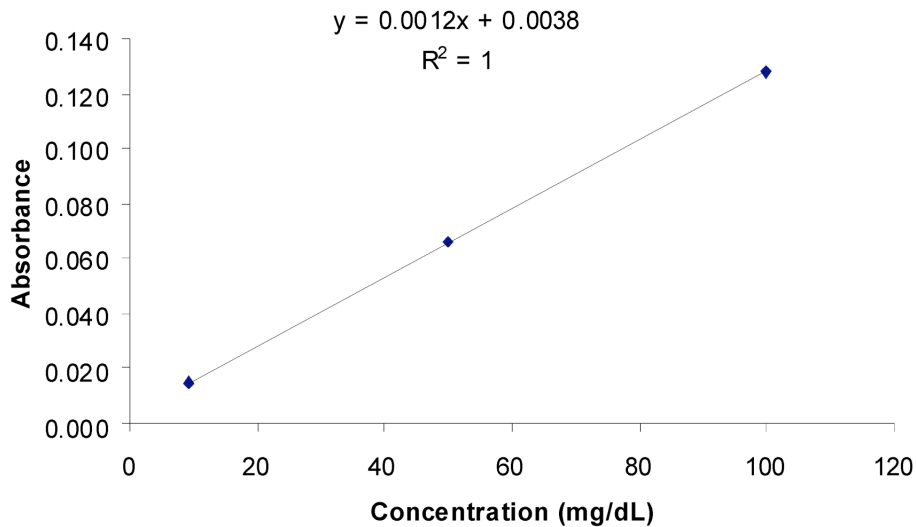
Figure 30. Calibration curve of cholesterol standards prepared in 0.05 M tris-HCl.

The cholesterol standards demonstrate linearity for the cholesterol analysis technique and cholesterol standard preparation. The following figure demonstrates the calibration for cholesterol concentration in RLP fractions from Subject 4 isolated by the RLP immunoseparation assay (Figure 31).
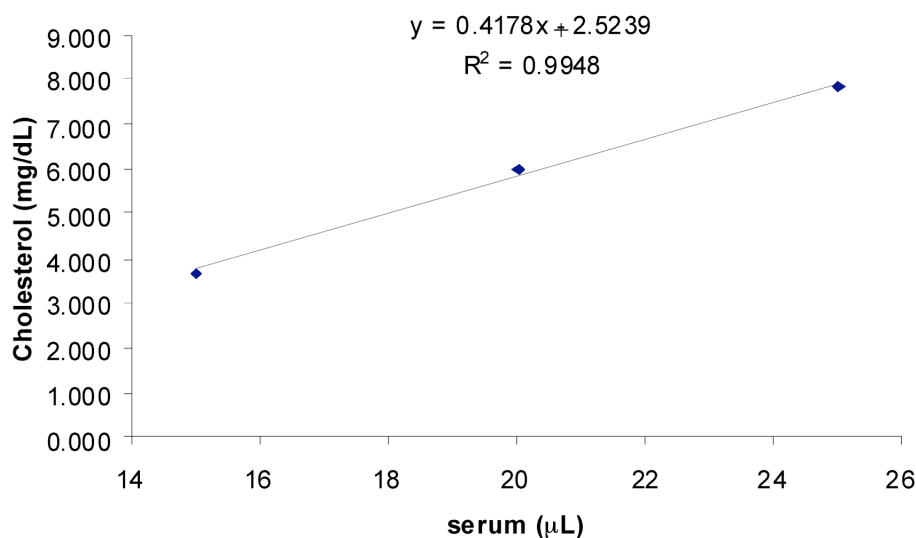
Figure 31. Calibration curve of cholesterol concentration of RLP fractions isolated from variable serum volume utilized in the RLP immunoseparation assay for Subject 4.

Again, a linear relationship exists between the amount of serum assayed in the RLP immunoseparation and the RLP cholesterol determined by this traditional enzymatic assay.

Typically, the RLP-cholesterol is determined by the Polymedco kit in conjunction with a chemistry analyzer from (Cobas MIRA S). The traditional RLP cholesterol determination involves incubation of the RLP immunoseparation assay in a mixer with built-in magnetic bars that drive steel beads up and down in each cup. After incubation, the supernatant (RLP, unbound fraction) is transferred for cholesterol analysis in a chemistry analyzer (Cobas MIRA S).[38]. With RLP-cholesterol, as isolated by the Polymedco assay, a detection limit of 0.12 mg/dL is needed since the samples are diluted 61-fold.[19] An enzymatic cycling method is utilized in the determination of RLP-

cholesterol. In this customary analysis, cholesterol ester hydrolase hydrolyzes esterified

cholesterol to free cholesterol and fatty acids. The cholesterol is then reversibly oxidized

in the presence thio-NAD and thio-NADH. The thio-NADH is measured by change in

absorbance per minute at 404 and 500 nm to measure the cholesterol concentration.[62]

However, as presented here, RLP-cholesterol can be measured by increasing the

amount of serum used in the assay to 15-25 µL out of a total of 300 µL in the assay. The

dilution factor then becomes, at the least, only 20-fold, and a traditional enzymatic

cholesterol assay may be used to detect the cholesterol in the RLP fraction as shown in

Figure 31. The following figure shows that in Subject 4, the incubation of 20 µL of

serum in the RLP immunoseparation assay still effectively removes the non-RLP content

(Figure 32).
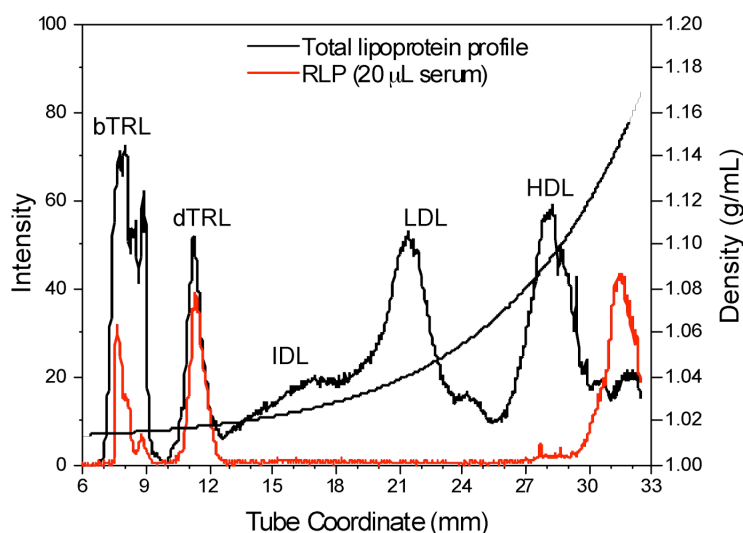
Figure 32. Lipoprotein and RLP density profiles in CsBiEDTA following the layering of water for Subject 4.

Since non-RLP components are removed with a 20 µL serum volume in the immunoseparation assay, the total RLP-cholesterol value can be extrapolated from the 15 µL value (3.66 mg/dL) in Figure 31 by multiplying it by its dilution (15 µL of serum in 300 µL) or 20. Therefore, the RLP-cholesterol value for Subject 4 is determined at a concentration of 73.2 mg/dL.

Summary on RLP Cholesterol Determination

This value would have to be compared against the RLP-cholesterol value determined by the traditional method, which is approved by the Food and Drug Administration, to determine its accuracy. This form of analysis shows potential to determine RLP-cholesterol clinically without the necessity of a cycling enzymatic assay detector. Instead, a ultraviolet-visible light spectrophotometer in conjunction with commercially available cholesterol enzymatic assays would suffice in this measurement.

Triacylglycerol Distribution

<u>Objective</u>

The triglyceride content as well as the MAG (monoacylglycerol), DAG (diacylglycerol), and glycerol content were measured in different lipoprotein fractions separated by density gradient ultracentrifugation. These values were used to determine percent distribution throughout the lipoprotein classes as a function of density. This analysis is important since triglyceride-rich lipoproteins are involved in the metabolism of dietary fats and contain most serum triglycerides.[11] Also, the TRL class has a specific temporal sequence in its formation, metabolism and clearance pathways.[5] Since TRL have complex interactions with other lipoprotein particles, it is of interest to be able to measure the lipid content of all the lipoprotein classes at any given time in a subject's serum sample.

<u>Enzymatic Triglyceride Analysis</u>

After collecting the lipoprotein fractions by freezing in liquid nitrogen and subsequent slicing, each fraction was analyzed for triglyceride and free glycerol content. After obtaining these raw concentration values, the mass of triglyceride content for each fraction was also determined and divided by the total mass of triglycerides that were ultracentrifuged to determine percent recovery.

Lastly, the distribution of the triglycerides was determined by assuming a 100% recovery and multiplying each fraction by its dilution coefficient. The following figure

details the distribution of true triglycerides in a fasting serum sample from Subject 2 (Figure 33).
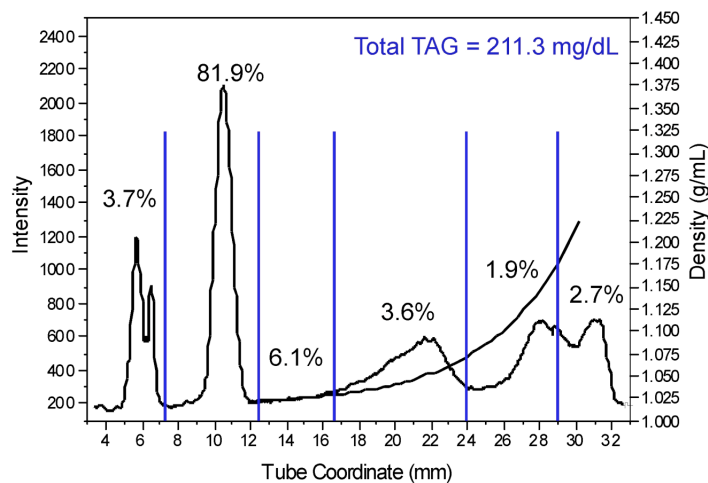
Figure 33. Triacylglycerol distribution as a function of density in a fasting serum sample from Subject 2.

As seen in this figure, the measured total true triglyceride concentration for this subject was 211.3 mg/dL in the fasting state. The percentages detailed in this figure represent the distribution of this total concentration in different lipoprotein subclasses as a function of density. It is clear from this analysis that the majority of triglycerides are carried in the dTRL fraction at a percentage of 81.9%.

When the bTRL fraction was collected by aspiration, the bTRL fraction had less absolute TAG content. The aspirated fraction contained 86% of the triglyceride mass in the bTRL fraction collected by freezing and cutting. The freeze/cut method was adopted for the analyses due to greater percent recovery. The analyses for the fasting serum sample had a total 73.5% recovery by mass with the freeze/cut method. To establish a

distribution trend, it was assumed that the recovery was consistent throughout the tube.

The following figure depicts the percent distribution from the free glycerol measurement

of the fasting serum from Subject 2 (Figure 34).
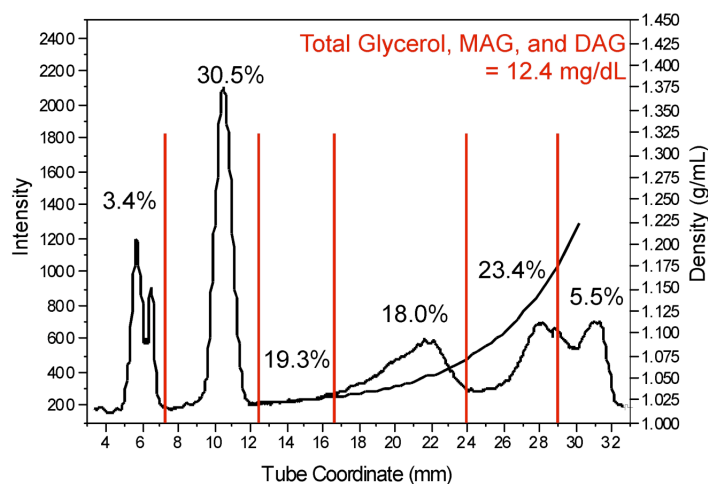
Figure 34. Glycerol, MAG, and DAG distribution as a function of density in a fasting serum sample from Subject 2.

The free glycerol measurement takes into account more than just free glycerol

since monoacylglycerols (MAG) and diacylglycerols (DAG) have an available free

hydroxyl group for phosphorylation in the first step of the free glycerol measurement.

Since most samples do not have significant glycerol content,[60] it is assumed that this

measurement accounts for the other products of the catabolism of triglycerides in the

form of MAGs and DAGs. The total concentration from this measurement is relatively

small when compared to the triglyceride concentration value.

In the fasting state, most of these metabolic intermediates appear in the dTRL

fraction; however, a significant percentage is distributed in the HDL, IDL, and LDL

subclasses as well. The least percentage of glycerol, MAG, and DAG content is located in the bTRL subclass. The following figure illustrates the TAG distribution as a function of density in a postprandial serum sample from Subject 2 collected 5 hours after a high-fat meal (Figure 35).

Figure 35. Triacylglycerol distribution as a function of density in a postprandial serum sample from Subject 2.

In this postprandial state, the total TAG value increases dramatically from 211.3 mg/dL to 287.5 mg/dL. Another difference that is visible in Figure 35 is the distribution of this TAG content in the different lipoprotein subclasses. The bTRL here carries a higher percentage of the TAG content at 9.5% as compared to 3.7% in the fasting state (Figure 33). The dTRL carries 65.5% diminished from 81.9% in the fasting state.

Interestingly, the LDL and HDL subclasses carry a greater percentage of TAGs in the postprandial state when compared to their contribution in the fasting state. LDL carries 8.8% in comparison to 3.6% of the TAG in the fasting state, and the HDL carries

5.2% in comparison to 1.9% of the TAG in the fasting state. Moreover, part of the HDL

is also found in the bottom fraction in this density separation, and so, the TAG content

increases to 5.7% in the postprandial state for dense HDL in comparison to 2.7% in the

fasting state. HDL carries a significant portion of the TAG in the postprandial state when

both these fractions are taken into consideration.

Again, the analyses for the postprandial serum sample had a 73.7% recovery by

mass, and to establish distribution trends, it is assumed that the recovery was consistent

throughout the tube. The following figure shows the glycerol, MAG, and DAG

distribution as a function of density in the postprandial state for Subject 2 (Figure 36).

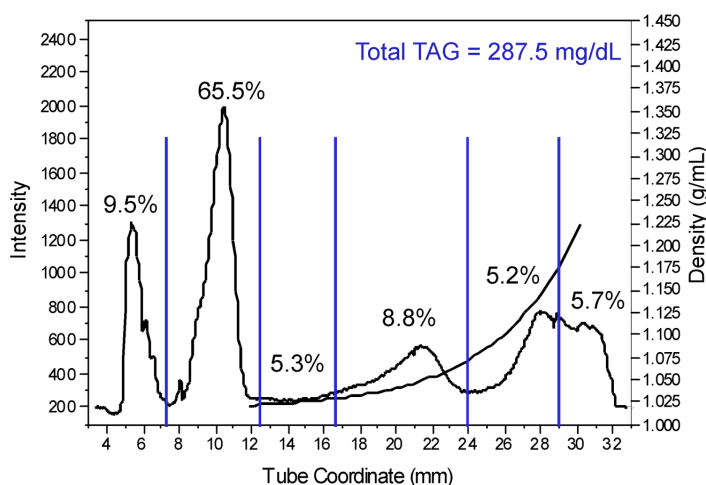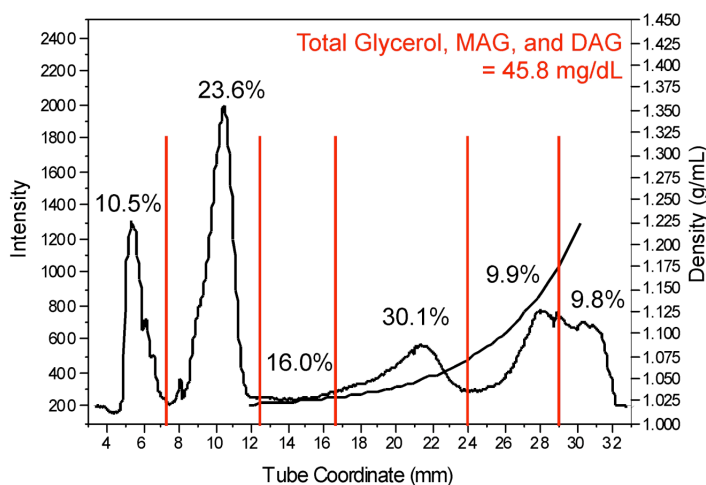**Figure 36. Glycerol, MAG, and DAG distribution as a function of density in a postprandial serum sample from Subject 2.**

In the postprandial state, the free glycerol measurement results in a higher

concentration of 45.8 mg/dL when compared to the fasting state value of 12.4 mg/dL.

Since this is the postprandial state, it is more likely that this measurement accounts for

MAG and DAG content.

The distribution trend in the postprandial state for these catabolic intermediates is very different from the fasting state. First of all, the majority of the MAG and DAG content is now found in LDL at 30.1% in comparison to 18.0% in the fasting state where the dTRL carried the majority of the glycerol/MAG/DAG content at 30.5% as well. In this postprandial state, the dTRL contain 23.6% and the bTRL contain 10.5% of the glycerol/MAG/DAG content. The bTRL in the fasting state only carried 3.4%. Interestingly, together the bTRL and dTRL fractions carry the same percentage of the glycerol/MAG/DAG content in both the postprandial (34.1%) and fasting (33.9%) states.

The contribution of IDL does not change significantly from 19.3% in the fasting state to 16.0% in the postprandial state. Therefore, the major changes in the distribution can be accounted for among the LDL, HDL and dense HDL subclasses. The dense HDL increases to 9.8% of the glycerol/MAG/DAG burden in the postprandial state from 5.5% in the fasting state.

Another interesting trend in this analysis was in the integrated fluorescence intensities for the TRL fractions of the fasting state. When the fluorescence intensity of the bTRL and dTRL are integrated they account for 21.8% and 78.2% of the fluorescence intensity in the TRL. The percent distributions of total TAG concentration for the bTRL and dTRL fractions are 18.2% and 81.8% respectively of the total TRL class. The total TAG distribution correlates to the integrated fluorescence intensity distribution for the bTRL and dTRL classes. This trend is not observed for the other lipoprotein fractions. This correlation also does not occur for the bTRL and dTRL in the

postprandial state. This is most likely due to the fact that the TRL may be closer to saturation with NBD C_6-ceramide in the fasting state than in the postprandial state.

This observation indicates that NBD C_6-ceramide correlates with the hydrophobic content of a particle and exhibit preference for more hydrophobic particles. This is the case with TRL as they consist primarily of TAG. Further studies that take into account saturation conditions of NBD C_6-ceramide and TRL are necessary to establish this correlation as well as to determine the correlation of the fluorescence in other lipoprotein subclasses with their hydrophobic content.

Summary on Triacylglycerol Distribution

The trends in TAG distribution and glycerol/MAG/DAG distribution are interesting from a metabolic perspective. The changes in this distribution may provide information regarding the mechanism through which plasma triglycerides promote cardiovascular disease since there is little understanding to their indirect role.[4] Monitoring the distribution of the TAG and their catabolic products as a function of density is important in regard to understanding and diagnosing the atherogenic lipoprotein phenotype, which is associated with hypertriglyceridemia and small dense LDL and HDL. This combination of phenotypes increases cardiovascular disease risk.[4] In fact, elevated triglycerides in conjunction with low HDL-cholesterol is a very common lipid disorder and causes more documented cases of coronary artery disease than familial hypercholesterolemia, which is associated with elevated LDL.[81]

A similar technique allows for the measurement of the TAG distribution

following a density gradient separation of lipoprotein subclasses from a potassium bromide salt gradient.[61] The technique presented here allows for a more specific diagnosis in that the distribution of the TAG content and glycerol/MAG/DAG content is also available with total triglyceride and density data. In addition, the clearance of TAG content can potentially be monitored by this technique, which is important since the cardioprotective role of HDL can be monitored as a function of its metabolic role in the transport of dietary triglycerides and triglyceride metabolic products in the hours after a meal.

Lastly, since NBD C_6-ceramide fluorescence in a TRL particle correlates to its triglyceride content, the necessity of this form of analysis may potentially be eradicated. Instead, the integrated fluorescence intensity of TRL particles may be potentially be measured and used to determine the triglyceride level in a subject's serum sample without the use of expensive enzymatic assay reagents. This would still allow for a measurement of triglyceride content of TRL particles as a function of density.

In vitro *Lipolysis*

Objective

In this study, serum samples were incubated with lipoprotein lipase to induce triglyceride hydrolysis in an *in vitro* setting. These serum samples were then examined by density gradient ultracentrifugation to determine changes in the lipoprotein density profile as well as subsequent triglyceride distribution analysis to determine the extent of

triglyceride hydrolysis and generation of glycerol/MAG/DAG in the lipoprotein

fractions isolated by density gradient ultracentrifugation. This study allows a simplified

in vitro analysis out of circulation of the complex interaction of LpL with TRL particles

in vivo.

Determination of Incubation Time and LpL Concentration

       Different concentrations of lipoprotein lipase with fasting serum from Subject 1

were examined for different incubation intervals. The following figure illustrates the

effect of increasing LpL concentration in a 2-hour incubation period on the total

lipoprotein profile for Subject 1 (Figure 37).

Figure 37. Changes in the total lipoprotein profile following a 2 hour incubation with different concentrations of lipoprotein lipase for fasting serum from Subject 1

       Dramatic changes following a 2-hour incubation with varying concentrations of

LpL are evident in Figure 37. The bTRL fraction changes the least visibly due to minimal lipoprotein content at this density from the fasting serum sample of this subject. The dTRL fluorescence intensity decreases dramatically with increasing concentrations of LpL; whereas, the fluorescence intensity of the LDL initially decreases, increases slightly, and then dramatically increases in fluorescence intensity from the control assay of 0 U/μL to the assay of 0.25 U/μL of LpL. This may be attributed to the conversion of VLDL particles to LDL upon lipolysis. The LDL subclass also shifts to a higher tube coordinate at a higher density.

In addition, many changes are perceptible in the HDL class. The intensity initially increases, stabilizes, and then dramatically increases with the 0.25 U/μL LpL assay. Again, this dramatic change in fluorescence intensity is not due to the synthesis of HDL particles in this *in vitro* setting, but rather a change in the lipid content of HDL upon lipolysis of TRL particles. The dense HDL/protein content has a consistent decrease in fluorescence intensity in concert with the increase in LpL concentration. The following figure illustrates the changes in the total lipoprotein profile of fasting serum from Subject 1 following an incubation of 4 hours (Figure 38).
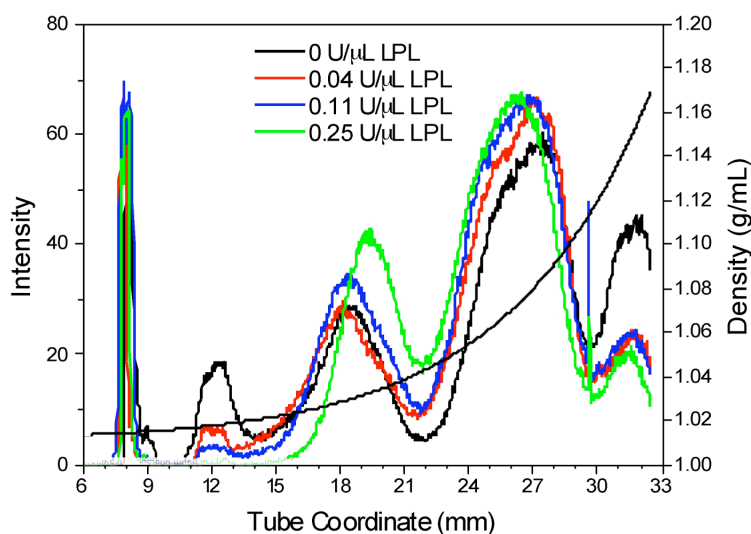
Figure 38. Changes in the total lipoprotein profile following a 4 hour incubation with different concentrations of lipoprotein lipase for fasting serum from Subject 1.

Again, similar trends to the 2-hour incubation are seen here. The bTRL exhibit stable fluorescence intensities for the varying LpL concentrations. The dense TRL exhibit less fluorescence intensity due to lipolysis in order of increasing LpL concentration. On the other hand, the LDL fluorescence intensity directly correlates to increasing LpL concentration. In addition, at an LpL concentration of 0.25 U/µL, the LDL shifts to a tube coordinate corresponding to a higher density. The HDL intensity is also directly related to LpL concentration in the assay. These trends indicate a shift in triglyceride content from the dTRL to HDL and a conversion of VLDL to LDL. Lastly, the serum protein intensity decreases as the LpL concentration increases. The figure below represents the changes in the total lipoprotein profile following 6 hours of incubation with the varying LpL concentrations (Figure 39).
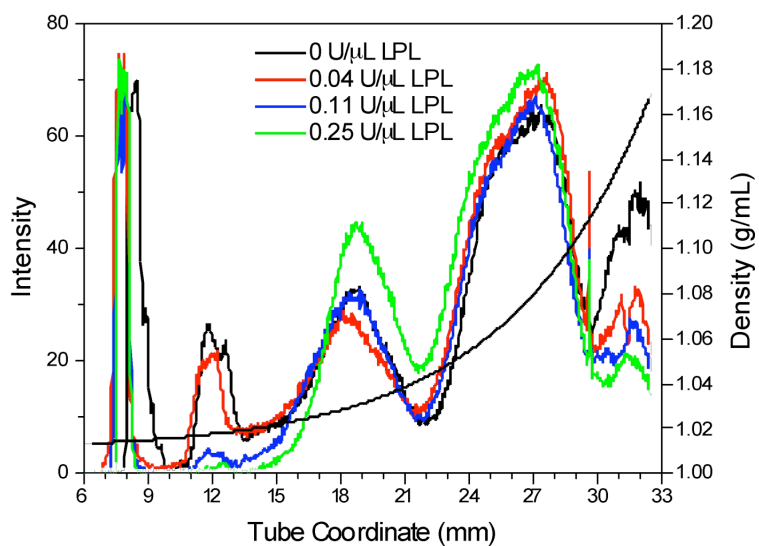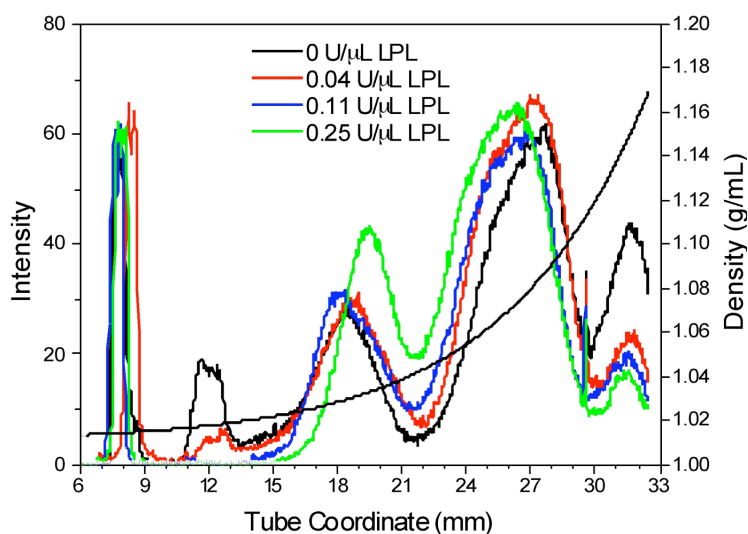
Figure 39. Changes in the total lipoprotein profile following a 6 hour incubation with different concentrations of lipoprotein lipase for fasting serum from Subject 1.

Following a 6-hour incubation period, the dTRL exhibit no fluorescence intensity due their complete hydrolysis in the assays with the 0.11 U/µL and 0.25 U/µL concentrations of LpL. Again, the bTRL intensity is fairly stable. LDL fluorescence intensity again follows the same direct relationship with LpL concentration with a significantly more dramatic shift in density in the assay with 0.25 U/µL LpL concentration. HDL, too, exhibits the exact same trend with a shift to lower density in the assay of 0.25 U/µL LpL concentration. This shift in density is not apparent at the 2 hour and 4 hour incubation profiles (Figure 37 and Figure 38). The subsequent figure illustrates the final incubation period at 8 hours (Figure 40).
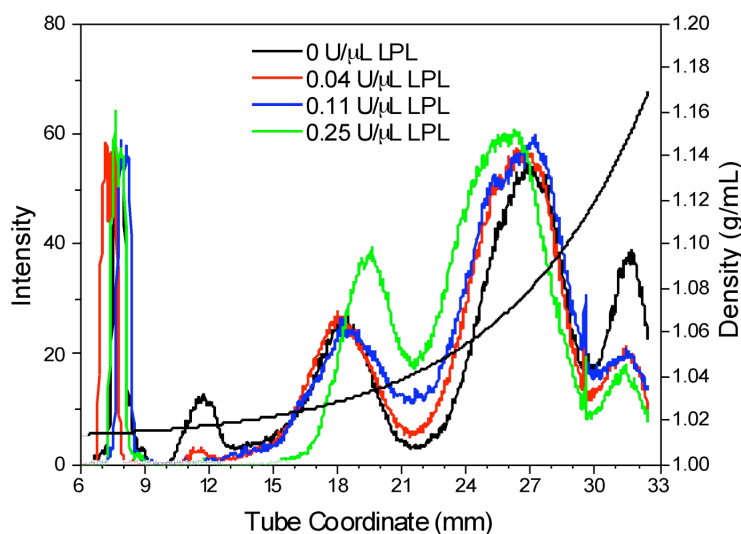
Figure 40. Changes in the total lipoprotein profile following an 8 hour incubation of fasting serum from Subject 1 with different concentrations of lipoprotein lipase.

As seen in the previous figures, the bTRL intensity does not change. The dTRL intensity decreases as a function of increasing LpL concentration in each assay. At the eighth hour, all of dTRL fluorescence intensity vanishes for the assays with 0.11 U/µL and 0.25 U/µL. Even the assay with 0.04 U/µL LpL shows a significant drop in fluorescence intensity for the dTRL. Interestingly, the fluorescence intensities of the LDL subclass do not change significantly in the control assay (0 U/µL) and the assays of the two lower LpL concentrations. Again, the 0.25 U/µL of LpL causes a dramatic shift in density for the LDL as well as an increase in fluorescence intensity. Lastly, changes in the HDL fluorescence intensity follow the same trend as before with a shift to lower density in the assay of 0.25 U/µL of LpL.

Triglyceride Distribution Following *in vitro* Lipolysis

In vitro lipolysis assays with the 0 U/µL LpL (control) and 0.11 U/µL LpL with shorter varied incubation periods of 30 minutes, 60 minutes, 90 minutes and 120 minutes were applied to fasting serum samples. In this study, serum from both Subject 1 and Subject 2 were examined for subject variation. The density profile of Subject 1 was stable at 2 hours with the 0.11 U/µL of LpL as seen in Figure 37. Here, 30 minute intervals of lipolysis were examined in these two subjects up to 2 hours.

Serum and LpL or serum and water were separated by density gradient ultracentrifugation in 0.2 M NaBiEDTA. Following the separation, fractions were collected by the freeze/cut manner described before and percent distribution of triglycerides was determined for the fasting serum of Subject 2. The following figure illustrates the changes in the total lipoprotein profile following a 30 minute incubation with water or 0.11 U/µL of LpL for Subjects 1 and 2 (Figure 41).

Figure 41. Changes in the total lipoprotein profile in NaBiEDTA following a 30 minute incubation with 0.11 U/µL of lipoprotein lipase for fasting serum from (a) Subject 2 and (b) Subject 1.

Greater changes in the lipoprotein profile are apparent from incubation with LpL in Subject 2's profile than Subject 1's profile. The bTRL and dTRL in Subject 2's profile (Figure 41a) increases in fluorescence height intensity upon lipolysis. The LDL gains fluorescence intensity and shifts to a lower density and lower tube coordinate as does the HDL. The dense HDL/protein area loses fluorescence intensity upon lipolysis. Subject 1 has a more stable density profile (Figure 41b). The bTRL maintain fluorescence intensity upon lipolysis, and the dTRL lose a small amount of intensity. LDL fluorescence intensity in this subject remains stable, and the HDL gain an insignificant amount of fluorescence intensity. Again, the dense HDL/proteins lose fluorescence intensity upon lipolysis. The following figure illustrates the changes in the lipoprotein profiles after a 60-minute incubation period (Figure 42).

Figure 42. Changes in the total lipoprotein profile in NaBiEDTA following a 60 minute incubation with 0.11 U/µL of lipoprotein lipase for fasting serum from (a) Subject 2 and (b) Subject 1.

Again, changes in the lipoprotein profile for Subject 2 are more dramatic than in Subject 1's profile. As seen in Figure 42a, the bTRL gain fluorescence intensity upon lipolysis at 60 minutes. This increase in fluorescence intensity may be attributed to a higher triglyceride concentration in this subject's serum for which the conversion of TAG to MAG and DAG may delay their movement out of the TRL particles. The dTRL have a fairly stable fluorescence intensity but shift to a higher density at a lower tube coordinate. The LDL and HDL exhibit the same trend as before with an increase in fluorescence intensity and a shift to a lower density at lower tube coordinates. This result may be attributed to the movement of TAG, MAG, and DAG to HDL and a conversion of the VLDL to LDL particles as well. Subject 1's density profile in Figure 42b proves to be a good control as the fluorescence intensity of the bTRL and LDL remain constant. The fluorescence intensity of the dTRL decreases further in concert with a slight increase in fluorescence intensity for the HDL fraction. This subject's profile reveals itself as a simpler model for lipolysis and the movement of TAG, MAG, and DAG content to HDL. Subject 2's profile in Figure 42a proves to be more complex. The following figure exhibits the changes in these two subjects' profiles following a 90-minute incubation period (Figure 43).
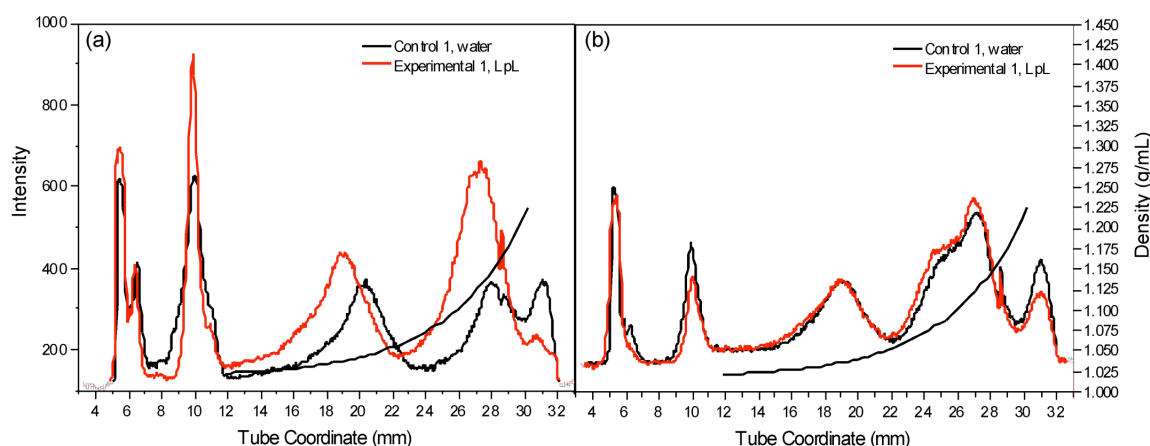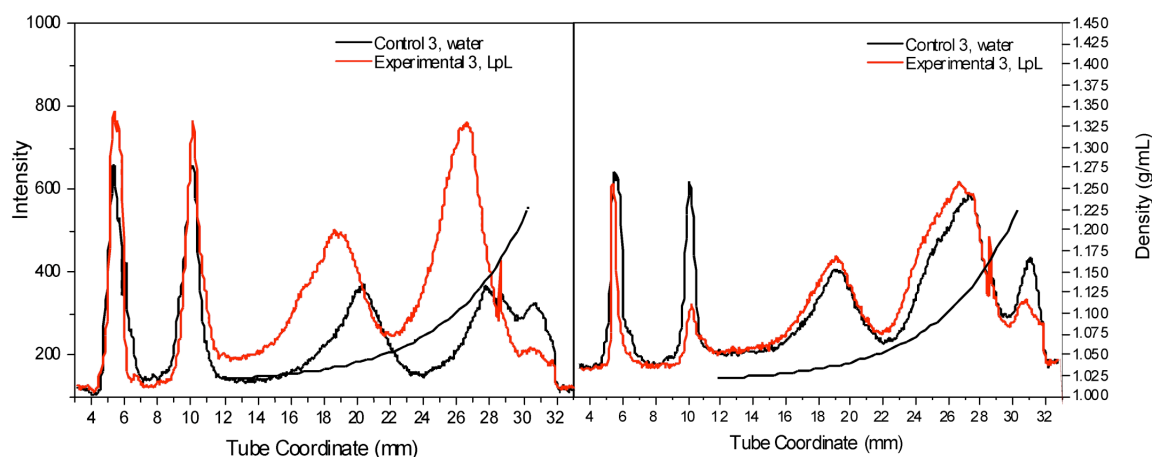
Figure 43. Changes in the total lipoprotein profile in NaBiEDTA following a 90 minute incubation with 0.11 U/µL of lipoprotein lipase for fasting serum from (a) Subject 2 and (b) Subject 1.

Again, Subject 2's density profile, Figure 43a, exhibits more complex phenomena with lipolysis. The bTRL and dTRL fluorescence intensities do not vary greatly from the previous 60-minute incubation period. Again, the LDL and HDL exhibit an increase in fluorescence intensity as well as a shift to lower density and a lower tube coordinate. The cessation of changes in fluorescence intensity may be due to a saturation of TAG content in HDL, in which case the lipolytic products cannot move out of the TRL fractions. This is an interesting finding in that it partially mimics the ability of this subject's HDL to process triglycerides and inherently its cardioprotective role when there is no HDL generation. On the other hand, the density profile of Subject 1 follows a continual trend with a decrease in dTRL intensity and an increase in HDL fluorescence intensity. The final incubation period with this concentration of LpL for these two subjects is presented in the following figure (Figure 44).
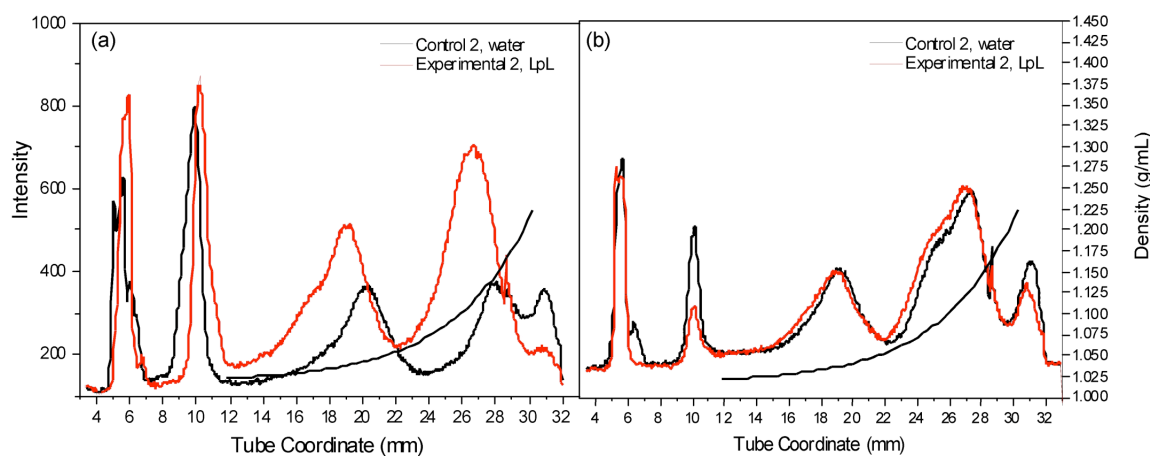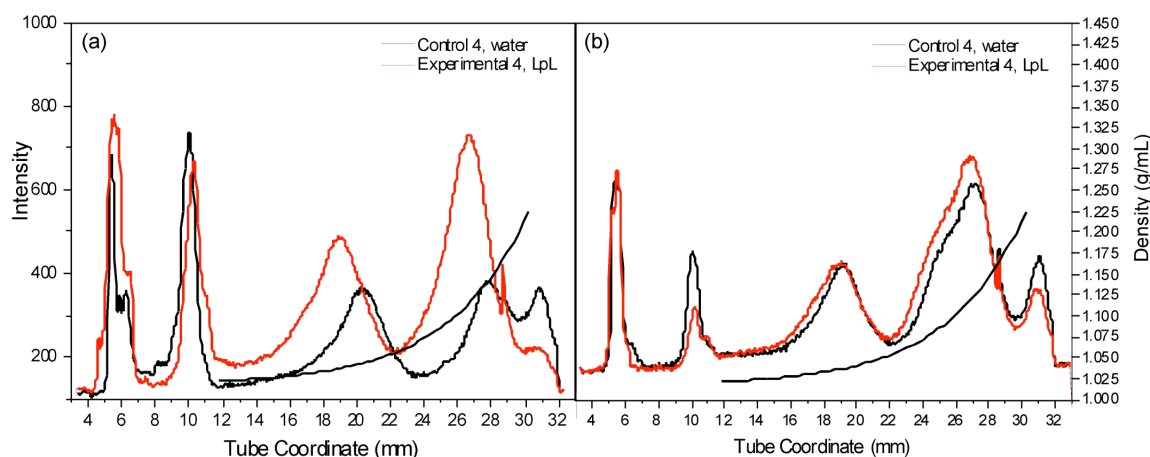
Figure 44. Changes in the total lipoprotein profile in NaBiEDTA following a 120 minute incubation with 0.11 U/µL of lipoprotein lipase for fasting serum from (a) Subject 2 and (b) Subject 1.

Again, the same trends in both Subjects are observed in these density profiles. Subject 2's dTRL loses some fluorescence intensity here, and the LDL shifts to a lower density more significantly. In Subject 1's profile (Figure 44b), the HDL has an increase in fluorescence intensity in conjunction with a decrease in the fluorescence intensity of the dTRL. In this subject, the cardioprotective role of HDL as a receptacle for triglycerides seems to hold.

Lastly, the triglyceride distribution for the 1 hour control (0 U/µL LpL) and experimental (0.11 U/µL) assays for Subject 2 were determined by fraction collection and subsequent enzymatic analysis in the manner described previously. Figure 45 displays the changes in the TAG distribution and glycerol/MAG/DAG distribution for these two assays.
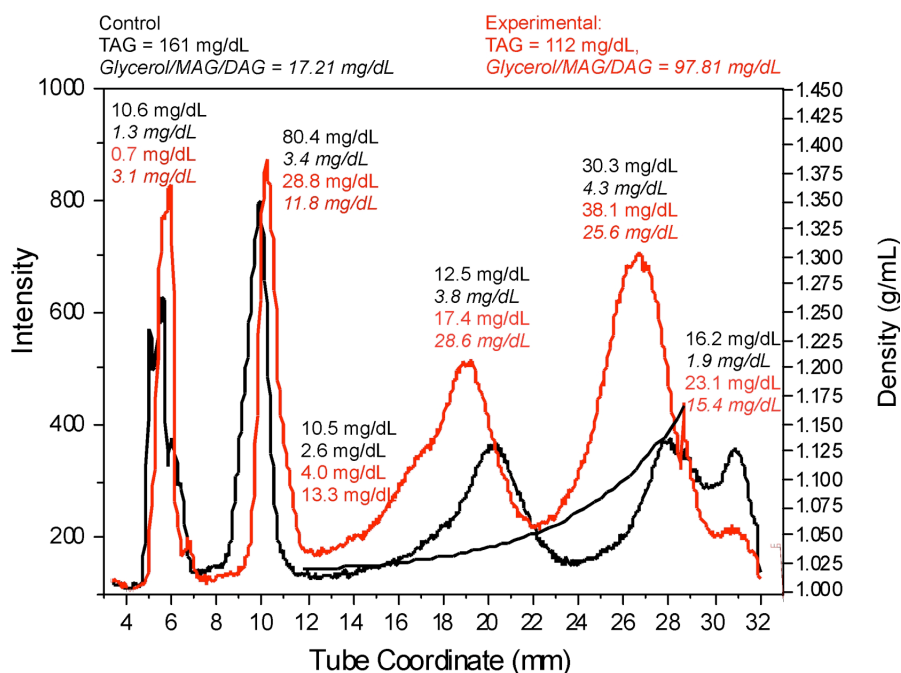
Figure 45. Changes in TAG and Glycerol/MAG/DAG concentration in lipoprotein subclasses separated by DGU in NaBiEDTA following in vitro Lipolysis by LpL.

In Subject 2's density profile we can see the increase in intensity of the LDL and buoyant HDL classes, which correlates to the increase in the concentration of TAG and lipolysis products in both fractions. The buoyant HDL clearly contain a higher concentration of these particles in the control and lipolyzed samples, which correlates with a greater intensity in the buoyant HDL. Due to the separation conditions of NaBiEDTA, denser HDL separates below the seam in the tube, and so, TAG and lipolysis products are detected in the bottom fraction as well in lower concentrations.

In all the TRL fractions (bTRL, dTRL, and IDL), the overall TAG concentration decreases due to lipolysis, but the concentration of lipolysis products increases. The reason that total TAG and glycerol/MAG/DAG concentrations do not sum up to the

same total in the control and experimental assays is probably inherent to the mechanism of the assay. Though the free glycerol analysis can account for MAG and DAG concentrations, phosphorylation of the hydroxyl group on the first position may have a decreased probability of reaction due to steric hindrance. If this occurs, this value may be an underestimation. Therefore, it is expected that following *in vitro* lipolysis, more of the MAG, DAG, and TAG are converted to glycerol increasing the responsiveness of the assay to this particular measurement.

Summary on *in vitro* Lipolysis

Overall, much information about the metabolic features of the different lipoprotein subclasses can be examined by this technique. We can observe changes in density and core TAG and lipolysis product content from density gradient ultracentrifugation coupled to enzymatic analyses. This method provides us with fundamental information regarding the behavior and metabolic interactions among the particles in an *in vitro* setting mimicking the *in vivo* interactions. The method also furthers and elaborates the phenotypic qualities associated with the Atherogenic Lipoprotein Phenotype (ALP), which is characterized by elevated TAG level, dense LDL, and dense HDL.[6] This technique also presents, potentially, a more specific diagnostic tool for ALP and susceptibility to hypertriglyceridemia.

In addition, this study shows the variability in the susceptibility to lipolysis in two different subjects. At the time of this study, Subject 1 had a non-vegetarian diet and Subject 2 had a vegetarian diet. Also, Subject 2 had normal triglyceride levels,

diagnosed clinically, and Subject 1 had elevated triglycerides. The changes seen in the density profiles following the *in vitro* lipolysis may be attributed to differences in the diets of these two subjects as well as their triglyceride levels.

The limitations and also controls of this study are the lack of nascent formation of LP particles in response to the perturbation as well as the clearance and movement of these particles in circulation and in the liver.

From this study, we also gain understanding of the relationship of NBD fluorescence intensity and hydrophobic content of lipoprotein particles. NBD fluorescence intensity seems to correlate with the major nonpolar class in each lipoprotein. In the case of LDL, there may be an increase in particle number due to the conversion of VLDL to LDL upon lipolysis. This could partially explains the increase in the intensity in this region, which also correlates to an increase in the general TAG and lipolysis products concentration as well. LDL is also involved in the shuttling of TAGs from VLDL to LDL.[4] The conversion of VLDL to LDL particles may be proven in the future by assaying the LDL for apo B-100 concentration for quantification purposes.

This study proves the feasibility of monitoring the lipolysis of triglycerides *in vitro* by the addition of lipoprotein lipase to simulate lipolysis that occurs *in vivo*. This tells us whether there is enough LpL in a subject's serum to complete the hydrolysis reaction by the point the fasting state is achieved. We can also study the movement of TAG and lipolysis products (Glycerol/MAG/DAG) among the different lipoprotein subclasses in order to assess the efficacy of LpL, the conversion of VLDL→LDL, and the cardio-protective role of HDL, specifically buoyant HDL.

TRL Analysis by Capillary Zone Electrophoresis

Objective

Intact triglyceride-rich lipoprotein fractions were further characterized by

capillary zone electrophoresis after collection from preparative density gradient

ultracentrifugation in 20% (w/v) sucrose. The different TRL classes were examined by

CZE in order to define subclasses by electrophoretic mobility.

Fraction Collection

The following figure shows the separation of TRL in a 20% (w/v) sucrose

density gradient (Figure 46).
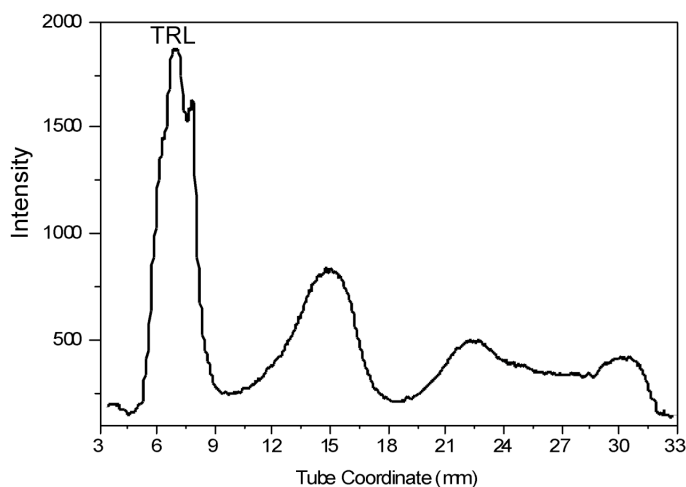
Figure 46. Separation of intact TRL in preparative ultracentrifugation in 20% (w/v) sucrose.

The TRL that separated at the meniscus in the separation depicted in Figure 46,

were collected by freezing in liquid nitrogen and subsequently slicing out as described before. This fraction was not subjected to any additional separation by layering and so contained a mixture of bTRL and dTRL particles together.

CZE Separation of TRL in 12.5 mM Sodium Borate BGE Solution on P/ACE Model 5510 Capillary Electrophoresis Instrumentation

The TRL fraction in this preparative separation was collected and concentrated for analysis by capillary zone electrophoresis. The fractions were first analyzed in a 12.5 mM sodium borate in water uniform electrolyte solutions in a Beckman P/ACE Model 5510 capillary electrophoresis instrument equipped with a photodiode array detector (Beckman Coulter, Inc.).

Deionized water was injected (8 seconds) as an electroosmotic flow marker (EOF) followed by a sample injection of 10-15 seconds at 17 kV for variable electrophoretic separation time periods. Fractions corresponding to the lipoprotein subclasses were detected at 214 nm for their relative migration time, electrophoretic mobilities, and intensities.

The figure below is an example of an electrophoretic separation of an intact TRL fraction separated in a 12.5 mM sodium borate in water BGE (background electrolyte) solution (Figure 47).
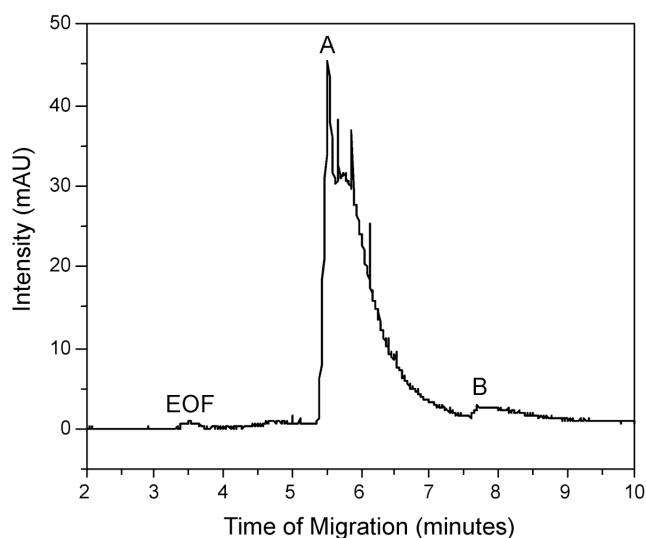
Figure 47. Separation of intact TRL by capillary zone electrophoresis in a 12.5 mM sodium borate background electrolyte solution detected at 214 nm.

The sodium borate BGE solution does not offer an effective separation of the TRL class as evidenced in Figure 47. The TRL class of lipoproteins is a complex mixture of CM, CMR, VLDL, and rVLDL; yet, the electrophoretic separation offers only two major fractions, A and B, around -21.7×10^{-5} cm^2/Vs and -31.6×10^{-5} cm^2/Vs respectively. The effective mobility is determined by the following equation.[72]

$$\mu_{eff} = \frac{L_c L_d}{U} \left(\frac{1}{t} - \frac{1}{t_{EOF}} \right)$$

(Equation 5)

In this equation the L_c and L_d represent the length of the capillary and the length of the capillary to the detector window respectively. The values t and t_{EOF} represent the time of migration of the peak of interest and the electroosmotic marker or water in this case.[71]

The resolution between fractions A and B is also not very effective as fraction A exhibits a tailing effect that runs into fraction B. Intact RLP isolated from the RLP immunoseparation assay was collected by preparative density gradient ultracentrifugation in 20% (w/v) sucrose in the same manner as the intact TRL. The following figure displays the electrophoretic separation of intact RLP in 12.5 mM sodium borate in water BGE solution (Figure 48).
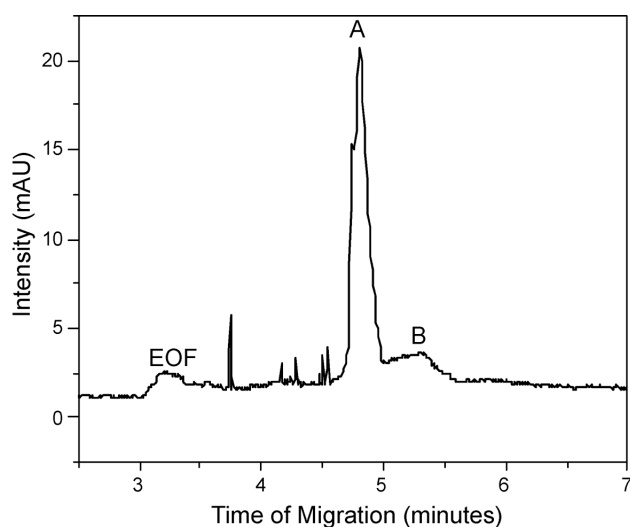
Figure 48. Separation of intact RLP by capillary zone electrophoresis in a 12.5 mM sodium borate background electrolyte solution detected at 214 nm.

A similar separation result to the intact TRL class is observed here. The intact RLP separate into two major fractions (A and B) as seen in Figure 48. These two fractions have electrophoretic mobilities at approximately -20.1×10^{-5} cm^2/Vs and -33.4×10^{-5} cm^2/Vs. The two fractions have slightly better resolution than in TRL most likely due to lipoprotein concentration. These fractions exhibit similar mobilities to the intact

TRL at overall lower intensities due to a lower concentration of RLP collected from serum.

The low resolution of the TRL subclasses in the sodium borate BGE solution is most likely due to the low molar solubility of large TRL particles. Like LDL, these particles are probably displaying a tendency toward aggregate formation.[82]

CZE Separation of TRL in 12.5 mM Sodium Borate, 3.5 mM SDS, 20% (v/v) ACN in Water BGE Solution on P/ACE Model 5510 Capillary Electrophoresis Instrumentation

Since lipoprotein particles have a high affinity for dodecyl sulfate ions of SDS, a new BGE solution was applied to obtain a better electrophoretic separation of the TRL subclasses. The dodecyl sulfate ions interact with lipoprotein particles through nonpolar interactions and increase the particles' negative charge.[82]

The TRL fractions were analyzed in a 12.5 mM sodium borate, 3.5 mM SDS, 20% (v/v) acetonitrile in water background electrolyte solutions in the Beckman P/ACE Model 5510 capillary electrophoresis instrument. Deionized water was injected (8 seconds) as an electroosmotic flow marker (EOF) followed by a sample injection of 10-15 seconds at 17 kV for variable electrophoretic separation time periods. Fractions corresponding to the lipoprotein subclasses were detected at 214 nm for their relative migration time, electrophoretic mobilities, and intensities.

When the intact TRL and intact RLP are separated in a 12.5 mM sodium borate, 3.5 mM sodium dodecyl sulfate, 20% ACN (v/v) in water background electrolyte buffer, greater resolution of the lipoproteins is achieved. The following figure depicts the

separation of intact TRL in this SDS buffer (Figure 49).

Figure 49. Separation of intact TRL by capillary zone electrophoresis in a 12.5 mM sodium borate, 3.5 mM SDS, 20% (v/v) acetonitrile in water background electrolyte solution detected at 214 nm.

The electrophoretic separation of intact TRL in the sodium borate/SDS buffer yields 8 major peaks. The electrophoretic mobilities of these fractions are listed in the following table (Table 4).

Table 4. Effective electrophoretic mobilities (μ_{eff}) of TRL subclasses separated by CZE in a 12.5 mM sodium borate, 3.5 mM SDS, 20% (v/v) acetonitrile in water background electrolyte solution detected at 214 nm on P/ACE^{TM} 5510 capillary electrophoresis instrumentation.

Peak	μ_{eff} (* 10^{-5} cm^2/Vs)
A	-23.8
B	-29.7
C	-31.8
D	-33.2
E	-33.7
F	-36.2
G	-36.4
H	-36.6

In addition, the μ_{eff} values for the TRL subclasses are higher in the sodium borate/SDS buffer as previously seen with LDL and HDL. The presence of acetonitrile as an organic modifier is known to decrease the μ_{eff} values of lipoprotein particles at varying degrees dependent on the particle's overall polarity.[82] This may be a useful way of determining the triglyceride content of TRL particles, which have the highest percentage of nonpolar constituents in the form of triglycerides. CM consist of approximately 85% triglyceride content, and VLDL particles consist of approximately 60% triglyceride content.[83] The effective mobilities of these particles correspond to their major nonpolar component due to interaction with the SDS probe in the BGE solution.[82] These particles vary greatly in their composition, and capillary electrophoretic separations in a buffer with sodium borate and detergent (SDS) offer great potential to study the changes in the triglyceride content of these particles by changes in effective mobility.

However, it is important to remember that the volume of the particle itself is inversely related to particle electrophoretic mobility. The greater the lipoprotein volume, the lower is its effective mobility. CM may have larger nonpolar content but have a significantly larger radius in the range of 375-6,000 Å compared to 150-400 Å for VLDL.[83]

The following figure illustrates the electrophoretic separation of intact RLP isolated from the RLP immunoseparation assay (Figure 50).
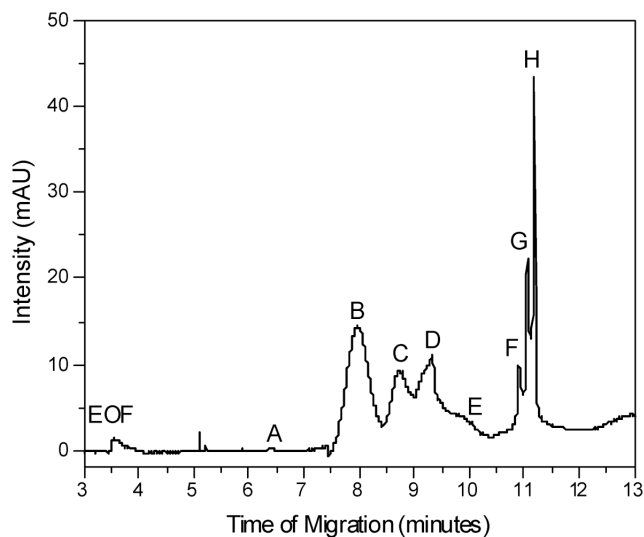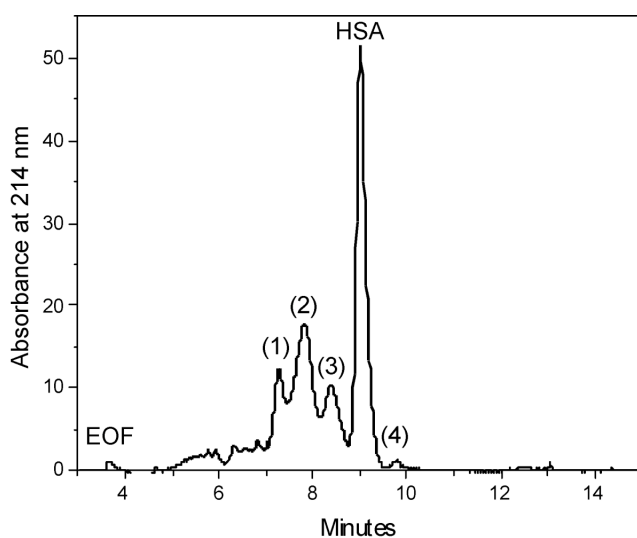

Figure 50. Separation of intact RLP, isolated from RLP immunoseparation assay, by capillary zone electrophoresis in a 12.5 mM sodium borate, 3.5 mM SDS, 20% (v/v) acetonitrile in water background electrolyte solution detected at 214 nm.

The electrophoretic separation of the intact RLP isolated from the RLP immunoseparation assay yielded 5 major peaks. Some of these peaks are derived from the serum protein content and some from the actual RLP particles. The mobility of peaks 1-4 are -25.5×10^{-5} cm^2/Vs, -27.2×10^{-5} cm^2/Vs, 28.8×10^{-5} cm^2/Vs, and 32.1×10^{-5}

cm^2/Vs. The identity of the largest peak labeled HSA (human serum albumin) with an

μ_{eff} of 30.3 × 10^{-5} cm^2/Vs in Figure 50 was proven with an electrophoretic separation of

a HSA standard in the 12.5 mM, 3.5 mM SDS, 20% (v/v) ACN in water BGE buffer

depicted below (Figure 51).

Figure 51. Separation of Human Serum Albumin (HSA) standard by capillary zone electrophoresis in a 12.5 mM sodium borate, 3.5 mM SDS, 20% (v/v) acetonitrile in water background electrolyte solution detected at 214 nm.

The μ_{eff} of the HSA standard is -29.8 × 10^{-5} cm^2/Vs corresponding to the large

peak labeled HSA seen in the total RLP electropherogram in Figure 50. The identity of

this peak was expected since HSA is the most abundant serum protein constituent.[84, 85]

To remove the protein content and obtain an RLP profile by CZE, RLP were

collected from preparative ultracentrifugation in 20% (w/v) sucrose. The following

electropherogram shows the recovered RLP following removal of the protein content

(Figure 52).

Figure 52. Separation of intact RLP by capillary zone electrophoresis in a 12.5 mM sodium borate, 3.5 mM SDS, 20% (v/v) acetonitrile in water background electrolyte solution detected at 214 nm.

The electrophoretic mobilities of the RLP subclasses are very similar to those of the total TRL electrophoretic separation. The following table summarizes the μ_{eff} values from the separation of RLP by CZE depicted in Figure 52 (Table 5).

Table 5. Effective electrophoretic mobilities (μ_{eff}) of RLP subclasses separated by CZE in a 12.5 mM sodium borate, 3.5 mM SDS, 20% (v/v) acetonitrile in water background electrolyte solution detected at 214 nm on P/ACE^{TM} 5510 capillary electrophoresis instrumentation.

Peak	μ_{eff} (* 10^{-5} cm^2/Vs)
1	-24.5
2	-29.8
3	-32.8
4	-33.6
5	-35.9
6	-36.4
7	-36.7
8	37.2

Peak 1 has an μ_{eff} of 24.5 × 10^{-5} cm^2/Vs similar to the μ_{eff} of peak A at -23.8 × 10^{-5} cm^2/Vs for total TRL listed in Table 4. Peak 2 has a μ_{eff} of -29.8 × 10^{-5} cm^2/Vs, which correspond to peak B for the total TRL listed in Table 4. Likewise, peaks 3 and 4 have μ_{eff} of -32.8 × 10^{-5} cm^2/Vs and -33.6 × 10^{-5} cm^2/Vs, which correspond to peaks C and D listed in Table 4 for the total TRL. Lastly, peaks 5, 6, 7 and 8 have μ_{eff} of -35.9 × 10^{-5} cm^2/Vs, -36.4 × 10^{-5} cm^2/Vs, -36.7 × 10^{-5} cm^2/Vs, and -37.2 × 10^{-5} cm^2/Vs respectively. These peaks have similar mobilities to peaks F, G, and H in the TRL electrophoretic separation as listed in Table 4.

The TRL collected from preparative ultracentrifugation in sucrose was added to the RLP presented in the previous figure. The following figure depicts the electrophoretic separation when the TRL was added to the RLP in order to see if the peaks were additive with the same electrophoretic separation when combined (Figure 53).
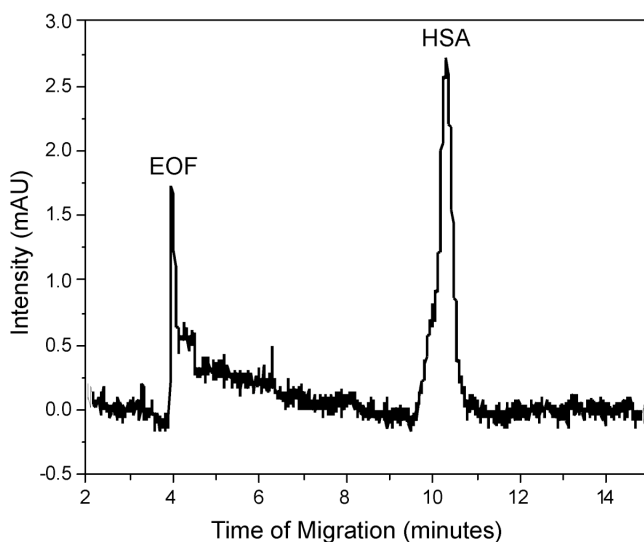
Figure 53. Separation of intact TRL added to intact RLP by capillary zone electrophoresis in a 12.5 mM sodium borate, 3.5 mM SDS, 20% (v/v) acetonitrile in water background electrolyte solution detected at 214 nm by P/ACE 5510^{TM} capillary electrophoresis instrumentation.

The electrophoretic separation observed in Figure 53 is identical to the total TRL

and RLP electrophoretic separations observed in Figure 49 and Figure 52 respectively

with identical effective electrophoretic mobility values. The reproducibility of the

electrophoretic separations in the sodium borate/SDS background electrolyte solution is

evidence of the structural stability of the TRL lipoprotein particles even with their

interaction with the dodecyl sulfate ions. A similar finding was observed with LDL and

HDL particles.[82]

To identify the last few peaks (F, G, H) in Figure 53, a cholesterol standard of 3 mg/dL was prepared and subjected to electrophoretic separation depicted below (Figure 54).
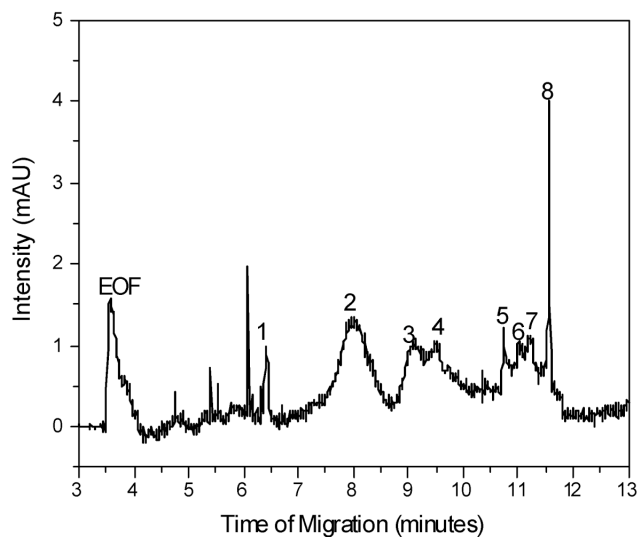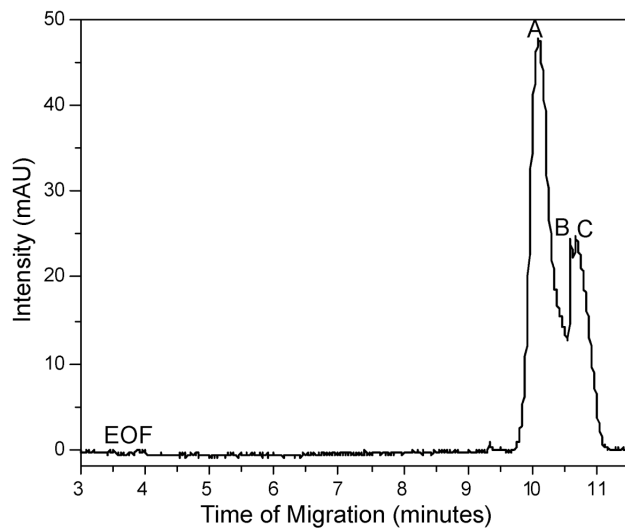

Figure 54. Separation of cholesterol standard by capillary zone electrophoresis in a 12.5 mM sodium borate, 3.5 mM SDS, 20% (v/v) acetonitrile in water background electrolyte solution detected at 214 nm.

Three major peaks are visible in the electrophoretic separation of the cholesterol standard. The electrophoretic mobilities of the cholesterol peaks A, B and C are -35.6×10^{-5} cm^2/Vs, -36.6×10^{-5} cm^2/Vs, and -37.2×10^{-5} cm^2/Vs respectively. Since the cholesterol standard is free unesterified cholesterol, this provides support for the identification of peaks F, G, and H seen in the TRL and RLP electrophoretic separations. Free unesterified cholesterol must dissociate from the TRL particles during the on-line separation by CZE in the sodium borate/SDS buffer. This measurement may potentially provide information in further characterizing the TRL subclasses according to the surface free unesterified cholesterol content. Also, the three peaks seen here in Figure 54 may be free cholesterol and cholesterol that may be modified by oxidative stress or simply differ in the extent of coupling with the dodecyl sulfate ions from SDS.

CZE Separation of TRL in 12.5 mM Sodium Borate, 3.5 mM SDS, 20% (v/v) ACN in Water BGE Solution on P/ACE™ MDQ Capillary Electrophoresis Instrumentation

Buoyant and dense TRL fractions were also analyzed by capillary electrophoresis with newer CE instrumentation (P/ACE™ MDQ Capillary System, Beckman Coulter Inc). These fractions were collected from water layering following a preparative density gradient ultracentrifugal spin in 20% (w/v) sucrose. The following figure shows the electrophoretic separation of the bTRL and dTRL classes from Subject 1 (Figure 55).
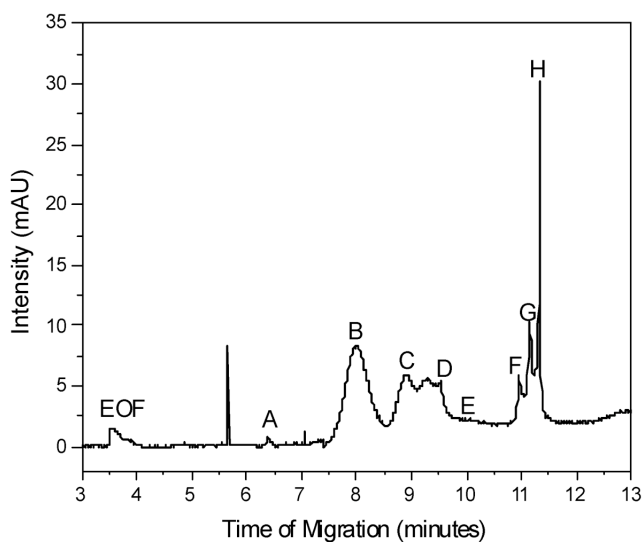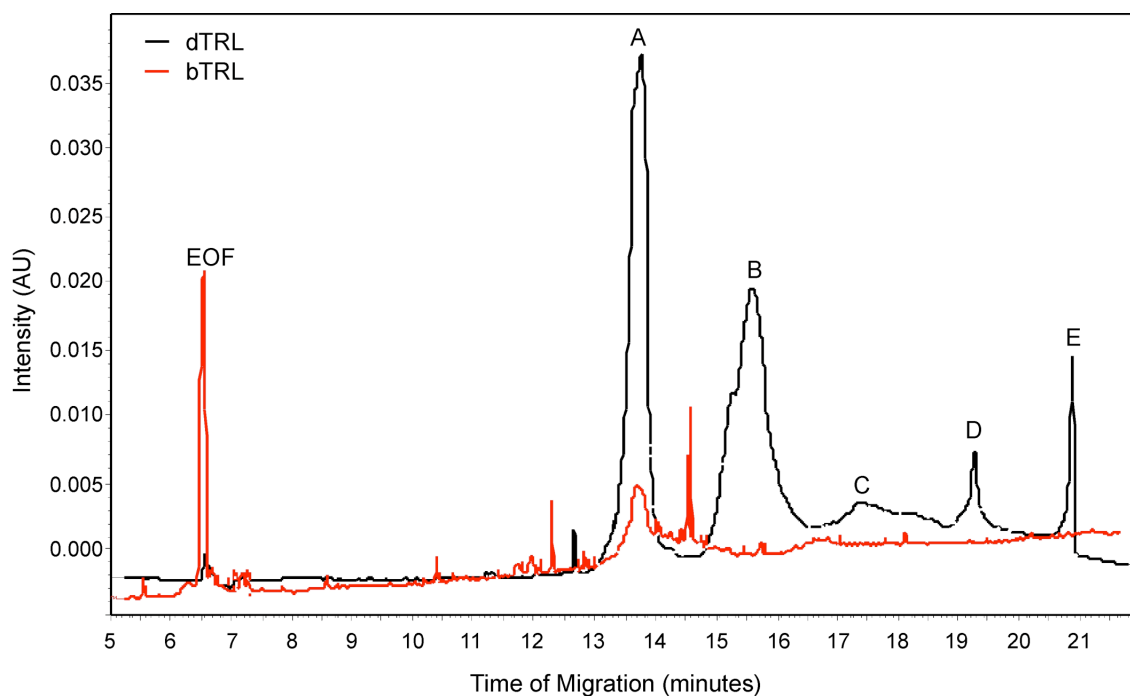
Figure 55. Separation of intact buoyant TRL and intact dense TRL by capillary zone electrophoresis in a 12.5 mM sodium borate, 3.5 mM SDS, 20% (v/v) acetonitrile in water background electrolyte solution detected at 214 nm on P/ACE^{TM} MDQ capillary electrophoresis instrumentation.

The electrophoretic separation of the bTRL and dTRL from Subject 1 in the P/ACE MDQ instrumentation is similar to the electrophoretic separation of TRL from Subject 2 seen in the P/ACE 5510 instrumentation. The following table lists the μ_{eff} values for the electrophoretic separation of TRL in Figure 55 (Table 6).

Table 6. Effective electrophoretic mobilities (μ_{eff}) of TRL subclasses separated by CZE in a 12.5 mM sodium borate, 3.5 mM SDS, 20% (v/v) acetonitrile in water background electrolyte solution detected at 214 nm on CE P/ACE MDQ^{TM} capillary electrophoresis instrumentation.

Peak	μ_{eff} ($* 10^{-5}$ cm^2/Vs)
A	-28.2
B	-31.0
C	-33.2
D	-35.0
E	-36.2

There is greater resolution between peaks in Figure 55, and the μ_{eff} values are different from TRL separated on the P/ACE^{TM} 5510 instrumentation mainly due to differences in TRL composition inherent to Subjects 1 and 2.

The actual separation structure of the fractions is similar. The electrophoretic separation of TRL subclasses from Subject 1 produces higher effective mobilities most likely due to smaller TRL volume. As presented earlier, the results from the *in vitro* lipolysis study indicate that Subject 1 has lesser TAG content in the TRL subclasses than Subject 2. Also, the fact that the bTRL here yield such a low intensity indicates that Subject 1 has denser and therefore smaller TRL particles inherently.

The most interesting finding from the bTRL and dTRL separation depicted in Figure 55 is the fact that the bTRL class separates into one major fraction that coincides with a portion of the dTRL class at an μ_{eff} value of -28.2×10^{-5} cm^2/Vs. This lends credence to the hypothesis that the first fraction of TRL to separate at a lower μ_{eff} is CM due to their large volume. Both CM and VLDL are composed largely of triglycerides. This major nonpolar constituent correlates to their interaction with dodecyl sulfate ions from SDS in the BGE solution.[82] Therefore, their size difference would affect the separation more than their interaction with the dodecyl sulfate ions. However, as seen before, the interaction with SDS is necessary to prevent aggregation of the particles and achieve better resolution.

CM particles are more buoyant than VLDL, and in this fasting serum separation, it is expected that the CM content would not be significant. This observation is apparent in the fact that the majority of the TRL fractions are detected in the dTRL range. The following figure depicts the electrophoretic separation of TRL from serum subjected to a one-hour incubation at 37 ℃ (LpL Control, no enzyme) and TRL from serum subjected to a one-hour incubation at 37 ℃ with lipoprotein lipase (LpL Experimental, with enzyme) in Figure 56.
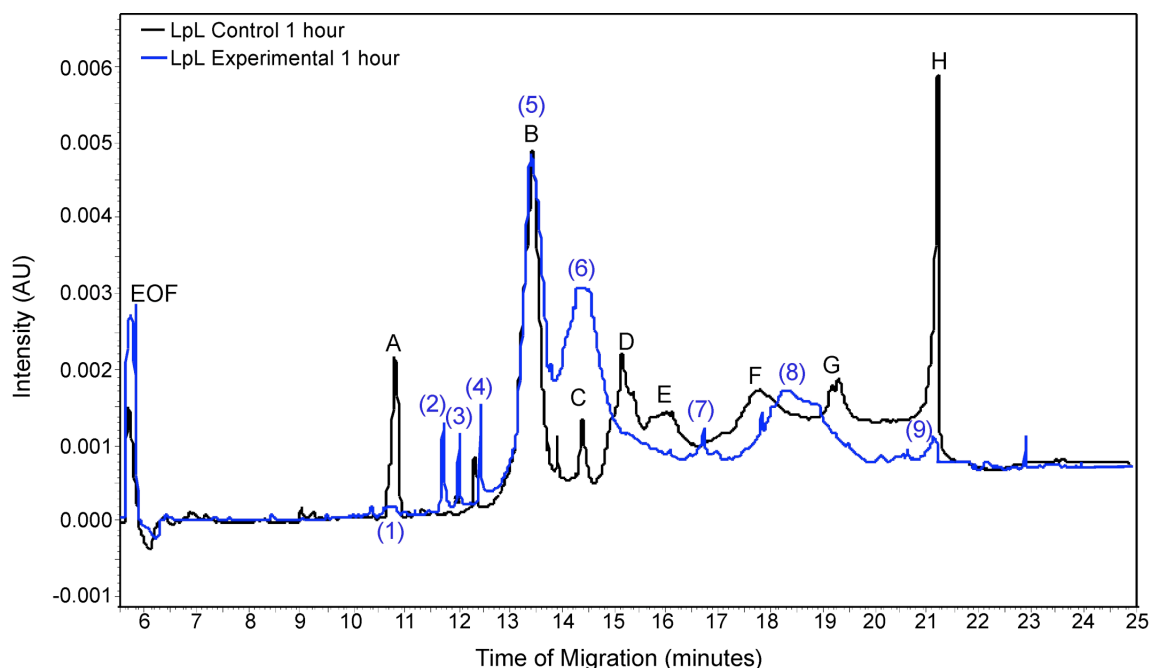
Figure 56. Separation of TRL control and TRL subjected to lipolysis by LpL by capillary zone electrophoresis in a 12.5 mM sodium borate, 3.5 mM SDS, 20% (v/v) acetonitrile in water background electrolyte solution detected at 214 nm in P/ACE^{TM} MDQ capillary electrophoresis instrumentation.

This result again lends credence to the concept that size plays the most significant role in the electrophoretic separation of TRL particles in a sodium borate/SDS buffer solution. The identities of peaks A-H (LpL Control, no enzyme) and peaks 1-9 (LpL Experimental, with enzyme) remain unidentified (Figure 56). Upon lipolysis, new peaks at higher mobilities than the parent peaks appear. The parent peaks appear to diminish in intensity for the most part. The *in vitro* lipolysis does not actually create TRL remnants since the interaction is different than the synthesis of RLP in circulation *in vivo*. The most important finding of this analysis is the fact that as the

triglyceride content of TRL particles is hydrolyzed and the TRL particle decreases in size, the μ_{eff} values of the particles increase.

<u>Summary on the Separation of TRL by Capillary Zone Electrophoresis</u>

Capillary zone electrophoresis (CZE) is a powerful technique to analyze the heterogeneous population of triglyceride-rich lipoproteins.[69] These particles vary significantly in their triglyceride content and size due to their derivation from dietary lipids. This technique allows for a rapid analysis of small amounts of sample, and we specifically employ CZE, the simplest form of capillary electrophoresis, to analyze these particles according to their charge to mass ratio.[67] Previous studies show a separation of IDL, VLDL, and LDL by capillary isotachophoresis, in which a discontinuous electrolyte system is employed to produce zones.[67, 69] However, CZE is simpler and shows great potential in the analysis of TRL subclasses as presented here.

The CZE results presented here prove the feasibility of studying the TRL class in as intact lipoprotein particles in a sodium borate/SDS/ACN background electrolyte system. The reproducibility of the separation authenticates the interaction of SDS and the intact particles. Since these particles are mostly composed of nonpolar constituents, the SDS buffer is an excellent choice to prevent aggregation and may even correlate to the triglyceride content, the major nonpolar component, of TRL particles. The electrophoretic mobilities of the TRL fractions in various subjects may provide information in regard to total triglyceride level and triglyceride levels in individual subclasses. In addition, free cholesterol seems to dislodge from the TRL particles and elutes with a very high mobility. This is again probably due to the interaction of the

dodecyl sulfate ions with the TRL particles. Since dodecyl sulfate ions interact with exposed nonpolar regions of lipoprotein particles,[82] it is likely that their interaction with TRL would be at the highest level in the lipoprotein classes. This interaction probably causes the free cholesterol on the surface to dissociate and elute separately from the intact particle. This measurement in itself may have clinical utility in determining the amount of free cholesterol that dissociates as a function of the amount of TRL.

Another interesting finding in this study is the fact that the size of the particle separated in this medium inversely correlates to its effective mobility. In contrast, in this background electrolyte solution, LDL and HDL separate according to their exposed nonpolar regions and not according to their sizes. HDL has a lower μ_{eff} value than LDL even though it has a smaller size.[82] *In vitro* lipolysis has an interesting effect on the μ_{eff} values of the TRL subclasses. Upon the hydrolysis of the particles' triglyceride content and size reduction, the μ_{eff} values increase again lending credence to the hypothesis that larger TRL particles in the form of CM have lower μ_{eff} values than smaller TRL particles in the form of VLDL.

Overall, this study proves the feasibility of studying the TRL class by capillary zone electrophoresis in a continuous buffer system with a detergent and organic modifier. In the future, different detergents can also be examined to see if they have similar interactions with TRL particles. Also, the identification of CM and VLDL classes in the separations can be made by the use of standards. The free cholesterol content that dislodges from the particles may be quantified by linear calibration against cholesterol standards. Finally, triglyceride levels may potentially be quantified by μ_{eff}

values and TRL particles may be quantified by their intensity values.

Postprandial Study

Objective

Total lipoprotein density profiling and RLP density profiling were applied in this postprandial study to monitor the changes in the density profiles as a function of time following a high fat meal. As mentioned previously, TRL particles are carriers for TAG derived from both dietary and endogenous production, and an elevated level of TAG is a risk factor for cardiovascular disease.[7, 22] Because this relationship is not well understood, it is important to study the metabolism of TRL in terms of their formation and metabolism. This study shows the potential of this novel method in studying the postprandial state to understand the complex mechanisms behind the synthesis, metabolism and clearance of triglyceride-rich lipoproteins.

Total Lipoprotein Density Profiling

The following figure depicts the changes in the total lipoprotein density profile from the fasting state baseline draw (0 hour) through the 8 hours following the high-fat meal (Figure 57).
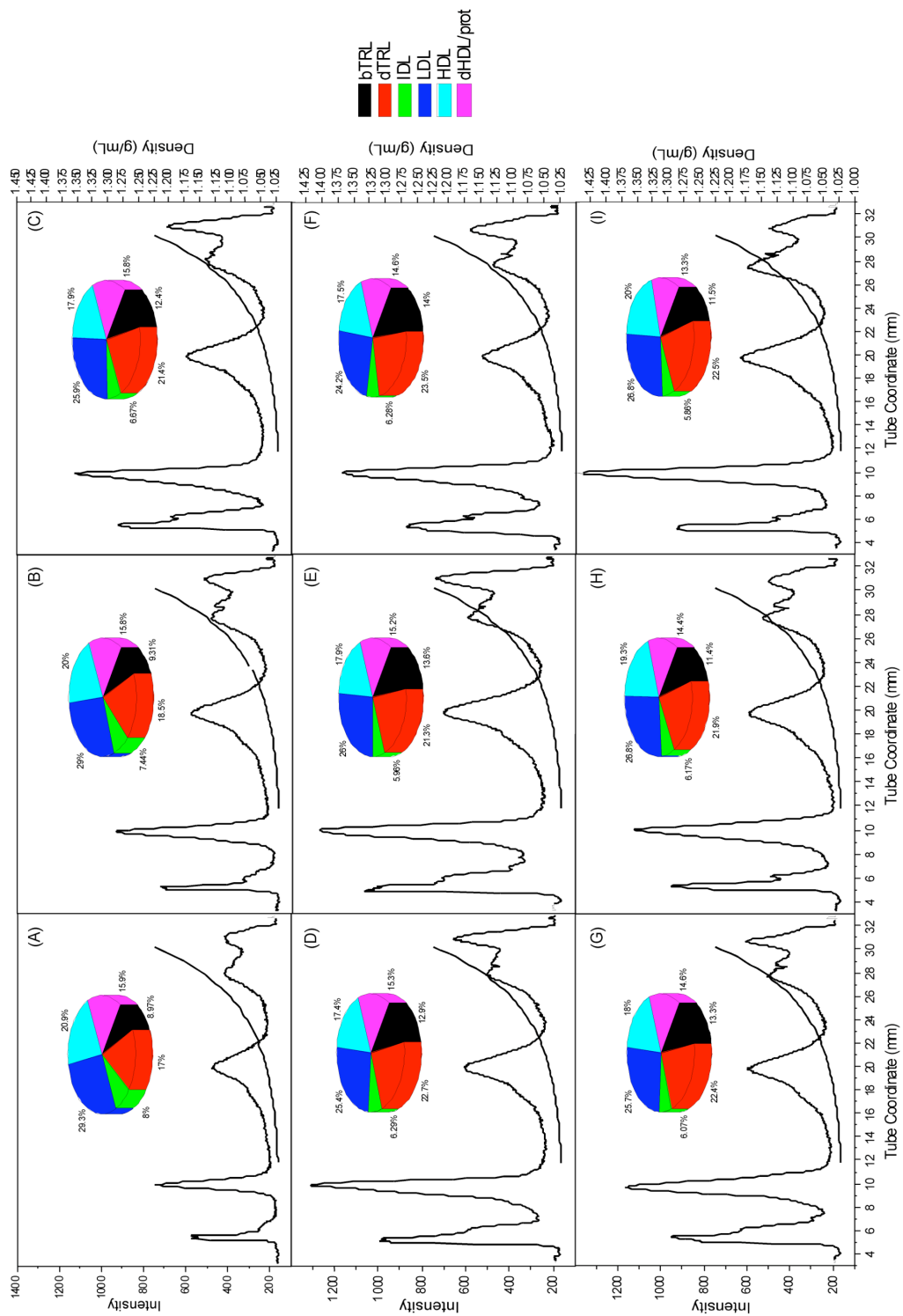
Figure 57. Lipoprotein density profiles and relative fluorescence intensities of lipoprotein subclasses from nutrition based clearance study in NaBiEDTA: (A) 0 hour baseline blood draw, (B) 1 hour blood draw, (C) 2 hour blood draw, (D) 3 hour blood draw, (E) 4 hour blood draw, (F) 5 hour blood draw, (G) 6 hour blood draw, (H) 7 hour blood draw, and (I) 8 hour blood draw from Subject 2.

There are many changes that are observed in the lipoprotein subclasses from this time dependent nutrition study. It is interesting to note that the relative fluorescence of the lipoprotein subclasses does not change drastically from the fasting state to the postprandial and clearance states. This result may evidence some equilibrium of lipid content among the lipoprotein classes at a given time. The absence of change in the relative fluorescence is probably caused by a limited time span for lipid transfer among the particles or another physiological mechanism for this regulation in terms of particle number and limited capacity.

The following figure depicts the absolute fluorescence intensities of the lipoprotein subclasses over the hours of the time study (Figure 58).
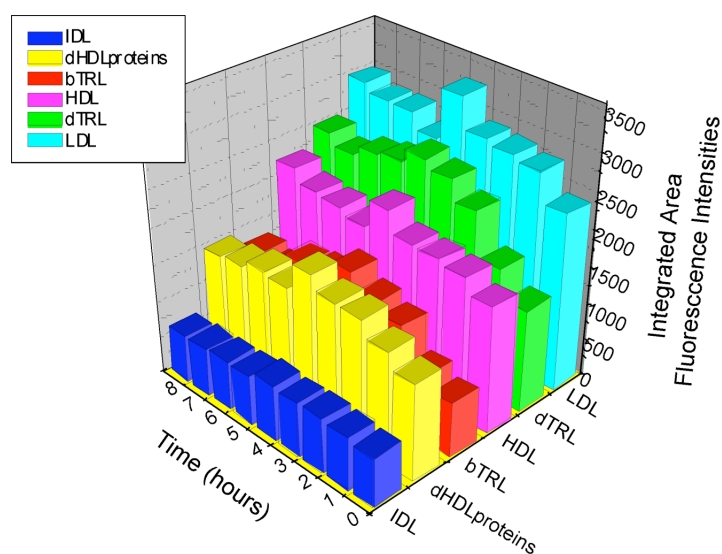
Figure 58. Absolute integrated fluorescence intensities of the lipoprotein subclasses.

RLP Density Profiling

The RLP density profiling method was applied to the 0 hour, 2 hour, 4 hour, 6 hour, and 8 hour serum samples from the time based nutrition study. The following figure illustrates the changes in the RLP density profiles relative to the total lipoprotein density profiles for the baseline, 0 hour blood draw (Figure 59).
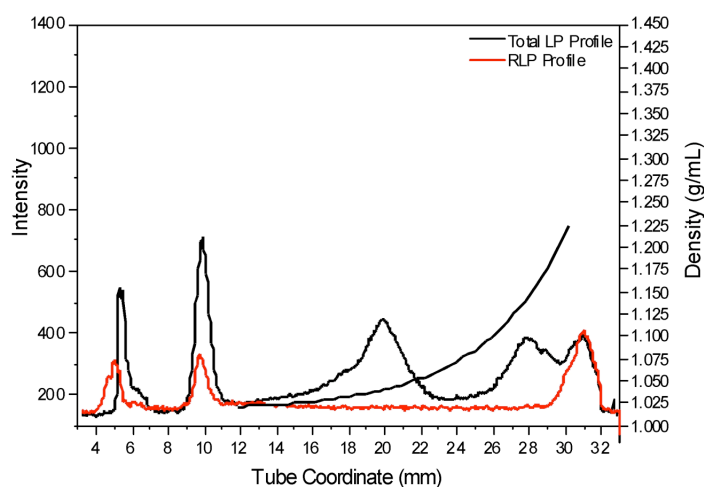
Figure 59. Total lipoprotein and RLP density profiles of the 0 hour, baseline draw in NaBiEDTA for Subject 2.

In Figure 59, the baseline draw displays a basal level of RLP as bRLP and dRLP. The following figure is the RLP density profile and total lipoprotein density profile 2 hours after the meal (Figure 60).

Figure 60. Total lipoprotein and RLP density profiles of the 2 hour blood draw following the meal in NaBiEDTA for Subject 2.

Two hours after the meal (Figure 60), there is a significant elevation of dRLP, which is most likely due to the appearance of CM, which appear as early as one hour after a meal in circulation.[25] Another interesting feature of this RLP profile is the appearance of dense HDL. In the postprandial state, HDL triglyceride level is elevated even though its cholesterol content does not change after a meal.[75] At the stage of metabolism observed here, it is likely that the HDL has taken on a significant amount of triglyceride content, which can cause a dissociation of apo A-1 as mentioned previously.[75] If the apo A-1 dissociates from the HDL, it would explain its temporary appearance in the RLP profile at this stage of metabolism. This provides a lot of information regarding the timing of the stages of TRL metabolism in terms of *reverse cholesterol transport.* This profile tells us that by two hours after a high fat meal, HDL and TRL have undergone an exchange of lipid content and the TRL particles have been converted to RLP.

The highest level of fluorescence intensity is observed at the fourth hour after the meal as depicted in Figure 58. The following figure shows the RLP density profile relative to the total lipoprotein profile at this stage of metabolism (Figure 61).

Figure 61. Total lipoprotein and RLP density profiles of the 4-hour blood draw following the meal in NaBiEDTA for Subject 2.

It is interesting that even though overall fluorescence is most elevated at the 4th hour after the meal, the RLP density profile shows lower levels of fluorescence intensity. At this stage, the RLP have cleared from circulation, and triglyceride-rich, apo A-1 deficient HDL are not observed either. The elevation in TRL suggests that there is a synthesis of nascent particles most likely in the form of VLDL from the liver. Also, the RLP content that previously appeared at the 2 hour profile are removed as seen in this profile. This indicates that the lipid content of these particles has been deposited in the liver and re-packaged in the form of VLDL. Since there is an elevation in TRL

fluorescence intensity in this profile, it is likely that the newly synthesized VLDL have

not been converted to rVLDL. The following figure depicts the RLP and total

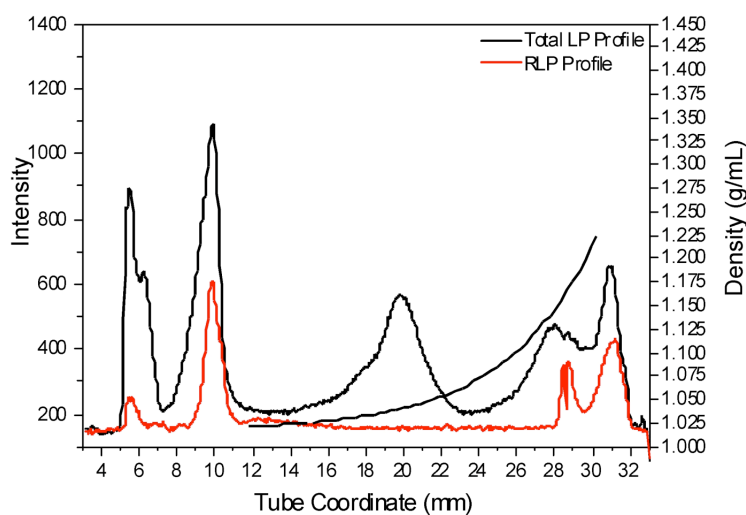lipoprotein density profiles at the sixth hour following the meal (Figure 62).
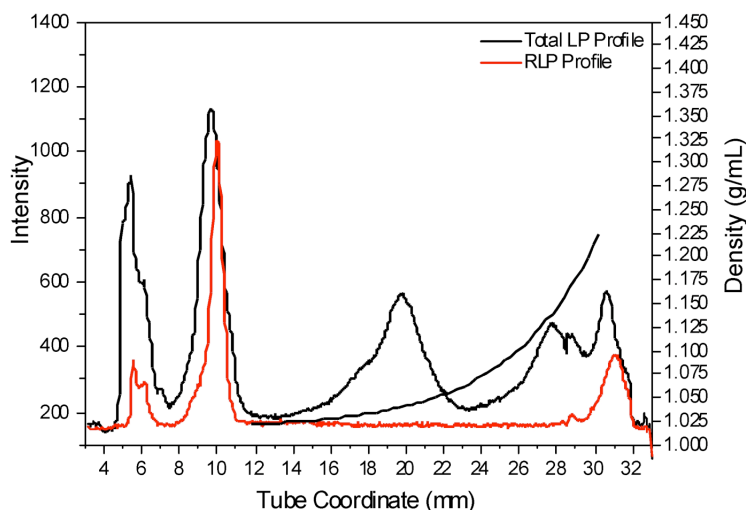
**Figure 62. Total lipoprotein and RLP density profiles of the 6-hour blood draw
following the meal in NaBiEDTA for Subject 2.**

It is evident that at the sixth hour following the meal, the VLDL have been

converted to rVLDL. In addition, a small level of dense HDL again appears along with

the elevation in RLP. Again, this is most likely due to the triglyceride-enrichment of

HDL due to its lipid exchange with VLDL in circulation. The triglyceride enrichment

can cause a dissociation of apo A-1.[75] This would lead to the appearance of dense

triglyceride-rich, apo A-1 deficient HDL in the RLP profile as observed here. The figure

that follows depicts the RLP and total lipoprotein density profiles of the final blood draw
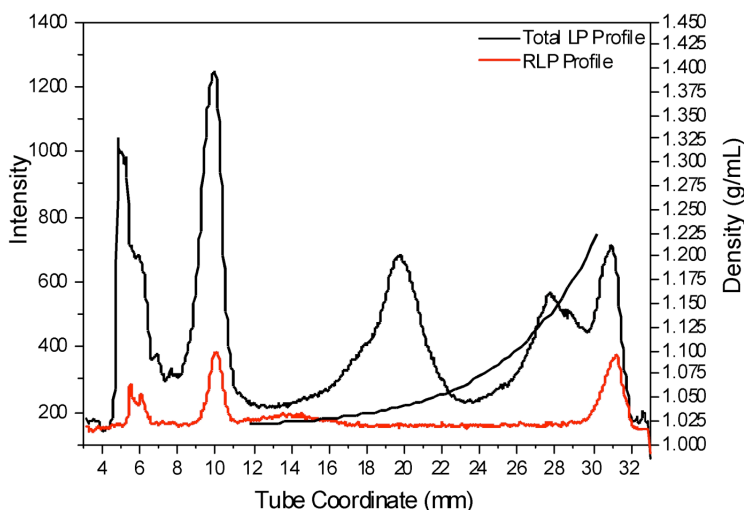
of this time-based nutrition study (Figure 63).
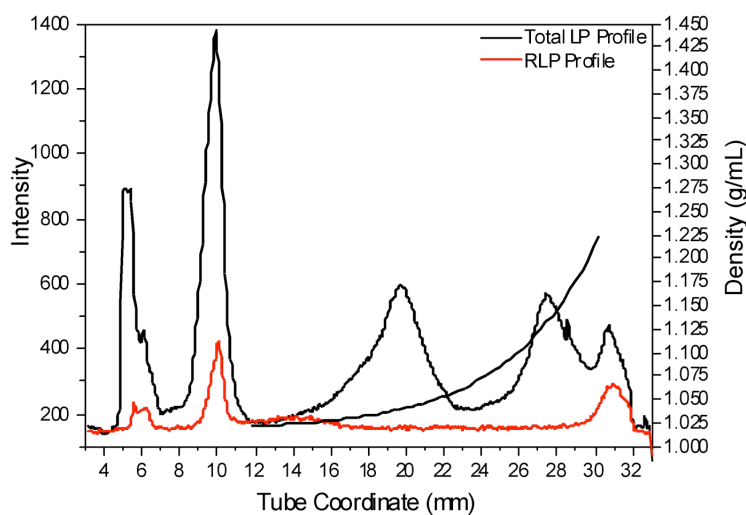
Figure 63. Total lipoprotein and RLP density profiles of the 8-hour blood draw following the meal in NaBiEDTA for Subject 2.

A dramatic decrease in RLP fluorescence intensity is observed at the final blood draw. This effect is accompanied by an increase in dTRL fluorescence intensity. It seems that a second synthesis of VLDL occurs two hours following the initial VLDL surge. The integrated fluorescence intensities of the RLP and TRL subclasses were evaluated by performing area under curve calculations. The following figure depicts the integrated fluorescence intensities of the RLP classes within each respective TRL class (Figure 64).
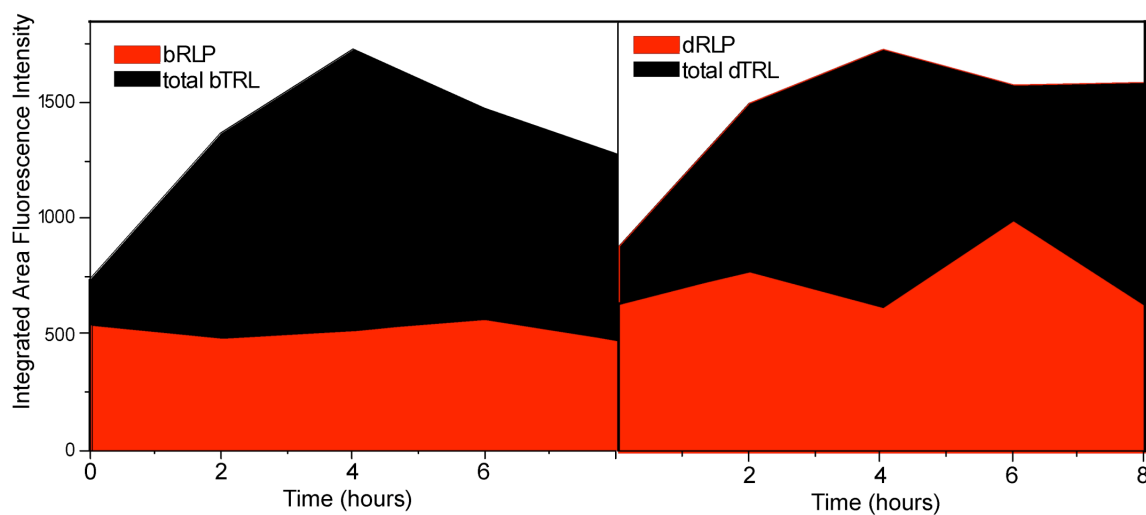
Figure 64. Integrated fluorescence intensities of the buoyant and dense RLP and TRL classes.

The postprandial study revealed that there are many changes in the TRL and RLP subclasses in the 8 hours following ingestion of a large fatty meal. This data provides more detailed information than the total lipoprotein density profiles alone.

These trends are most easily observed in Figure 58, where the absolute fluorescence intensities show that TRL are most elevated at the fourth hour after the meal. The dTRL and dRLP exhibit the most variability in their intensities from which useful metabolic information can be derived. At the second hour, there is an increase in fluorescence intensity in both the dTRL and bTRL classes with a slight increase in dRLP. This is the first stage of chylomicron synthesis. At the fourth hour, again dTRL increase with a slight drop in dRLP and an increase in bTRL. This is indicative of VLDL synthesis due to the clearance of CMR in the liver. At the sixth hour, the dRLP is dominated by dRLP most likely in the form of rVLDL, and the overall fluorescence intensity of the TRL diminishes. Lastly, at the eight hour, the dTRL fluorescence

intensity increases relatively as the dRLP fluorescence intensity decreases due to rVLDL clearance and more VLDL synthesis by the liver.

Summary of Postprandial Study

This entire study indicates a dynamic equilibrium in the synthesis and clearance of TRL particles. It seems that at least in the liver, synthesis of triglyceride-rich particles is controlled and time-dependent on the delivery of fats from the exogenous pathway. The results here corroborate information in the literature in regard to the metabolic processes involved in TRL synthesis, conversion to RLP, and clearance.[5, 25, 75, 11-13, 27] This technology allows the researcher and clinician to evaluate these stages in a subject's metabolism as a function of time. The appearance of triglyceride-rich, dense HDL, a form of HDL_3 as observed by density profiling methods, completes our understanding of the relationship between RLP formation and *reverse cholesterol transport* by providing a time marker for this conversion and interaction.

Patients who suffer from peripheral arterial disease continue to have elevated levels of triglycerides even at the eight hour following a oral fat load test. In studies related to this disease, elevations in postprandial triglyceride levels are observed at the fourth, sixth, and eight hours.[86] These previous findings correlate with the increase in TRL fluorescence intensities seen at the fourth, sixth, and eight hours following the high-fat meal in our study.

In addition, this study provides even more information in terms of the formation and clearance of RLP particles in between these hours as well as the appearance of the

triglyceride-rich, apo A-1 deficient HDL with the decrease in HDL cholesterol levels at the fourth, sixth, and eight hours following a meal indicating its exchange of cholesteryl esters and triglycerides with TRL particles via cholesteryl ester transfer protein in *reverse cholesterol transport.*[86] Our observations on the appearance of the apo A-1 deficient, triglyceride-rich, dense HDL in the RLP profiles is in agreement with these observations indicating a lipid transfer between TRL and HDL at the second and sixth hours following the meal.

Special Case Study: Hypertriglyceridemia and Megacystis-Microcolon-Intestinal Hyperperistalsis Syndrome

Objective & Background

Megacystis-Microcolon-Intestinal Hypoperistalsis Syndrome (MMIHS) is a rare, congenital disease characterized by abdominal distention due to a distended non-obstructed urinary bladder with associated hydronephrosis, microcolon, hypoperistalsis, and malrotation of the small intestine. The pathogenesis of this disorder is not fully understood although intestinal smooth muscle atrophy is described in such patients. In this study, serum from a female subject with MMIHS, who developed profound hypertriglyceridemia, was evaluated by lipoprotein density profiling and RLP density profiling. Lipoprotein density profiling and RLP density was performed, and testing by this technique suggests a unique cholesterol metabolism defect that may be present in

MMIHS. This method provides a safe and useful technique to evaluate lipid processing abnormalities for rare pediatric diseases such as MMIHS.

RLP Density Profiling

The RLP density profiling method (Chapter II, *Method 1*) was applied to this subject's non-fasting and fasting serum samples. The non-fasting and fasting density profiles are shown below in Figure 65 and Figure 66 respectively.
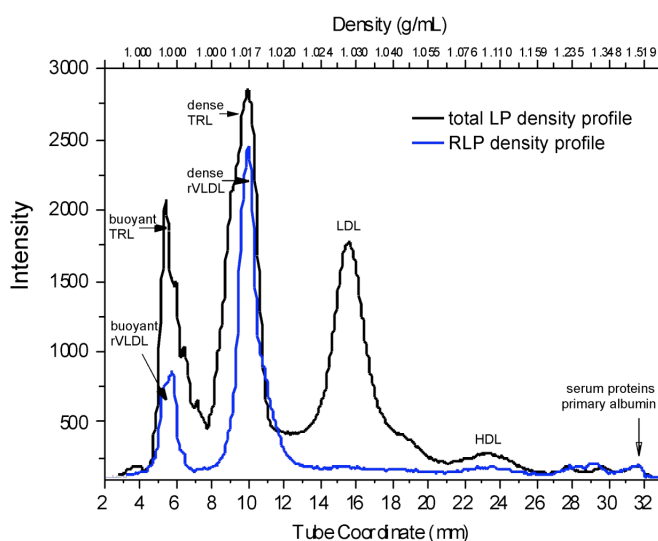
Figure 65. Total lipoprotein and RLP density profiles of non-fasting serum in CsBiEDTA.
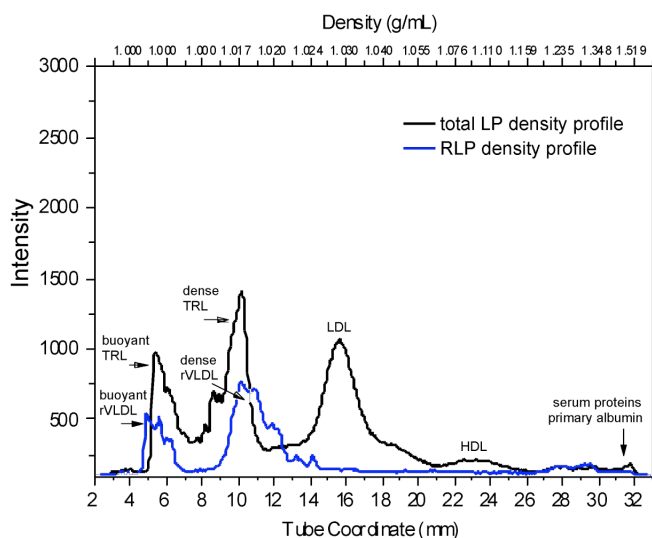
Figure 66. Total lipoprotein and RLP density profiles of fasting serum in CsBiEDTA.

The features of the lipoprotein density profile included triglyceride-rich lipoprotein fractions such as buoyant VLDL, dense VLDL, and rVLDL. Other noted features included LDL, HDL, and serum proteins. Overall, all lipoprotein fractions were diminished in the "fasting" serum density profile; however, the relative intensities of the various lipoprotein fractions remained nearly constant except that the concentration of rVLDL particles were higher in the fasting TRL fraction compared to the non-fasting samples.

Apolipoprotein Analysis

SDS-PAGE analysis as described in Chapter II, *Method 3* was performed on the

buoyant and dense TRL and RLP fractions collected from the density gradient

ultracentrifugal separation to determine the apo B-100 and apo B-48 content of the

subclasses. The figure that follows depicts the SDS-PAGE analysis in a 3-8% tris-acetate

gel (Figure 67).
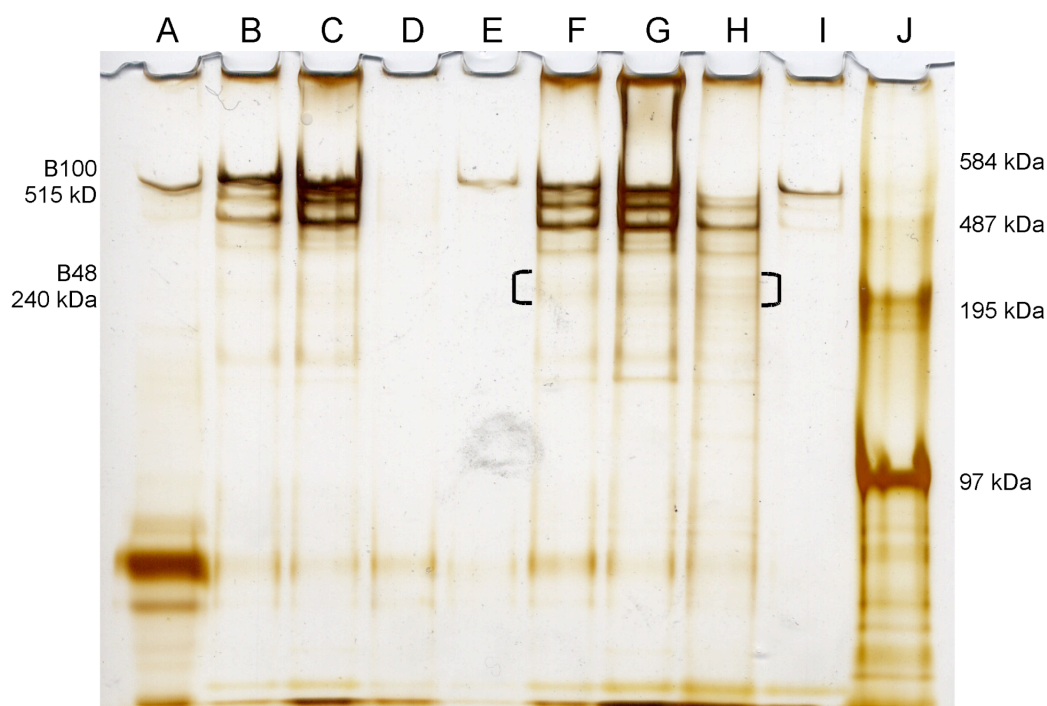
Figure 67. SDS-PAGE analysis of (A) apo B-100 standard, (B) non-fasting buoyant TRL, (C) non-fasting dense TRL (D) non-fasting buoyant RLP, (E) non-fasting dense RLP, (F) fasting buoyant TRL, (G) fasting dense TRL (H) fasting buoyant RLP, and (I) fasting dense RLP in a 3-8% tris-acetate gel.

Particles containing apo B-48 including CM and/or their remnants (CMR) were

not detected by SDS-PAGE analysis with the exception of minimal intensity noted in the

lanes containing buoyant TRL, dense TRL, and buoyant RLP (Figure 6). The lanes with

minimal apo B-48 detection possibly are attributed to absorption of biliary lipids and

lipids from desquamated intestinal epithelium since there was no other source of

chylomicron synthesis in the patient.[12] The main apolipoprotein constituent detected in

both the fasting and nonfasting buoyant and dense VLDL fractions was apo B-100. If

chylomicrons and their remnants were present, the meniscus fraction produced by RLP

immunoseparation should have contained chylomicrons, buoyant VLDL, and remnants

of these particles.[21] These fractions contained exceedingly small amounts of apo B-48,

since the silver staining method can detect even nanograms of apolipoprotein. Again,

this is due to the formation of CM from absorption of intestinal epithelium[12] since this

subject had no oral source for lipids.

Summary on Special Case Study: Hypertriglyceridemia and Megacystis-Microcolon-Intestinal Hyperperistalsis Syndrome

The most common, albeit rare, cause of primary hypertriglyceridemia is

attributable to low or absent lipoprotein lipase (LpL) activity due to a defect in the lipase

enzyme or apo C-2, which is required for lipoprotein lipase activation. These two

proteins are required for triglyceride hydrolysis contained in CM and VLDL particles.

Genetic mutations of either protein result in severe hypertriglyceridemia,

chylomicronemia, and elevated VLDL.[11-13, 27] Diagnosis of LpL and apo C-2 deficiency

typically is performed by measuring LpL activity in post-heparin plasma (for example,

after intravenous administration of 60 unit heparin per kilogram of body weight).[40, 87]

VLDL particles are assembled in the liver and released into the bloodstream. The first stage of catabolism involves activation of LpL on the endothelium of capillaries in adipose and muscle tissue by apo C-2 on the surface of the VLDL particles, which results in the hydrolysis of associated triglycerides to free fatty acids and formation of RLP.[80] Therefore, the presence of RLP density profiles presented here in Figure 65 and Figure 66 provides indirect confirmation of the presence of LpL activity as well as apo C-2. The use of RLP density profiling is a simpler technique compared to heparin injection to determine the possibility of familial LpL deficiency, since it does not require systemic heparinization.

In conclusion, remnant lipoprotein density profiling indirectly proves that this patient did not have lipoprotein lipase or apo C-2 deficiency. It was further demonstrated that hepatic production of VLDL and its catabolism was intact. The method of RLP density profiling provides a safe and useful technique to assess LpL and apo C-2 deficiencies as well as the liver's ability to produce VLDL and remove TRL particles.

CHAPTER IV

CONCLUSIONS

The overall objective of this research was to develop an array of methods for the analysis of triglyceride-rich lipoproteins in human serum and to apply these methods to clinical samples. This objective was achieved in the development of a novel RLP density profiling method that combines an established immunoseparation assay with density gradient ultracentrifugation, recovery of TRL classes by density gradient ultracentrifugation, analysis of TRL by gel electrophoresis for apolipoprotein content, and the development of TRL analysis by capillary zone electrophoresis. Lastly, this objective was also achieved by examination of the variability of the fasting and postprandial (following a meal) states in a subject in a time-based study. Furthermore, the RLP density profiling technique was applied to a special case study involving a patient from Scott & White Hospital, Temple, Texas who exhibited a disorder involving hypertriglyceridemia. This special case study yielded a specific diagnosis of this patient. The RLP density profiling method provides tremendous information in regard to the metabolism of TRL. From this new methodology, the dynamics of TRL formation, metabolism, and clearance can be studied in the hours after a meal. This technique can be used to assess metabolic disorder involving lipoprotein lipase specifically in the assessment of lipoprotein lipase and apo C-2 deficiencies. The use of this technique evades the traditional diagnostic procedure that involves an invasive heparin injection. Furthermore, this technique also allows for the detection of triglyceride-rich, apo A-1

depleted dense HDL. The detection of such atherogenic HDL in fasting serum samples also proves to be a useful for diagnostic capacity for patients suffering from cardiovascular disease.

The proper application of this technique to time-based nutrition studies can provide insight into the synthesis of TRL by the small intestine and liver, the metabolism of TRL and RLP in association with LpL and HDL, and the clearance rate of TRL and RLP particles by the liver in a particular subject. This entire technique of RLP density profiling and lipoprotein profiling was applied to serum samples collected at one-hour time intervals following a high-fat content meal. The results of this analysis provided great insight in the ability of this subject's lipoproteins to metabolize the dietary fats by monitoring changes in the lipoprotein and RLP density profiles. This novel methodology provides useful information in regard to the atherogenicity of these particles and in the assessment of an individual's risk factor for developing coronary artery disease.

The separation of bTRL and dTRL by the layering of different solvents exhibits great potential in achieving a separation between apo B-48 containing TRL particles in the form of CM and CMR from apo B-100 containing TRL particles in the form of VLDL and rVLDL. The limitation of water based density gradient solutions is the density of water, which falls in between the density values of the TRL class. The use of solvents such as acetonitrile and 50% methanol may potentially achieve a separation of the TRL subclasses. Further studies on the integrity of the TRL particles are needed to determine the efficacy of such solvents in the separation of TRL subclasses by density.

The analysis of bTRL and dTRL for their apolipoprotein content by SDS-PAGE gel electrophoresis was developed successfully. The result of this analysis proved that the bTRL and dTRL do not achieve a separation between the apo B-100 and apo B-48 containing TRL particles. However, the majority of apo B-48 containing particles do migrate to the meniscus when a water layering is applied and more so when a 50% methanol layering is applied.

The apo B-100 and apo B-48 bands can be easily distinguished to also analyze bRLP and dRLP fractions as seen in the special case study on MMIHS. The results of that study proved that the patient did not have a significant amount of apo B-48 containing TRL in circulation due to lack of an oral fat source. Moreover, the RLP density profiling method was applied to this patient's fasting and nonfasting serum samples and the result led to the elimination of a diagnosis of LpL or apo C-2 deficiency. This expedited the treatment of this patient without requiring the traditional heparin based diagnosis.

The coupling of the RLP immunoseparation assay with enzymatic cholesterol analysis proved to be an effective and successful measurement in terms of achieving a linear response. This new analytical technique shows promise in the determination of RLP-cholesterol in a clinical setting without the use of the traditional enzymatic cycling assay and detector. Instead, the new method requires a simple detector that has visible light detection capabilities and commercially available cholesterol enzymatic assays.

The development of triglyceride distribution analysis as a function of density also proved to be a successful and useful technique from a metabolic perspective. Following

a density gradient ultracentrifugal separation and collection of serum lipoproteins fractions, traditional enzymatic triglyceride analysis was performed and a distribution trend was created within a subject's serum sample. This technique may also be applied in a similar fashion to establish cholesterol distribution trends as a function of density. The changes in the distribution of lipid components as a function of density may provide useful information for researchers regarding the mechanism by which plasma triglycerides promote cardiovascular disease. Lastly, it was observed that under certain conditions close to saturation, NBD C_6-ceramide integrated fluorescence intensity correlates with triglyceride content in the buoyant and dense TRL classes. This observation shows promise for the use of fluorescence measurement in the determination of TRL triglyceride levels as a function of density.

The use of an *in vitro* lipolysis assay with serum followed by density profiling and triglyceride distribution analysis provided interesting results with fundamental information regarding the behavior and metabolic interactions of TRL with other lipoprotein subclasses. From this study, we gained more information regarding the relationship of NBD C_6-ceramide fluorescence and hydrophobic content of lipoprotein particles. The fluorescence observed correlates with the major nonpolar class in each lipoprotein. Overall, this study proves the feasibility of monitoring the lipolysis of triglycerides *in vitro* to approximately simulate the complex mechanisms of lipolysis *in vivo*. The movement of lipolytic end products in the form of monoacylglycerols, diacylglycerols, and glycerol can also be monitored with this technology, and the

cardioprotective role of HDL may be assessed in its ability to carry the lipolytic products.

Capillary zone electrophoresis in the analysis of TRL subclasses proved to be a powerful technique in terms of providing a rapid analysis of this complex mixture of particles. Two different kinds of buffer solutions were assessed for separation efficacy, and it was determined that the presence of a detergent such as sodium dodecyl sulfate provides greater resolution and separation of TRL fractions. Moreover, an inverse relationship between TRL particle size and effective mobility was observed as being a greater determinant than particle polarity alone. The larger TRL particles had lower effective mobilities than smaller, less triglyceride-rich particles. In addition, it was observed that free cholesterol on TRL dislodge from the intact particle as a result of the presence of the SDS detergent in an on-line separation. This is also probably due to the interaction of dodecyl sulfate ions with the particles.

In conclusion, this study proves the feasibility of studying the TRL class by capillary zone electrophoresis in a continuous buffer system with a detergent and organic modifier. By the use of standards, the CM and VLD classes in these separations may be identified in the future. The free choleserol content that dissociates from the TRL particles may be quantified by a linear calibration against cholesterol standards. Furthermore, the nonpolar component in the TRL particles may potentially be evaluated by changes in effective mobility, and TRL particles may be quantified by their intensity values.

An array of methods for the analysis of triglyceride-rich lipoproteins was developed successfully and was applied to clinical samples to demonstrate the feasibility of their clinical utility. The described techniques may be used by researchers to further examine complex TRL samples collected from a variety of subjects and patients with clinically diagnosed dyslipidemias. Future studies may provide more insight into the mechanism of cardiovascular disease in terms of triglycerides and triglyceride-rich lipoproteins. These techniques may also be used in a clinical setting for specific diagnoses of patients who exhibit hypertriglyceridemia or other metabolic disorders involving the metabolism of triglyceride-rich lipoproteins.

REFERENCES

1.   Ross, R., *N Engl J Med.* **1999,** *340,* 115-26.

2.   Homma, Y., *J Atheroscler Thromb.* **2004,** *11,* 265-70.

3.   Barter, P., *Atherosclerosis Supplments 6.* **2005,** 15-20.

4.   Shepherd, J., Plasma Triglyceride and the Risk for Vascular Disease. In *Medscape Cardiology*, Del Negro, A., Good, D., Gruber, L., Wang, K., Eds. Medscape: New York, NY, 2005; Vol. 9, http://www.medscape.com/viewarticle/512941.

5.   Tulenko, T. N.; Sumner, A. E., *J Nucl Cardiol.* **2002,** *9,* 638-49.

6.   Austin, M. A.; King, M. C.; Vranizan, K. M.; Krauss, R. M., *Circulation.* **1990,** *82,* 495-506.

7.   Nakamura, T.; Kugiyama, K., *Current Atherosclerosis Reports.* **2006,** *8,* 107-110.

8.   Expert Panel on Detection, Evaluation, and Treatment of High Blood Cholesterol in Adults (Adult Treatment Panel III), *Journal of the American Medical Association.* **2001,** *285,* 2486.

9.   Gurr, M. I.; Harwood, J. L.; Frayn, K. N., *Lipid Biochemistry*. 5th ed.; Blackwell Science: Oxford Malden, MA, 2002.

10. Dominiczak, M. H., Apolipoproteins and Lipoproteins in Human Plasma. In *Handbook of Lipoprotein Testing*, Rifai, N.; Warnick, G. R.; Dominiczak, M. H., Eds. The American Association for Clinical Chemistry, Inc.: Washington D.C., 1997; pp 1-24.

11. Havel, R. J., Triglyceride-Rich Lipoprotein Remnants. In *Handbook of Lipoprotein Testing*, Rifai, N.; Warnick, G. R.; Dominiczak, M. H., Eds. The American Association for Clinical Chemistry, Inc.: Washington D.C., 1997; pp 451-464.

12. Havel, R. J., *American Journal of Clinical Nutrition.* **1994,** *59,* 795.

13. Marcoux, C.; Hopkins, P. N.; Wang, T.; Leary, E. T.; Nakajima, K.; Davignon, J.; Cohn, J. S., *Journal of Lipid Research.* **2000,** *41,* 1428.

14. Campos, E.; Nakajima, K.; Tanaka, A.; Havel, R. J., *Journal of Lipid Research.* **1992,** *33,* 369.

15. Chan, D. C.; Watts, G. F.; Barrett, P. H.; Mamo, J. C. L.; Redgrave, T. G., *Clinical Chemistry.* **2002,** *48,* 278.

16. Jialal, I.; Devaraj, S., *Clinical Chemistry.* **2002,** *48,* 217-219.

17. Karpe, F.; Boquist, S.; Tang, R.; Bond, G. M.; de Faire, U.; Hamsten, A., *Journal of Lipid Research.* **2001,** *42,* 17.

18. Masuoka, H.; Kamei, S.; Ozaki, M.; Kawasaki, A.; Shintani, U.; Ito, M.; Nakano, T., *Intern Med.* **2000,** *39,* 540-6.

19. Nakajima, K.; Okazaki, M.; Tanaka, A.; Pullinger, C. R.; Wang, T.; Nakano, T.; Masakazu, A.; Havel, R. J., *Journal of Clinical Ligand Assay.* **1996,** *19,* 177.

20. Nakajima, K.; Saito, T.; Tamura, A.; Suzuki, M.; Nakano, T.; Adachi, M.; Tanaka, A.; Tada, N.; Nakamura, H.; Campos, E.; et al., *Clin Chim Acta.* **1993,** *223,* 53-71.

21. Chandra, R.; Macfarlane, R. D., *Anal Chem.* **2006,** *78,* 680-5.

22. Hokanson, J. E.; Austin, M. A., *J Cardiovasc Risk.* **1996,** *3,* 213-9.

23. Mjos, O. D.; Faergeman, O.; Hamilton, R. L.; Havel, R. J., *Journal of Clinical Investigation.* **1975,** *56,* 603-615.

24. Havel, R. J.; Hamilton, R. L., *Hepatology.* **1988,** *8,* 1689-1704.

25. Cooper, A. D., *Journal of Lipid Research.* **1997,** *38,* 2173-2192.

26. Cohn, J. S.; Marcoux, C.; Davignon, J., *Arteriosclerosis, Thrombosis, and Vascular Biology.* **1999,** *19,* 2474-2486.

27. Yamada, N.; Shames, D. M.; Havel, R. J., *Journal of Clinical Investigation.* **1987,** *80,* 507-515.

28. Clavey, V.; Lestavel-Delattre, S.; Copin, C.; Bard, J. M.; Fruchart, J. C., *Arteriosclerosis, Thrombosis, and Vascular Biology.* **1995,** *15,* 963-971.

29. Kypreos, K. E.; Li, X.; van Dijk, K. W.; Havekes, L. M.; Zannis, V. I., *Biochemistry.* **2003,** *42,* 9841-9853.

30. van Dijk, K. W.; van Vlijmen, B. J. M.; van't Hof, H. B.; van der Zee, A.; Santamarina-Fojo, S.; van Berkel, T. J. C.; Mhavekes, L. M.; Hofker, M. H., *Journal of Lipid Research.* **1999,** *40,* 336-344.

31. Fisher, C. A.; Narayanaswami, V.; Ryan, R. O., *Journal of Biological Chemistry.* **2000,** *275,* 33601-33606.

32. Bjorkegren, J.; Silveira, A.; Boquist, S.; Tang, R.; Karpe, F.; Bond, M. G.; de Faire, U.; Hamsten, A., *Arteriosclerosis, Thrombosis, and Vascular Biology.* **2002,** *22,* 1470-1474.

33.   Smith, D.; Watts, G. F.; Dane-Stewart, C.; Mamo, J. C. L., *European Journal of Clinical Investigation.* **1999,** *29,* 204.

34.   Devaraj, S.; Vega, G.; Lange, R.; Grundy, S. M.; Jialal, I., *American Journal of Medicine.* **1998,** *104,* 445.

35.   Whitman, S. C.; Miller, D. B.; Wolfe, B. M.; Hegele, R. A.; Huff, M. W., *Arteriosclerosis, Thrombosis, and Vascular Biology.* **1997,** *17,* 1707-1715.

36.   Hinsdale, M. E.; Sullivan, P. M.; Mezdour, H.; Maeda, N., *Journal of Lipid Research.* **2002,** *43,* 1520-1528.

37.   Riches, F. M.; Watts, G. F.; Naoumova, R. P.; Kelly, J. M.; Croft, K. D.; Thompson, G. R., *International Journal of Obesity and Related Metabolic Disorders.* **1998,** *22,* 414-423.

38.   Hirany, S.; O'Byrne, D.; Devaraj, S.; Jialal, I., *Clinical Chemistry.* **2000,** *46,* 667.

39.   Hamano, M.; Saito, M.; Eto, M.; Nishimatsu, S.; Suda, H.; Matsuda, M.; Matsuki, M.; Yamamoto, S.; Kaku, K., *Annals of Clinical Biochemistry.* **2004,** *41,* 125-129.

40.   Brunzell, J. D.; Deeb, S. S., Familial Lipoprotein Lipase Deficiency, Apo C-II Deficiency. In *The Metabolic and Molecular Bases of Inherited Disease*, 8th ed.; Scriver, C. R.; Beaudet, A. L.; Sly, W. S.; Valle, D., Eds. McGraw-Hill: New York, 2001; Vol. 2, pp 2789-2816.

41.   Havel, R. J.; Eder, H. A.; Bragdon, J. H., *J Clin Invest.* **1955,** *34,* 1345-53.

42.   Caslake, M. J.; Packard, C. J., The Use of Ultracentrifugation for the Separation of Lipoproteins. In *Handbook of Lipoprotein Testing*, Rifai, N.; Warnick, G. R.;

Dominiczak, M. H., Eds. The American Association for Clinical Chemistry, Inc.: Washington D.C., 1997; pp 509-529.

43.   Nauck, M.; Warnick, G. R.; Rifai, N., *Clin Chem.* **2002,** *48,* 236-54.

44.   Hosken, B. D. *Density Gradient Ultracentrifugation of Lipoproteins Using Metal Ion Complex Solutes*. Ph.D. Dissertation, Texas A&M University, College Station, 2002.

45.   Foreman, J. R.; Karlin, J. B.; Edelstein, C.; Juhn, D. J.; Rubenstein, A. H.; Scanu, A. M., *J Lipid Res.* **1977,** *18,* 759-67.

46.   Schumaker, V. N.; Puppione, D. L., *Methods Enzymol.* **1986,** *128,* 155-70.

47.   Cockrill, S. L. *Lipoprotein density profiling - assessment of cardiovascular risk*. Ph.D. Dissertation, Texas A&M University, College Station, 1998.

48.   Hosken, B. D.; Cockrill, S. L.; Macfarlane, R. D., *Analytical Chemistry.* **2005,** *77,* 200-207.

49.   Johnson, J. D.; Bell, N. J.; Donahoe, E. L.; Macfarlane, R. D., *Anal Chem.* **2005,** *77,* 7054-61.

50.   Lovegrove, J. A.; Isherwood, S. G.; Jackson, K. G.; Williams, C. M.; Gould, B. J., *Biochimica et Biophysica Acta.* **1996,** *1301,* 221.

51.   Sclavons, M. M.; Cordonnier, C. M.; Mailleux, P. M.; Heller, F. R.; Desager, J. P.; Harvengt, C. M., *Clin Chim Acta.* **1985,** *153,* 125-35.

52.   Cornwell, D. G.; Kruger, F. A., *Proc Soc Exp Biol Med.* **1961,** *107,* 296-9.

53.   Schmitz, G.; Mollers, C.; Richter, V., *Electrophoresis.* **1997,** *18,* 1807-13.

54. Weiller, B. H.; Ceriotti, L.; Shibata, T.; Rein, D.; Roberts, M. A.; Lichtenberg, J.; German, J. B.; de Rooij, N. F.; Verpoorte, E., *Anal Chem.* **2002,** *74,* 1702-11.

55. Skoog, D. A.; Holler, F. J.; Nieman, T. A., Eds.; Molecular Luminescence Spectrometry. In *Principles of Instrumental Analysis*, 5th ed.; Harcourt Brace & Company: Orlando, FL, 1998; pp 355-379.

56. Espinosa, I. L.; McNeal, C. J.; Macfarlane, R. D., *Anal Chem.* **2006,** *78,* 438-44.

57. Sperry, W. M.; Brand, F. C., *Journal of Biological Chemistry.* **1943,** *150,* 315-324.

58. Artiss, J. D.; Zak, B., Measurement of Cholesterol Concentration. In *Handbook of Lipoprotein Testing*, Rifai, N.; Warnick, G. R.; Dominiczak, M. H., Eds. The American Association for Clinical Chemistry, Inc.: Washington D.C., 1997; pp 99-114.

59. Cole, T. G.; Klotzsch, S. G.; McNamara, J. R., Measurement of Triglyceride Concentration. In *Handbook of Lipoprotein Testing*, Rifai, N.; Warnick, G. R.; Dominiczak, M. H., Eds. The American Association for Clinical Chemistry, Inc.: Washington D.C., 1997; pp 115-125.

60. Jessen, R. H.; Dass, C. J.; Eckfeldt, J. H., *Clin Chem.* **1990,** *36,* 1372-5.

61. Belcher, J. D.; Egan, J. O.; Bridgman, G.; Baker, R.; Flack, J. M., *J Lipid Res.* **1991,** *32,* 359-70.

62. Kishi, K.; Ochiai, K.; Ohta, Y.; Uemura, Y.; Kanatani, K.; Nakajima, K.; Nakamura, M., *Clin Chem.* **2002,** *48,* 737-41.

63. Leary, E. T.; Wang, T.; Baker, D. J.; Cilla, D. D.; Zhong, J.; Warnick, G. R.; Nakajima, K.; Havel, R. J., *Clin Chem.* **1998,** *44,* 2490-8.

64. Perona, J. S.; Ruiz-Gutierrez, V., *J Sep Sci.* **2004,** *27,* 653-9.

65. Skoog, D. A.; Holler, F. J.; Nieman, T. A., Eds.; Capillary Electrophoresis and Capillary Electrochromatography. In *Principles of Instrumental Analysis*, 5th ed.; Harcourt Brace & Company: Orlando, FL, 1998; pp 778-795.

66. Cardin, A. D.; Price, C. A.; Hirose, N.; Krivanek, M. A.; Blankenship, D. T.; Chao, J.; Mao, S. J., *J Biol Chem.* **1986,** *261,* 16744-8.

67. Petersen, J. R.; Okorodudu, A. O.; Mohammad, A.; Payne, D. A., *Clin Chim Acta.* **2003,** *330,* 1-30.

68. Mukhopadhyay, R., *Anal Chem.* **2006,** *78,* 2109-2111.

69. Schlenck, A.; Herbeth, B.; Siest, G.; Visvikis, S., *J Lipid Res.* **1999,** *40,* 2125-33.

70. Tadey, T.; Purdy, W. C., *J Chromatogr A.* **1993,** *652,* 131-8.

71. Cruzado, I. D.; Cockrill, S. L.; McNeal, C. J.; Macfarlane, R. D., *J Lipid Res.* **1998,** *39,* 205-17.

72. Cruzado, I. D.; Song, S.; Crouse, S. F.; O'Brien, B. C.; Macfarlane, R. D., *Anal Biochem.* **1996,** *243,* 100-9.

73. Tsai, E. C.; Brown, J. A.; Veldee, M. Y.; Anderson, G. J.; Chait, A.; Brunzell, J. D., *BMC Pregnancy and Childbirth.* **2004,** *4,* 27-36.

74. Blum, H.; Beier, H.; Gross, H. J., *Electrophoresis.* **1987,** *8,* 93-99.

75. Lewis, G. F.; Uffelman, K. D.; Lamarche, B.; Cabana, V. G.; Getz, G. S., *Metabolism.* **1998,** *47,* 234-42.

76.   Clay, M. A.; Newnham, H. H.; Barter, P. J., *Arterioscler Thromb.* **1991,** *11,* 415-22.

77.   Patsch, J. R.; Karlin, J. B.; Scott, L. W.; Smith, L. C.; Gotto, A. M., Jr., *Proc Natl Acad Sci U.S.A.* **1983,** *80,* 1449-53.

78.   Horowitz, B. S.; Goldberg, I. J.; Merab, J.; Vanni, T. M.; Ramakrishnan, R.; Ginsberg, H. N., *J Clin Invest.* **1993,** *91,* 1743-52.

79.   O'Meara, N. M.; Cabana, V. G.; Lukens, J. R.; Loharikar, B.; Forte, T. M.; Polonsky, K. S.; Getz, G. S., *J Lipid Res.* **1994,** *35,* 2178-90.

80.   Havel, R. J., *Curr Opin Lipidol.* **1994,** *5,* 102-9.

81.   Castelli, W. P., *American Journal of Cardiology.* **1992,** *70,* 3H-9H.

82.   Cruzado, I. D.; Hu, A. Z.; Macfarlane, R. D., *J Capillary Electrophor.* **1996,** *3,* 25-9.

83.   Voet, D.; Voet, J. G.; Pratt, C. W., Biological Membranes. In *Fundamentals of Biochemistry*, Harris, D., Ed. John Wiley & Sons, Inc.: New York, 2002; Vol. Upgrade Edition, p 261.

84.   Mallik, R.; Jiang, T.; Hage, D. S., *Anal Chem.* **2004,** *76,* 7013-22.

85.   Sengupta, A.; Hage, D. S., *Anal Chem.* **1999,** *71,* 3821-7.

86.   Lupattelli, G.; Pasqualini, L.; Siepi, D.; Marchesi, S.; Pirro, M.; Vaudo, G.; Ciuffetti, G.; Mannarino, E., *Am Heart J.* **2002,** *143,* 733-8.

87.   Reina, M.; Brunzell, J. D.; Deeb, S. S., *J Lipid Res.* **1992,** *33,* 1823-32.

VITA

Richa Chandra graduated from Austin College in the spring of 1998 with a B.A. in chemistry and in Spanish. She matriculated at Texas A&M University in the fall of that same year and then joined the Laboratory for Cardiovascular Chemistry under the direction of Dr. Ronald D. Macfarlane. Richa's research involved the analysis of triglyceride-rich lipoproteins and the development of these techniques for clinical applications. She defended her research in June of 2006 and received her Ph.D. in August of 2006. Richa then matriculated at Texas Tech University School of Medicine in August of 2006. The author can be contacted at Mail Stop 3255, Texas A&M University, College Station, Texas 77843.